# "NEUTRINO-NUCLEON SCATTERING IN THE SECOND RESONANCE REGION"

Thesis submitted to qualify for the doctorate degree in the Universidad de Antioquia

**David F. Tamayo Agudelo**

---

Supervised by:

Dr. Alejandro Mariano (UNLP)

Dr. Daniel E. Jaramillo A. (UdeA)



**Physics Institute**

**UNIVERSIDAD DE ANTIOQUIA**

**MEDELLÍN, ANTIOQUIA - COLOMBIA**

**2022**

# Contents

# List of Figures

# ACKNOWLEDGMENT

First of all, I want to thank my family for their support during this time, without their support this would be impossible. I want to especially thank Professor Alejandro Mariano for all his patience, collaboration and guidance during this time. I thank Professor Daniel Jaramillo for the teachings at the beginning of this work, the GFIF group for the partial funding at the beginning.

I am grateful to professors Patricia Morales and Juan José Quiros for their collaboration and to the graduate students from the University of Antioquia

# INTRODUCTION

The standard model of elemental particles is the theory that describes the non-gravitational interactions between elementary particles, which make up matter and mediated their interactions [1]. The particles that make up matter are fermions, which have a half-integer spin and are classified into leptons ($e$, $\mu$, $\tau$, $\nu_e$, $\nu_\mu$, $\nu_\tau$ ), and quarks ($u$, $d$, $s$, $c$, $b$, $t$). Each fermion also has its antiparticle. However for neutrinos, that are electrically neutral there are two options: that they are their own antiparticle (Majorana fermions), or that differ from their antiparticle (antineutrino $\bar{\nu}$). The particles Interaction mediators are bosons. In the standard model these are: the photon ($\gamma$), the bosons $W^+$, $W^-$ and Z responsible for mediating the electroweak interaction and the eight gluons that are mediators in strong interaction. Additionally, the Higgs boson ($\Phi$) is included in the scalar sector of the standard model providing the particles mass.

In the standard model, neutrinos lack mass, but experimental evidence shows that although small, they do not vanish. This increases interest in their study as it leads to flavor oscillations, mixtures of angles between mass states, violations of quantum numbers, among others. The detection of neutrino masses is the first evidence of physics beyond the standard model. Neutrino physics has been one of the most studied topics in recent years for particle physics. Now it is known that neutrinos are massive particles that can oscillate (changing flavor), so it is essential to know precisely the cross section and the final state in the interactions of the neutrino with nucleons or with a nuclei. The interactions of the neutrinos are described with a high degree of precision by the standard model, no incompatibilities between it and the experimental data of the measurements of the interactions of the neutrinos with matter have yet been found. The interactions of neutrinos with nuclei and nucleons have received considerable attention in recent years stimulated by the need in the analysis of neutrino experiments that give information about the probability of oscillation.

There are several processes or reactions for the study of the interaction of neutrinos with nucleons. The dispersions of neutrinos by nucleons can be quasi-elastic, elastic or inelastic producing additional pions together the nucleon in charged current (CC) and neutral current (NC) interactions. Quasi-elastic interactions of neutrino and antineutrino charged currents with nucleons are described by the processes [3]:

$$\nu_\ell + n \to p + \ell^-,$$

$$\bar{\nu}_\ell + p \to n + \ell^+,$$

where $\ell = e,\ \mu,\ \tau$. In the laboratory only beam of electronic and muonic neutrinos are available, tauonic neutrinos are only available at high energies with cosmic rays interacting with the earth's atmosphere. The elastic interaction of neutrinos and antineutrinos with nucleons with neutral current is described by means of the process [4, 5]:

$$\nu_\ell + N \to \nu'_\ell + N'.$$

In order to have pion production (the process analyzed in this ph.d thesis work) we need that $E_\nu > m_\ell + m_\pi$, and these processes are schematized as:

$$\nu_\ell + N \to \ell^- + N'\pi,$$

$$\bar{\nu}_\ell + N \to \ell^+ + N'\pi,$$

where $N, N' = p,\ n$ .

Neutrino-nucleus scattering is a multi-scale problem, especially in the energetic region of interest for neutrino oscillation experiments in long-baseline experiments, that are hundreds to thousands of MeV, where the source of the neutrino beam and the distant detectors are separated by hundreds of km. On these scales of energy, it is convenient to describe neutrino interactions as the scattering of neutrinos from nucleons that are bound within nuclei. We should also mention the CP violation measurement in a long baseline experiment, or in a search for sterile neutrinos on short baselines. Finally there are experiments devoted to measure exclusively $\nu$-nucleon or nuclei cross sections.

The basic phenomenology of any oscillation experiment can be understood from the limit of two flavors. For two families of leptons in vacuum, the probability that a neutrino of flavor $\alpha$ will oscillate into flavor $\beta$, after propagating through a distance $L$ can be written as

$$P(\nu_\alpha \to \nu_\beta) \approx \sin^2(2\theta) \sin^2\left(\frac{\Delta m^2 L}{4E}\right), \tag{1}$$

where $\Delta m^2$ is the quadratic mass separation between the two mass eigenstates ($m_i$, $i = 1,2,3$) of the system, $\theta$ is the mixing angle that changes between the flavor basis and the mass basis , and $E$ is the energy of the

neutrinos. As can be seen from the equation, the oscillation probability is maximized for values of $L$ and $E$ such that $\Delta m^2 L/4E \sim (n+1)/2\pi$, where $n$ is an integer. The energy of the neutrino in which the maximum of the oscillation occurs, tells us the value of the mass separation (that is, the frequency of the oscillation), while the amplitude of the oscillation tells us the value of $\sin^2 2\theta$.

CP violation searches can be performed by combining measures from $P(\nu_\mu \to \nu_e)$ y $P(\bar{\nu}_\mu \to \bar{\nu}_e)$ , trying to observe a different behavior for particles and antiparticles. The information collected at different energies of neutrinos also generally help to reduce the size of the regions of trust allowed, which in general results in a better determination of the value of $\delta_{CP}$.

Apart from the fundamental importance in researching neutrino oscillation and CP violation, neutrino interaction analysis complements electron and photon scattering studies of hadronic physics by including axial-vector interactions in resonance excitations.

The basic setup of a neutrino-nucleus scattering experiment is that a neutrino of unknown energy that should be reconstructed (because the beams are not monochromatic) enters the detector made of heavier nuclei and interacts. In neutrino scattering in CC, the final state lepton is the charged partner of the incoming flavor ($\nu_{e,\mu,\tau}, l \equiv e, \mu, \tau$), while in NC dispersion, the lepton in the final state is a neutrino of the same flavor as the incoming neutrino $(\nu_{e,\mu,\tau}, \nu'_{e,\mu,\tau})$ that is not directly detectable. Usually, the exchanged momentum $W$ (charged) or $Z$ (neutral) boson interacts with a bound nucleon (one-body current), which is moving with a distribution of impulses $\mathrm{p}$ around the moment of Fermi $\mathrm{p}_F$ inside the nucleus, producing an outgoing nucleon of momentum $\mathrm{p}'$ and, if the neutrino energy is high enough and additional hadrons, mostly pions.

It is the initial neutrino energy spectrum as well as the available information about the particles in the final (detected) state, which must be used in the extraction of oscillation parameters. The strong dependence of the extraction of neutrino oscillation parameters with the neutrino interaction physics, can be best summarized by noting that the energy and configuration of the interactions observed in the experimental detectors (in addition to the effects of the detector) is the energy-dependent neutrino flux convolution with the energy-dependent neutrino-nucleon cross-section and the energy-dependent nuclear effects. In practice, experiments combine information about the energy dependence of all exclusive cross sections (referring to a given output channel), as well as nuclear effects, in a nuclear model. This model, together with the best estimate of the spectrum of incoming neutrino energies, then enters the Monte Carlo predictions of the target nucleus response and the topology of the final states, and is a critical component of the oscillation analysis. One of these channels is the pion production. Oscillation experiments measure event rates at their far detectors after the oscillation, which they use to extract the oscillation probabilities. For oscillations $\nu_\alpha \to \nu_\beta$, event rates with a given observable

topology can be calculated in principle as

$$N_{\alpha\to\beta}(p_{reco}) \;=\; \sum_i \varphi_\alpha(E_{true}) P_{\alpha\beta}(E_{true}) \sigma^i_\beta(p_{true}) \varepsilon_\beta(p_{true}) R_i(p_{true}; p_{reco}),$$

where $N_{FD}(p_{reco})$ represents the event rate as a function of of the reconstructed kinematic variables $p_{reco} \equiv (E_{reco}, \boldsymbol{p}_{reco})$, and $P_{\alpha\beta}(E_{true})$ is the oscillation probability in true neutrino energy function $E_{true}$. Here, $\varphi_\alpha$ is the neutrino flux of the flavor $\alpha$, $\sigma^i_\beta$ is the cross section of the neutrino for interaction $i$ and the flavor $\beta$, and $\varepsilon_\beta$ is the efficiency of the detector for the flavor $\beta$ as a function of its four-moment true $p_{true}$. Finally, the function $R_i(p_{true}\,; p_{reco})$ indicates the probability that the kinematic variables $p_{true}$ are reconstructed as $p_{reco}$ due to detector diffusion and nuclear effects and depends of the neutrino interaction type $i$. As can be seen from the equation, the sample of events for a given topology contains a sum of various interactions. This is the first way that the model of cross section *affects* oscillation analyses, and this model could be tested with experiments devotes to measure these cross sections.

From the experimental side, the Booster Neutrino Experiment (MiniBooNE) was designed to examine the indication of an oscillation signal $\bar{\nu}_\mu \to \bar{\nu}_e$ in the Liquid Scintillator Neutrino Detector (LSND) [6]. The MiniBooNE looks for data for $\nu_e$ appearing in a beam of $\nu_\mu$ when it is restricted to the range of $475 - 1250$ MeV, rebuilding the energy of the neutrino and refuting the interpretation of the LSND signal of the oscillation within a two neutrinos [7]. However, the results indicated an excess of event-type signals that persisted at a level of three standard deviations after several refinements of the analysis. The results obtained were of vital importance for the study of the oscillation of neutrinos that have great experimental interest, for physics beyond the Standard Model.

On the other hand several actual experiments have been designed to measure the cross section in the dispersion of neutrinos with nucleons such as MINER$\nu$A [8, 9] in the FERMILAB, where a beam of neutrinos is prepared to collide against a far detector and measure with high precision and statistics the cross section of the interaction Neutrino-nucleon and analyze the nuclear effects. These enable to analyze the models for the neutrino-nucleon and neutrino-nucleus cross sections, independently of the oscillation issue, giving the possibility of fixing resonances parameters and check nuclear dynamics. As normally, in these kind of experiments the FSI are treated through an event simulation code, we need the most free-less uncertainties model to introduce the primary interaction, in particular for the pion production process that both, contributes to backgrounds in the oscillation experiments and to knowledge of the resonances axial parameters.

For current and future neutrino oscillation experiments we need to understand single pion production by neutrinos with few-GeV energies. The pion production is either a signal process when scattering cross sections are analyzed, or a large background for analyses which select quasi-elastic events. At these energies the dominant production mechanism is via the excitation and subsequent decay of hadronic resonances.

By one side there are additional contributions and fake events different from de quasi-elastics signal coming from:

- Multinucleon emission that comes from pion absorptions, and not detected by a Cherenkov detector.
- $\pi^0$ emission where the pion could decay in two gammas, only one detected and confused with a muon.
- $\pi$ emission when it is absorbed through final state interactions (FSI) and thus does not emerge from the target.

On the othe side, experimental data on nuclear targets present a confusing picture, shown from the MINER$\nu$A [8, 9] and MiniBooNE [10] experiments in poor agreement with each other in the framework of current theoretical models [11, 12].

Complete models of neutrino–nucleus single pion production interactions are usually factorized into three parts:

- the neutrino–nucleon cross section
- additional nuclear effects which affect the initial interaction,as the two body currents
- and the “FSI” of hadrons exiting the nucleus.

The axial form factor of resonances cannot be constrained by electron scattering data, used normally to get the vector form factors (FF), so it relies upon data from Argonne National Laboratory’s 12 ft bubble chamber (ANL) and Brookhaven National Laboratory’s 7 ft bubble chamber (BNL), we will give the references in the results section, pion production experiments on free nucleons. The ANL neutrino beam was produced by focusing $12.4$ GeV protons onto a beryllium target. Two magnetic horns were used to focus the positive pions produced by the primary beam in the direction of the bubble chamber, these secondary particles decayed to produce a predominantly $\nu_\mu$ peaked at $\sim 0.5$ GeV. The BNL neutrino beam was produced by focusing $29$ GeV protons on a sapphire target, with a similar two horn design to focus the secondary particles. The BNL $\nu_\mu$ beam had a higher peak energy of $\sim 1.2$ GeV, and was broader then the ANL beam. These datasets differed in normalization by $30$–$40\%$ for the leading pion production process $\nu_\mu p \to \mu^- p \pi^+$, which conduced to large

uncertainties in the predictions for oscillation experiments [13, 14, 15, 16], as well as in the interpretation of data taken on nuclear targets[17].

It has long been suspected that the discrepancy between ANL and BNL was due to an issue with the normalization of the flux prediction from one or both experiments. Nevertheless, in Ref. [18], was presented a method for removing flux normalization uncertainties from the ANL and BNL for the mentioned leading channel measurements by taking ratios with charged-current quasi-elastic (CCQE) event rates in which the normalization cancels. Then, we obtained a measurement of $\nu_\mu p \to \mu^- p\pi^+$ multiplying the ratio by an independent measurement of CCQE (which is well known for nucleon targets). Using this technique, good agreement was found between the ANL and BNL data sets. Later in other work[19], was extend that method to include the subdominant $\nu_\mu n \to \mu^- p\pi^0$ and $\nu_\mu n \to \mu^- n\pi^+$ channels, and we will use the resulting data. We find that the reanalyzed data, where the normalization discrepancy has been resolved, is able to significantly reduce the uncertainties on the pion production parameters. This is one of the reasons that encourage us to return to the calculation of neutrino-nucleon cross sections with pion production. The other one is that there are many models to describe this process that do not not fulfill several important theoretical aspects

- There are problems from the formal point of view. Since the emission source of the pions is the excitation and decay of resonances, many of them spin $3/2$, we must maintain the amplitudes fulfilling the invariance by contact transformations. These transformations change the amount of the spin $1/2$ spurious contribution in the field that are present by construction. Many works keep the simpler forms of the free and interaction Lagrangians, and amplitudes lacks the mentioned invariance.

- In addition to the resonances pole contribution (normally referred as resonant terms) to the amplitude we have background terms coming from cross resonance contributions and non-resonance origin (called usually non resonant terms). Many works do not consider the interference between these both contributions and really, it is very important to describe the data.

- Another models detach the decay process of the resonance out of the whole weak production amplitude. However, resonances are non-perturbative phenomena associated to the pole of the S-matrix amplitude and one can not detach them from its production or decay mechanisms.

Between the contributions from another authors in this issue, we have an inconsistent model, from the point of view of spin $3/2$ contact transformations, that also include the second resonance region [20]. In addition, in that reference it seems that the cross resonance graphs contributions are omitted for the $\nu p \to \mu^- p\pi^+$ channel. It

is true that the direct or pole contribution of isospin- $\frac{1}{2}$ resonances cannot contribute to a isospin-$\frac{3}{2}$ amplitude, but the cross terms do. A last shortcoming to mention is that for non resonant backgrounds contributions, an arbitrary cutoff of $M_{\pi N} < 1.2$ GeV is applied changing artificially the behavior of these contributions independently from the rest of terms. This is done for all the regimes $M_{\pi N} < 1.4, 1.6$ GeV. As consequence the ANL and antineutrino results are poorly reproduced. A similar model was adopted in Ref. [21] but only with the $N^*(1520)$ resonance included, and the same inconsistency problems mentioned above are present.

On the other hand, the model adopted in Ref. [22] where the propagation of the resonances are described by a Breit-Wigner distribution separating production and decay, does not include a background amplitude and to get accordance in the data for the $\nu n \to \mu^- n\pi^+, \quad \nu n \to \mu^- p\pi^0$ processes they needed to add incoherently a spin $\frac{1}{2}$ background. The model adopted in Ref. [23] is similar to that in Ref. [22] but they adjust the background cross section contribution through a parameter $b^{\pi N}$ different for each channel. These two last works were improved in Ref. [24], where the Resonance (R) and Background (B) contributions were added coherently and the weak $\Delta$ production is treated within the parity conserving parametrization of the $WN \to \Delta$ vertex that is an approximation of the more general Sachs one. Nevertheless, there more energetic resonances were not included.

Finally in GENIE simulation [25] to describe the mentioned data [19], single pion production is separated into resonant and non-resonant terms, with interference between them neglected and interferences between resonances neglected too in the calculation. The resonant component is a modified version of the Rein and Seagal (RS) model [26], where the production and subsequent decay of 18 nucleon resonances with invariant masses $W \leq 2$ GeV are considered. In GENIE, only 16 resonances are included, based on the recommendation of the Particle Data Group (PDG) [27]. In this work they make the assumption that interactions on deuterium can be treated as interactions on quasi-free nucleons which are only loosely bound together, and so neglect FSI effects. In GENIE, there are a number of systematic parameters which can be varied to change the single pion production model. Resonant axial mass ($M_A^{RES}$), Resonant normalization (RES norm), Non-resonant normalization (DIS norm), and normalization of the axial form factor ($F_A(0)$). The total GENIE prediction is the incoherent sum of the RES and DIS contributions, where interference terms have been neglected. GENIE cannot describe all of the pion production channels well for the reanalyzed datasets. For example, the data of the $\nu_\mu n \to \mu^- p\pi^0, \nu_\mu n \to \mu^- n\pi^+$ channels are very similar, but there are large differences between the nominal GENIE predictions for these channels. The non-resonant component of the GENIE prediction, which contributes strongly to these channels, appears to be too large. Finally, it can be seen from Fig.(3) of Ref. [19], where neutrino energy distribution is shown, that the nominal GENIE prediction fails to describe the low-$Q^2$ data

well for some channels.We also note that the GENIE uncertainties are larger than the data suggests, and they may be reduced by tuning the GENIE model to the ANL and BNL data.

In this Ph.d thesis work we calculate the cross section of the inelastic dispersion of neutrinos on nucleons with the production of one pion, where we use a consistent formalism for the intermediate resonance states of spin $3/2$. We will consider only CC currents since they are the main contribution to the resonant pion production being the NC one small in this channel [28].

In addition, we incorporate states in the second resonance region up to $1.6$ GeV, we include N$^*(1440)$, N$^*(1520)$ and N$^*(1535)$ resonances. Also we compare different levels for dressing for the resonance propagators, and the consistency when do it in getting results. This work is organized as follows: In Chapter 1, we introduced the formalism of Rarita-Schwinger field for spin particles$-3/2$ . In the chapter 2 a didactic brief introduction for form factors is introduced, and the frame in which we will use them. The formalism of a dressed propagator for spin particles$-3/2$ $\Delta$ $(1232)$ ($P_{33}$) and a the consistent use of the vertexes and the propagator is introduce in the chapter 3. In the chapter 4 we introduce a special discussion on the the resonances of the second region (N$^*(1440)$, N$^*(1520)$, and N$^*(1535)$). In chapter 5 we show the results obtained with our model in the different regimes of the final $M_{\pi N}$ invariant mass for the total and differential cross sections comparing with another results. Finally in chapter 6 we summarize our conclusions.

# Chapter 1

# EQUATION FOR SPIN$-\frac{3}{2}$ PARTICLES

In the present section we will describe the formal background to build the spin$-3/2$ fields, and a novel form to introduce the relativistic spin projectors that enable to separate the field in its differents components. In addition, we show how to treat the unavoidable effects of having a spurious $1/2$ field, dragged by construction into the propagator and vertexes in order to avoid model dependences. We will introduce the concept of contact transformations and the way of fixing free parameters in the interaction Lagrangians.

Spin$-3/2$ particles are represented by Rarita-Schwinger fields, which result from the tensor product between a tensor of order 1 and a Dirac bispinor, which can be denoted by a irreducible representation $SU(2) \oplus SU(2)$ in the usual form:

$$\psi : \left(\frac{1}{2},0\right) \oplus \left(0,\frac{1}{2}\right). \tag{1.1}$$

The field of spin 1 or Lorentz vector $A_\mu$ can be built by direct product as:

$$A_\mu : \left(\frac{1}{2},0\right) \otimes \left(0,\frac{1}{2}\right) = \left(\frac{1}{2},\frac{1}{2}\right), \tag{1.2}$$

then $3/2$ spinor-vector $\psi_\mu$, according to Rarita and Schwinger, comes from the direct product of a vector and a spinor such as:

$$\psi_\mu \sim A_\mu \otimes \psi : \left(\frac{1}{2},\frac{1}{2}\right) \otimes \left(\left(\frac{1}{2},0\right) \oplus \left(0,\frac{1}{2}\right)\right) = \left(1,\frac{1}{2}\right) \oplus \left(0,\frac{1}{2}\right) \oplus \left(\frac{1}{2},1\right) \oplus \left(\frac{1}{2},0\right). \tag{1.3}$$

where the proper representation for the $3/2-$spin particle is contained in the direct sum $\left(\frac{1}{2},1\right)$ and $\left(1,\frac{1}{2}\right)$. The direct sum $\left(0,\frac{1}{2}\right) \oplus \left(\frac{1}{2},0\right)$ in Eq. 1.3 is an irreducible representation of spin$-\frac{1}{2}$ and we have another contained

in the direct sum $\left(1,\frac{1}{2}\right)\oplus\left(\frac{1}{2},1\right)$ (distinct), so that we can write the Rarita-Schwinger spinor as:

$$\psi^{\mu}=\psi^{\mu}_{3/2}\oplus\psi^{\mu}_{1/2}\oplus\tilde{\psi}^{\mu}_{1/2}. \tag{1.4}$$

where, the free Rarita-Schwinger spinor must also satisfy the Dirac equation (we will see below how to arrive this equation):

$$(i\partial\!\!\!/-m)\psi_{\nu}(x)=0, \tag{1.5}$$

with the on-shell constraints:

$$\gamma^{\mu}\psi_{\mu}=0, \tag{1.6}$$

$$p^{\mu}\psi_{\mu}=0, \tag{1.7}$$

which eliminate spin contributions $1/2$, and will be discussed below. We follows the conventions of Bjorken and Drell [30] and the convention $\hbar=c=1$ will be used throughout [31].

The spinor $\psi^{\mu}$ has 16 particle states distributed as (we have two $1/2$ different sectors):

$$\text{spin}\frac{3}{2}=\begin{cases}4\text{ particles}\\4\text{ anti-particles}\end{cases} \tag{1.8}$$

$$\text{spin}\frac{1}{2}=\begin{cases}2\text{ particles}\\2\text{ anti-particles}\end{cases} \tag{1.9}$$

$$\text{spin}\frac{1}{2}=\begin{cases}2\text{ particles}\\2\text{ anti-particles}\end{cases} \tag{1.10}$$

and in order to separate the components associated with the $1/2$ spin degrees of freedom from the proper Rarita-Schwinger, are introduced the constraints through a Gram-Schmidt procedure. This also enable us to find the projectors in the different space sectors. It is important to mention, that this is a novel form to get these projectors.

## 1.1 GRAM-SCHMIDT PROCESS

The Gram-Schmidt process is an algorithm to construct, from a set of linearly independent vectors forming a subspace, another orthonormal set of vectors that generates the same vector subspace.

Calling the projection of $\mathbf{v}$ on $\mathbf{u}$ as $\mathsf{P}_{\mathbf{u}}\mathbf{v}$ (Fig. 1.1), we have:

$$\mathsf{P}_{\mathbf{u}}\mathbf{v} = \hat{\mathbf{u}}(\hat{\mathbf{u}} \cdot \mathbf{v}), \tag{1.11}$$

where, $\hat{\mathbf{u}} \equiv \frac{\mathbf{u}}{u}$, with $u \equiv |\mathbf{u}|$. Given the set of vectors $\mathbf{v}_1, \cdots, \mathbf{v}_n$, can be constructed the set of orthogonal vectors $\mathbf{u}_1, \cdots, \mathbf{u}_n$ as follows,

$$\mathbf{u}_1 = \mathbf{v}_1, \tag{1.12}$$

$$\mathbf{u}_2 = (1 - \mathsf{P}_{\mathbf{u}_1})\mathbf{v}_2, \tag{1.13}$$

$$\mathbf{u}_3 = (1 - \mathsf{P}_{\mathbf{u}_1})(1 - \mathsf{P}_{\mathbf{u}_2})\mathbf{v}_3, \tag{1.14}$$

$$\mathbf{u}_n = \prod_{j=1}^{n-1}(1 - \mathsf{P}_{\mathbf{u}_j})\mathbf{v}_n \tag{1.15}$$

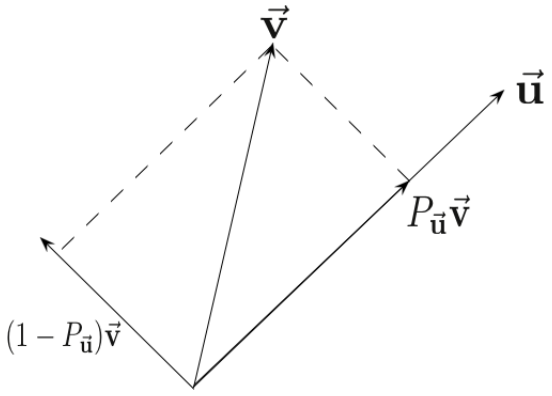


**Figure 1.1:** Parallel and orthogonal components of $\mathbf{v}$ on $\mathbf{u}$.

## 1.2 RARITA-SCHWINGER FIELD

With the Gram-Schmidt process described above we can find the components of $3/2-$spinor of Rarita-Schwinger field ($\psi^{\mu}$), doing the following correspondences (Fig. 1.2):

$$\mathbf{v}_1 \to p^{\mu},$$
$$\mathbf{v}_2 \to \gamma^{\mu},$$
$$\mathbf{v}_3 \to \psi^{\mu}.$$

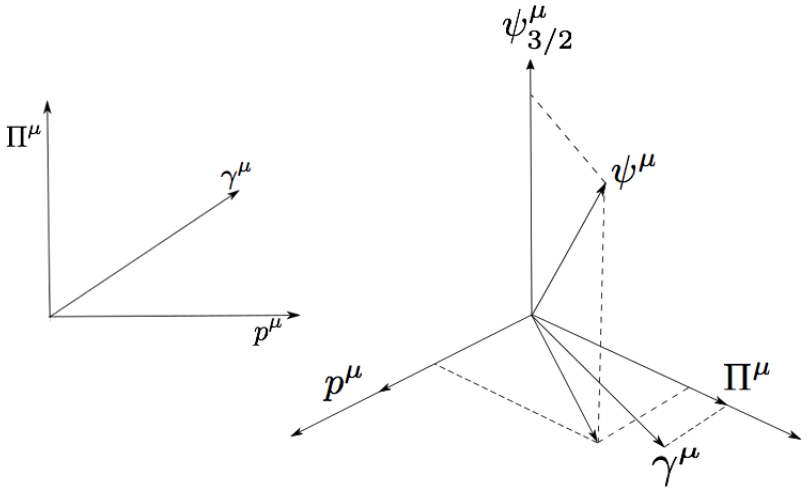


**Figure 1.2:** Geometric representation of the $1/2$-spin components and $3/2$ Rarita-Schwinger field.

and defining the vectors:

$$\hat{\mathbf{u}}_{\mathbf{1}} \to \hat{p}^{\mu} = \frac{p^{\mu}}{|p^{\mu}|}, \qquad\qquad \hat{\mathbf{u}}_{\mathbf{2}} \to \gamma^{\mu} - \gamma^{\nu}\frac{p_{\nu}p^{\mu}}{|p|^2}, \tag{1.16}$$

and with this,

$$\begin{aligned} |\hat{\mathbf{u}}_{\mathbf{2}}|^2 &= \left(\gamma^{\mu} - \gamma^{\nu}\frac{p_{\nu}p^{\mu}}{|p|^2}\right)\left(\gamma_{\mu} - \gamma^{\nu}\frac{p_{\nu}p_{\mu}}{|p|^2}\right) \\ &= \gamma^{\mu}\gamma_{\mu} - \frac{\not{p}\not{p}}{|p|^2} - \frac{\not{p}\not{p}}{|p|^2} + \frac{\not{p}\not{p}p^{\mu}p_{\mu}}{|p|^4} \\ |\hat{\mathbf{u}}_{\mathbf{2}}|^2 &= 4 - \frac{p^2}{|p|^2} - \frac{p^2}{|p|^2} + \frac{p^4}{|p|^4} = 4 - 1 - 1 + 1 = 3, \end{aligned}$$

$$|\hat{\mathbf{u}}_{\mathbf{2}}| = \sqrt{3}, \tag{1.17}$$

$$\hat{\mathbf{u}}_2 = \frac{\mathbf{u}_2}{|\mathbf{u}_2|} \to \frac{1}{\sqrt{3}}\left(\gamma^{\mu} - \gamma_{\nu}\frac{p^{\nu}p^{\mu}}{|p|^2}\right) = \frac{1}{\sqrt{3}}\left(\gamma^{\mu} - \frac{\not{p}p^{\mu}}{|p|^2}\right) \equiv \Pi^{\mu}, \tag{1.18}$$

where we have introduced the vector $\Pi^{\mu}$

$$\Pi^{\mu} = \frac{1}{\sqrt{3}}\left(\gamma^{\mu} - \frac{\not{p}p^{\mu}}{|p|^2}\right). \tag{1.19}$$

Taking now, $\mathbf{v}_3 = \psi^\mu$

$$\mathbf{u}_3 \to \psi^\mu_{3/2} = \psi^\mu - \left[\frac{p^\mu p_\nu}{|p|^2}\right]\psi^\nu - \Pi^\mu\Pi_\nu\psi^\nu, \tag{1.20}$$

renaming the projectors as ($|p|^2 = p^\mu p_\mu = p^2$):

$$P^{1/2}_{22} \equiv \left[\frac{p^\mu p_\nu}{p^2}\right]$$
$$P^{1/2}_{11} \equiv \Pi^\mu\Pi_\nu,$$

and the Rarita-Schwinger spinor can be written in terms of the projectors as:

$$\boxed{\psi^\mu_{3/2} = \left[g^\mu_\nu - \left(P^{1/2}_{11}\right)^\mu_\nu - \left(P^{1/2}_{22}\right)^\mu_\nu\right]\psi^\nu}, \tag{1.21}$$

from where

$$P^{3/2} \equiv \left[g^\mu_\nu - \left(P^{1/2}_{11}\right)^\mu_\nu - \left(P^{1/2}_{22}\right)^\mu_\nu\right]. \tag{1.22}$$

## 1.3 RARITA-SCHWINGER LAGRANGIAN

In this subsection we analyze the Rarita-Schwinger Lagrangian and the contact transformations to get infinite equivalent forms for it all giving the same amplitude. The Lagrangian of the Rarita-Schwinger field can be written as [29]:

$$\mathcal{L} = \overline{\psi}_\mu\Lambda^{\mu\rho}\psi_\rho, \tag{1.23}$$

where,

$$\Lambda^{\mu\rho} = i\partial_\nu\gamma^{\mu\nu\rho} + m\gamma^{\mu\rho} \tag{1.24}$$

being

$$\gamma^{\nu\mu\rho} = \frac{1}{2}\left(\gamma^\mu\gamma^\nu\gamma^\rho - \gamma^\rho\gamma^\nu\gamma^\mu\right) \tag{1.25}$$
$$\gamma^{\mu\nu} = \frac{1}{2}\left(\gamma^\mu\gamma^\nu - \gamma^\nu\gamma^\mu\right), \tag{1.26}$$

and after working a little bit we get

$$\Lambda^{\mu\rho} = \left(i\partial\!\!\!/ - m\right) g^{\mu\rho} + i\gamma^{\mu}\partial\!\!\!/\gamma^{\rho} - i\left(\partial^{\mu}\gamma^{\rho} + \gamma^{\mu}\partial^{\rho}\right) + m\gamma^{\mu}\gamma^{\rho}. \tag{1.27}$$

Now, using the Euler-Lagrange equation one can get for the Rarita-Schwinger equation ,

$$\boxed{i\partial_{\nu}\gamma^{\mu\nu\rho}\psi_{\rho} - m\gamma^{\mu\rho}\psi_{\rho} = 0}. \tag{1.28}$$

or the equivalent form (see Appendix A):

$$\boxed{\gamma^{5}\epsilon^{\mu\nu\sigma\rho}\partial_{\nu}\gamma_{\sigma}\psi_{\rho} - 2im\sigma^{\mu\nu}\psi_{\nu} = 0,} \tag{1.29}$$

with $\sigma^{\mu\nu} = -\frac{i}{2}\left[\gamma^{\mu},\gamma^{\nu}\right] = -\frac{i}{2}(\gamma^{\mu}\gamma^{\nu} - \gamma^{\nu}\gamma^{\mu})$. Since in Eq. 1.23 only it is fixed the $3/2$ component of the states through the constraints Eq. 1.6 (obtained in the Appendix A), being certainly arbitrary as regards the $1/2$ ones, it should be invariant under the contact transformation:

$$\psi^{'\rho} = R^{\rho}{}_{\sigma}(a)\psi^{\rho}, \tag{1.30}$$

where, $R^{\rho}{}_{\sigma}(a) = \delta^{\rho}_{\sigma} + a\gamma_{\sigma}\gamma^{\rho}$, since $\psi_{3/2}\gamma_{\nu} = 0$ does not affect the $3/2$ sector. Usually it is used to write $a$ in terms of a parameter $A$, $a = \left(\frac{1+3A}{2}\right)$, with $A \neq -1/2$. Applying this transformation on Eq. 1.23, we get the most general one-parameter Lagrangian

$$\mathcal{L}(A) = \overline{\psi}_{\mu}\Lambda^{\mu\rho}(A)\psi_{\rho}, \tag{1.31}$$

where

$$\Lambda^{\mu\rho}(A) = R^{\mu}{}_{\sigma}\left(\frac{1+3A}{2}\right)\Lambda^{\sigma\delta}R^{\rho}{}_{\delta}\left(\frac{1+3A}{2}\right), \tag{1.32}$$

being $\Lambda^{\sigma\delta}(-1/3) \equiv \Lambda^{\sigma\delta}$ in Eq. 1.27. Finally, using the properties of $R(a)$ , it is easy to show that the Lagrangian Eq. $1.31$ is also invariant under the change

$$A \to A' = \frac{A-2a}{1+4a},\ a \neq -1/4,\ A \neq -1/2, \tag{1.33}$$

when the transformation Eq. 1.30 is done. The spin$-3/2$ propagator $G(p,A)^{\beta\nu}$ should satisfy (in momentum space, we replace $i\partial \to p$),

$$\Lambda(p,A)^{\beta\mu}G(p,A)_{\beta\nu} = g^{\mu\nu}, \tag{1.34}$$

for any value of $A$ and to keep consistence, it should be transformed as

$$G(p,A)_{\mu\nu} = R^{-1}(A)_{\mu\alpha}G^{\alpha\beta}(p)R^{-1}(A)_{\beta\nu}. \tag{1.35}$$

where $G(p)$ is the Rarita-Schwinger propagator (omitting indexes)

$$G(p) = -\left[\frac{\not{p}+m}{p^2-m^2}P^{3/2} + 2/m^2(\not{p}+m)P_{11}^{1/2} + \sqrt{3}/m(P_{12}^{1/2}+P_{21}^{1/2})\right]. \tag{1.36}$$

Alternatively, Eq. 1.35 can be expressed as

$$\begin{aligned} G_{\alpha\beta}(p,A) &= -\frac{1}{p^2-m^2}\left\{(\not{p}+m)\left[-g_{\alpha\beta}+\frac{1}{3}\gamma_\alpha\gamma_\beta+\frac{1}{3m}(\gamma_\alpha p_\beta-\gamma_\beta p_\alpha)+\frac{2}{3m^2}p_\alpha p_\beta\right]\right. \\ &- \left.\frac{2(p^2-m^2)b(A)}{3m^2}\left[\gamma_\alpha p_\beta-(b(A)-1)\gamma_\beta p_\alpha-(\frac{b(A)}{2}\not{p}+(b(A)-1)m)\gamma_\alpha\gamma_\beta\right]\right\}, \end{aligned} \tag{1.37}$$

where $b(A) = \frac{A+1}{2A+1}$.

The invariance of the free Lagrangian Eq. 1.23 under the contact transformations means that the physical quantities (and thus the amplitudes) should be independent of $A$. Consequently, we demand the interaction Lagrangian for the $3/2$ field coupled to a nucleon ($\psi$) and a pseudoscalar meson ($\phi$) or boson ($W$), as usually appear in a resonance production-decay, be invariant under Eq. 1.30 and Eq. 1.33. The most general interaction Lagrangian satisfying such requirement is

$$\mathcal{L}_{int}(A,Z) = g\bar{\Psi}_\mu R(\frac{1}{2}(2Z+(1+4Z)A))_{\mu\nu}F^\nu(\psi,\phi,W,...)+h.c., \tag{1.38}$$

where $F_\nu$ is a function of the fields and its derivatives, and $g$ is the coupling constant and $Z$ a new arbitrary parameter. Using the property $R(a)_{\mu\nu}R(b)^\nu_\lambda = R(a+b+4ab)_{\mu\lambda}$ it is posible to demonstrate

$$R(1/2(2Z+(1+4Z)A)_{\alpha\beta} = R(A)_{\alpha\mu}R^{-1}(1/2(1-6Z/(1+4Z))^\mu_\beta \tag{1.39}$$

that would be replaced in Eq. 1.38 . Note that the $A-$dependence introduced by the propagator Eq. 1.35 in the

$W\psi \to \phi\psi$ amplitude is canceled by the $R(A)_{\mu\nu}$ in the vertex generated from Eq. 1.38. That is, for any value of $Z$ we get an $A$-independent amplitude and could introduce reduced A-independent Feynman rules. Then, the value for $Z$ must be chosen for each interaction and fixed by a criteria independent from contact transformations. The specific reduced Feynman rules to be used in our calculations will be explained in the Chapter 4 and 5 for each $3/2-$resonance.

# Chapter 2

# FORM FACTORS

We are going to built our amplitudes from effective Lagrangians that consider to the involved hadrons as elementary particles, and also the strong interactions vertexes do not consider particles with structure. This description would be appropriate for certain energy range, but surely will lost its validity for higher energies, being necessary form factors (FF) that take into account the particles sizes or simulating the inclusion of more energetic resonances not included explicitly in the model. Due to this, we find constructive to make a short review on the concept of FF. At the end of the chapter we will resume the use of them to introduce rescattering in the amplitude and contributions of more energetic resonances, not included explicitly in the model.

Hadron spectroscopy makes possible to build the quark model (the quark model should not be confused with QCD, which is the fundamental theory of strong interactions), which can give us information about the static nature of the hadron, for example, its mass, electric charge, spin, isospin and strangeness. But the quark model cannot be solved (perturbative methods are not applicable) to give us information on the internal structure of the hadron or to generate the wave functions for the resonances. To obtain information, we need a test object that can go inside the hadron and shows us its structure. For the test object enter and give us the information of the internal structure of the hadron, we need that: (1) its own properties are well known, (2) it has small size and (3) it can penetrate deeply inside the hadron. From this point of view, the entities that best qualify are the leptons. It can be compared to the situation at the beginning of the 20th century, when there were several models for the atomic structure, where, particle $\alpha$ were used as the test object to reveal the structure of the atom, and the investigation of the scattering patterns in a golden white led for the Rutherford model to be established.

In the 1960's, particle physics theory was in tension. In the field of strong interactions, confidence in field theory was weak and the idea of particle democracy based on the analyticity of the scattering amplitudes was at its peak. Above all the bootstrap theory told us that all particle are equal, no elementary particle exist and that

they themselves are building blocks of other particles, namely they are their own fundamental constituents. Part of the reasoning came from an experimental observation of the nucleon form factor. Experiments showed that, unlike the atom, the nucleon has no nucleus and the entire structure is soft like jelly. There was no reason to believe in the existence of an internal structure within the nucleon. The situation changed when deep inelastic scattering data were presented in 1969. This was the updated Rutherford experiment, in the sense that it clarified the structure of the nucleon, that is, that the nucleon is composed of point-like particles. A series of deep inelastic scattering data, beginning with those from the MIT-SLAC group, clarified that the nucleon is a quark compound and that the quark has fractional charge, which paved the way for quantum chromodynamics (QCD) to appear as the strong interaction theory. To clarify the internal structure of the nucleon so that it is a compound of point-like particles that are generically called partons, the role of the deep inelastic dispersion of leptons such as: electrons (muons) and neutrinos are the best test for the identification of partons as quarks and gluons.

The electron is the best-known and easiest-to-obtain test object of all time. To use the electron, we need to know the formula for its reaction with other particles. The basic equation is the Rutherford dispersion formula is the matrix element:

$$\langle f|H_{IS}|i\rangle = \int d^3x \psi_f^*(x) H_{IS} \psi_i(x), \tag{2.1}$$

where the wave functions are given by

$$\psi_i = N e^{i\mathbf{p}_i \cdot x}, \qquad \psi_f = N e^{i\mathbf{p}_f \cdot x}, \tag{2.2}$$

being $N = 1/\sqrt{V}$ is a normalization factor, normalized the wave function to one particle per unit volume. The electrostatic Hamiltonian is given by:

$$H_{IS} = \frac{Ze^2}{4\pi}\frac{1}{r}. \tag{2.3}$$

Inserting the Eqs. 2.2 and 2.3 in the Eq. 2.1

$$\langle f|H|i\rangle = \frac{Ze^2}{4\pi V}\int d^3x \frac{e^{i(\mathbf{p}_i - \mathbf{p}_f)\cdot x}}{r}; \qquad r = |x|, \tag{2.4}$$

putting $\mathbf{q} = \mathbf{p}_i - \mathbf{p}_f$ and carrying out the integration we find,

$$
\begin{aligned}
I \equiv \int d^3x \frac{e^{i\mathbf{q}\cdot x}}{r} &= 2\pi \int_0^\infty dr \int_{-1}^1 dz \frac{e^{iqrz}}{r} r^2 \\
&= \frac{2\pi}{iq} \int_0^\infty dr (e^{iqr} - e^{-iqr}),
\end{aligned} \tag{2.5}
$$

This integral diverges formally, but we may consider that the potential has a damping factor $e^{-\mu r}$ due to the screening effect of the surrounding repulsive charge. Then

$$
\begin{aligned}
I &= \frac{2\pi}{iq} \int_0^\infty (e^{\mu r + iqr} - e^{-\mu r - iqr}) = \frac{2\pi}{iq} \left( \frac{1}{\mu - iq} - \frac{1}{\mu + iq} \right) \\
&= \frac{4\pi}{q^2 + \mu^2} \to \frac{4\pi}{q2},
\end{aligned} \tag{2.6}
$$

and inserting this equation in Eq. 2.4 we have

$$
\langle f|H|i\rangle = \left( \frac{Ze^2}{4\pi V} \right) \frac{4\pi}{q^2} = \frac{Z\alpha 4\pi}{Vq^2}, \qquad \alpha = \frac{e^2}{4\pi} \simeq \frac{1}{137} \tag{2.7}
$$

$$
q^2 = |\mathbf{p}_i - \mathbf{p}_f|^2 = 4p^2 \sin^2 \frac{\theta}{2}, \tag{2.8}
$$

where $\theta$ is the angle between $\mathbf{p}_i$ and $\mathbf{p}_f$, and $|\mathbf{p}_i| = |\mathbf{p}_f| = p$ by the energy conservation. The final state density is calculated to be

$$
\rho = \delta(E_i - E) \frac{V d^3 p}{(2\pi)^3} = V \left[ \frac{mdE}{p} \right] \frac{p^2 d\Omega}{8\pi^3} = \frac{Vmpd\Omega}{8\pi^3}, \tag{2.9}
$$

where we used $E = \frac{p^2}{2m} \to dE = \frac{p}{m} dp$ and integrated over $E$. Inserting Eq. 2.7 and Eq. 2.8 in the Fermi Golden rule $W_{fi} = 2\pi |\langle f|T|i\rangle|^2 \rho$ we have the transition probability:

$$
W_{fi} = 2\pi \left( \frac{Z\alpha}{V} \right)^2 \left( \frac{4\pi}{q^2} \right)^2 V \frac{mpd\Omega}{8\pi^3} = \frac{p}{V} \frac{4Z^2\alpha^2 m}{q^4} d\Omega. \tag{2.10}
$$

To convert the transition probability to cross section, it must be divided by the incoming flow. The flux is the number of particles passing through unit area in unit time. When the wave function is normalized to one particle per unit volume, the incoming flux can be given as $v/V$, where $v = p/m$ is the velocity of the particle,

$$\therefore \qquad \frac{d\sigma}{d\Omega} = \frac{4Z^2\alpha^2m^2}{q^4} = \frac{Z^2\alpha^2m^2}{4p^4\sin^4\theta/2}., \tag{2.11}$$

which is the useful Rutheford formula. Let's rewrite the Eq. 2.11 as:

$$\frac{d\sigma}{d\Omega} = \left|\frac{m}{2\pi}\int d\mathbf{r}V(\mathbf{r})e^{i\mathbf{Q}\cdot\mathbf{r}}\right|^2 = \frac{4Z^2\alpha^2m^2}{Q^4}, \tag{2.12}$$

and

$$d\sigma = \frac{2\pi}{v}|H_{fi}|^2\delta(E-E_i)\frac{d^3\mathbf{p}}{(2\pi)^2}\frac{mp}{v}|V_{fi}|^2d\Omega \tag{2.13}$$

where $m$, $Z$ is the mass and electric charge of the target

$$V(\mathbf{r}) = \frac{Ze^2}{4\pi}\frac{1}{r} = \frac{Z\alpha}{r} \tag{2.14}$$

$$Q^2 = |\mathbf{Q}|^2 = |\mathbf{k}_i - \mathbf{k}_f|^2 = 4k^2\sin^2\frac{\theta}{2} \tag{2.15}$$

being $k$, $\theta$ is the momentum and scattering angle of the electron. $Q$ is the momentum that the electron transfers to the target, and is called the momentum transfer. The equation Eq. 2.12 holds when the the target is a point particle. If the target is spreaded and has a charge distribution $\rho(\mathbf{r})$, the potential is modified to

$$V(\mathbf{r}) \to V'(\mathbf{r}) = \int d\mathbf{r}'V(\mathbf{r}-\mathbf{r}')\rho(\mathbf{r}') \tag{2.16}$$

and the matrix element to

$$\begin{aligned} V_{fi} \to V'_{fi} = \int d\mathbf{r}V'(\mathbf{r})e^{i\mathbf{Q}.\mathbf{r}} &= \left[\int d(\mathbf{r}-\mathbf{r}')V(\mathbf{r}-\mathbf{r}')e^{i\mathbf{Q}.(\mathbf{r}-\mathbf{r}')}\right]\int d\mathbf{r}'\rho(\mathbf{r}')e^{i\mathbf{Q}.\mathbf{r}'} \\ &= V_{fi}F(Q^2) \end{aligned} \tag{2.17}$$

$$F(Q^2) = \int d\mathbf{r}\rho(\mathbf{r})e^{i\mathbf{Q}.\mathbf{r}} \tag{2.18}$$

where, for simplicity, the distribution was assumed to be spherically symmetric. $F(Q^2)$ is called the form factor

and is a measure of the target spreading. Normalizing the charge distribution by

$$\int d\mathbf{r}\rho(\mathbf{r}) = 1, \tag{2.19}$$

we have

$$F(0) = 1. \tag{2.20}$$

From this discussion, we know that the cross-section formula for an extended target is obtained from the point target by multiplying by the form factor (squared)

$$d\sigma(\theta) = d\sigma_{_{pt}}|F(Q^2)|^2, \tag{2.21}$$

where the above equation says that if we know the cross-section formula of a point target, we can obtain information about the target spread by measuring the scattering pattern. As it is clear from the Eq. 2.18, the part of $\rho(\mathbf{r})$ where $\mathbf{Q}.\mathbf{r} >> 1$ does not contribute to the integral because of the rapid oscillation due to the phase $e^{i\mathbf{Q}.\mathbf{r}}$. This means that the form factor is a measure of total charge integrated over the region $r < 1/Q$. In other words, the electron has penetrated to the distance given by $r \simeq 1/Q$. The maximum value of the momentum transfered $Q$ gives the limit to which we can probe the inner structure of target.

## 2.1 TARGET SIZE

When $\mathbf{Q}.\mathbf{r} << 1$, the form factor can be expanded as

$$\begin{aligned} F(Q^2) &= \int d\mathbf{r}\rho(\mathbf{r})\Big[1 + (i\mathbf{Q}.\mathbf{r}) + \frac{1}{2}(i\mathbf{Q}.\mathbf{r})^2 \ldots\Big], \\ &= \int d\mathbf{r}\rho(\mathbf{r}) + \frac{1}{2}\int d\mathbf{r}\rho(\mathbf{r})(i\mathbf{Q}.\mathbf{r})^2, \\ &= \int d\mathbf{r}\rho(\mathbf{r}) - \frac{1}{2}\int d\mathbf{r}\rho(\mathbf{r})(Q^2|r|^2\cos\theta), \\ &= \int d\mathbf{r}\rho(\mathbf{r}) - \frac{1}{2}\int dr d\phi d\cos\theta |r|^2\rho(\mathbf{r})(Q^2|r|^2\cos\theta), \end{aligned}$$

making $z = \cos\theta$ and the integral $\int_{-1}^{1} z^2 dz = 2/3$

$$
\begin{aligned}
F(Q^2) &= 1-\frac{Q^2}{6}\int 4\pi|r|^2 dr(\rho(r)|r|^2), \\
&= 1-\frac{Q^2}{6}\int d\mathbf{r}\rho(r)|r|^2 \\
F(Q^2) &= 1-\frac{Q^2}{6}\langle r^2\rangle
\end{aligned} \tag{2.22}
$$

and expanding the form factor $F(Q)$ into a Taylor serie,

$$
F(Q^2) = F(Q^2)\Big|_{Q^2=0} + Q^2\frac{dF(Q^2)}{dQ^2}\Big|_{Q^2=0} + \dots
$$

and comparing with Eq. 2.22 we obtain

$$
\langle r^2\rangle = -6\frac{dF(Q^2)}{dQ^2}\Big|_{Q^2=0}, \tag{2.23}
$$

where this means that if we can measure the cross section for small values of $Q$, the information we can obtain is limited to the total charge ($Z\alpha$) and the size of its spreading. The higher the value of $Q$ that we can obtain, that is, the higher the energy and the scattering angle, the deeper we can probe the internal structure. It helps to understand the physical meaning of the form factor if we know the spectral shape of typical spatial distributions. For a spherical constant density distribution $\rho(\mathbf{r}) = \rho_o$ for $r \le R$ and $\rho(\mathbf{r}) = 0$ for $r > R$ (Fig. 2.1a-2.1b)

$$
F(\xi) = \frac{3(\sin\xi - \xi\sin\xi)}{\xi^3}, \qquad \xi = QR, \tag{2.24}
$$

and this is similar to light on through a pinhole making a diffraction pattern of rings.

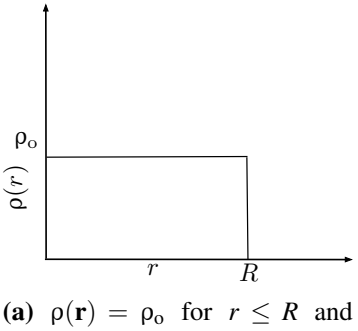


**(a)** $\rho(\mathbf{r}) = \rho_o$ for $r \le R$ and $\rho(\mathbf{r}) = 0$ for $r > R$.

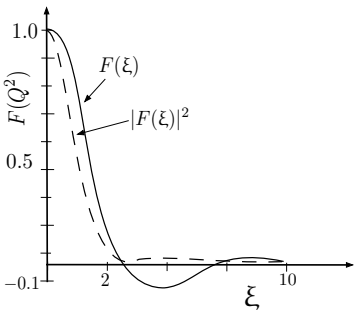


**(b)** $F(\xi) = 3(\sin\xi - \xi\cos\xi)/\xi^3$

If we look for example the nucleus, like a blurred sphere with radius $R = r_o A^{1/3}$, the charge distribution that

reproduces the observed pattern is depicted in Fig. 2.2 where $R$ represents the nuclear size, $t = (4\ln 3)a$ the thickness of the surface or the degree of blurriness. When the distribution becomes harder smoothly towards the core it may be represented by an exponential or a Gaussian respectively [32]:

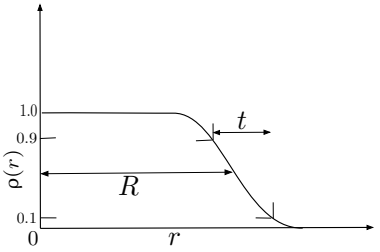


**Figure 2.2:** $\rho(r) = \rho_o/[1+\exp(r-R)/a]$, $t = (4\ln 3)a$.

$$\rho(\mathbf{r}) = \rho_o e^{-r/R}, \tag{2.25}$$

$$F(Q^2) = \frac{1}{(1+Q^2R^2)^2}. \tag{2.26}$$

$$\rho(\mathbf{r}) = \rho_o e^{-r^2/2\sigma^2}, \tag{2.27}$$

$$F(Q^2) = e^{-Q^2\sigma^2/2}. \tag{2.28}$$

## 2.2 Rescattering and hadrons FF

Here we concentrate in the using of FF in our problem of weak production pion amplitudes, where the hadronic ($h$) contribution would be expressed in general as

$$\mathcal{M}_h^\lambda = \bar{u}(p')\chi^\dagger \boldsymbol{\Phi}^* \cdot \left[\boldsymbol{I}^\dagger O^\lambda \boldsymbol{I}\right] \cdot \boldsymbol{W} u(p)\chi, \tag{2.29}$$

being $\bar{u}\chi^\dagger, u\chi$ the final and initial nucleon spinors (isospin wave function included), $\boldsymbol{\Phi}^*, \boldsymbol{W}$ the final pion and initial $W-$boson wave functions and $\boldsymbol{I} = \boldsymbol{\tau}, \boldsymbol{T}^\dagger$ the isospin and resonance isospin excitation operators. Firstly $O^\lambda$ is splitted in a resonant $s$-type (or pole $P$) contribution $O_R^\lambda$ and $u+t-$type (or non-pole $NP$) background one $O_B^\lambda$. All these will be clarified in the next chapters.

Now, omitting isospin coefficients we will support our discussion on the already pion photoproduction reaction analyzed previously in Ref.[33], and we will have the analogy $O^\lambda \equiv \hat{B}^\lambda$ and $O^\lambda_{B,R} \equiv \hat{B}^\lambda_{NP}, \hat{B}^\lambda_P$ with the photoproduction vertexes in that Reference. The minimum approximation that it is possible to implement can be resumed as

$$O^\lambda \approx O^\lambda_B + O^\lambda_R \equiv O^\lambda_B + \sum_R V_{R\pi N} G_R W^\lambda_{WNR}, \tag{2.30}$$

where $V_{R\pi N}$ and $W^\lambda_{WNR}$ represent schematically the $R \to N\pi$ and $WN \to R$ vertexes respectively, while $G_R$ a resonance propagator. Normally $G_R$ within the $O^\lambda_R$ contribution can be dressed by a self-energy mainly due to $\pi N$ rescattering , as will be shown in the next chapter. Nevertheless, the $O^\lambda_B$ contributions in special the $u$-resonance contributions can not do so. As consequence, grows rapidly for certain final $M_{\pi N}$ invariant mass. As described in Ref. [33] for the case of photoproduction, but valid also here, there are other effects not considerate in the approximation Eq. 2.30 of Eq. 2.29. The complete $\mathcal{M}^\lambda_h$ amplitude in the final $\pi N$ center of mass (CM) can be obtained with

$$\begin{aligned} O^\lambda(k,q) &= \left[-i(2\pi)^4\delta^4(k-k') + T_{NP}(k')G_{\pi N}(k')\right]\left(O^\lambda_B(k',q) + \sum_R V_{R\pi N}(k',k)G_R(k)\widetilde{W}^\lambda_{WNR}(k,q)\right) \\ \widetilde{W}^\lambda_{WNR}(k,q) &= W^\lambda_{WNR}(k,q) + \left(V_{R\pi N}(k,k'') + V_{R\pi N}(k,k')G_{\pi N}(k')T_{NP}(k',k'')\right)G_{\pi N}(k'')O^\lambda_B(k'',q), \end{aligned} \tag{2.31}$$

where with $k,q$ we indicate $\pi$ and $W$ momenta respectively, and where $k',k''$ are intermediate $\pi$ momenta and a repeated $k,k',k''$ are indicate $i\frac{\int d^4k,k',k''}{(2\pi)^4}$,

$$G_{\pi N}(k') = S_N(p+q-k')\Delta_\pi(k'),$$

is the pion-nucleon intermediate propagator, and $T_{NP}$ the non-pole scattering T-matrix that iterates to all orders the potential $V_{NP} \equiv V_{N\pi,N'\pi'}$ built with nucleon Born terms, meson exchange $t-$contributions and $u-$resonant contributions. In summary, in the full amplitude the rescattering of the final $\pi N$ pair through $T_{NP}$ is considered as well as the decay into a resonance of $O^\lambda_B$. We will not introduce in this thesis work unitarizartion corrections, done through imaginary contributions in Eq. 2.31, since as we will analyze the total and differential cross

sections, where corrections to each multipole compensate out in the multipole expansion of the cross section Ref. [33]. In Fig. 2.3 we show schematically the contributions in Eq. 2.31 and with FF we indicate the possible places where FF would be necessary.

As we wish to deal with effective real coupling constants ($T_{NP}$ dresses but is a complex operator), it is convenient to express the $\pi N$ T-matrix operator in terms of the real $K$-matrix Ref. [33], and after a three dimensional reduction we get

$$\begin{aligned} O^{\lambda}(\boldsymbol{k},\boldsymbol{q},W_{\pi N}) &\approx \left[(2\pi)^3\delta^3(\boldsymbol{k}-\boldsymbol{k'}) + \mathcal{P}\left(K_{NP}(\boldsymbol{k},\boldsymbol{k'})G_{TH}(\boldsymbol{k'},\sqrt{s})\right]\right. \\ &\times \left[O_B^{\lambda}(\boldsymbol{k'},\boldsymbol{q},W_{\pi N})\Big) + \sum_R V_{R\pi N}(\boldsymbol{k'},\boldsymbol{p})\Big)\, G_R(\boldsymbol{p},W_{\pi N})\widetilde{W}^{\lambda}_{WNR}(\boldsymbol{p},\boldsymbol{q},W_{\pi N})\right], \quad (2.32) \\ \widetilde{W}^{\lambda}_{WNR}(\boldsymbol{p},\boldsymbol{q},W_{\pi N}) &= W^{\lambda}_{WNR}(\boldsymbol{p},\boldsymbol{q}) + \mathcal{P}\left[V_{R\pi N}(\boldsymbol{p},\boldsymbol{k'})G_{TH}(\boldsymbol{k'},W_{\pi N})\,O_B^{\lambda}(\boldsymbol{k'},\boldsymbol{q})\right], \quad (2.33) \end{aligned}$$

where $G_{\pi N}(k')$ is replaced by the Thompson propagator $G_{TH}(\boldsymbol{k'},W_{\pi N}) = \frac{m_N}{2E_\pi(\boldsymbol{k'})E_N(\boldsymbol{k'})}\sum_{ms'}\frac{u(-\boldsymbol{k'},m'_s)\bar{u}(\boldsymbol{k'},m'_s)}{W_{\pi N}-E_\pi(\boldsymbol{k'})-E_N(\boldsymbol{k'})}$ and where with $\mathcal{P}$ is the principal value on the integral in repeated momenta.

The momenta integrals present in Eq. 2.32 and Eq. 2.33 are normally divergent, and in order to reproduce the experimental data FF have to be introduced for getting good agreement with data, which affect both $O^{\lambda}_{B,R}$ to regularize the mentioned integrals. They are meant, as seen above, to model the deviations from the point-like couplings due to the quark structure of nucleons and resonances, analogs of the electromagnetic ones reflecting the extension of the hadrons, and should be calculated from the underlying theory or quark models [34]. Because it is not clear a priori which form these additional factors should have, they introduce a source of systematical error in all models [35]. The use of individual different FF in each vertex of a graph would requiere vertex corrections when the propagators are dressed to fulfill electromagnetic gauge invariance in the radiative processes. Then, guided by previous calculations in $\pi N$ scattering and $\pi$-photoproduction in Ref. [36] and Ref. [37], and the description of NC1$\pi$ data obtained by the CERN Gargamelle experiment without applying cuts in the neutrino energies [38], we multiply $O_B^{\lambda}+O_R^{\lambda}$ by a global regularizing FF of the $R\pi N$ and $N\pi N'$ vertexes ($\mathrm{k}=|\boldsymbol{k}|$)

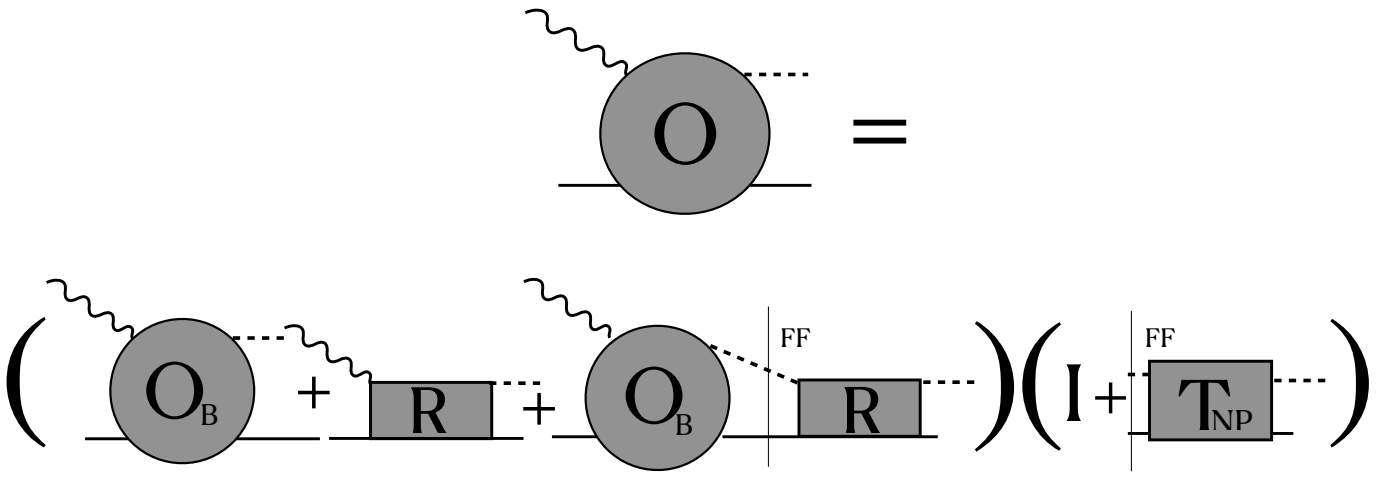


**Figure 2.3:** Rescattering and dressed vertex contributions

$$F(\mathrm{k}, M_{\pi N}) = \frac{(\Lambda)^4}{(\Lambda)^4 + \mathrm{k}(\mathrm{W}_{\pi\mathrm{N}})^2 \left(W_{\pi N} - W_{\pi N}^{th}\right)^2 \theta(W_{\pi N} - 1.6 \text{ GeV})}, \tag{2.34}$$

$$\mathrm{k}(W_{\pi N}) = \sqrt{\frac{(W_{\pi N}^2 - m_N^2 - m_\pi^2)^2 - 4m_N^2 m_\pi^2}{4W_{\pi N}^2}}, \tag{2.35}$$

being the threshold invariant mass $W_{\pi N}^{th} = m_\pi + m_N$ and which is consistent with that introduced in Refs.[36] and [37], but lighting it above the second resonance region that begins around $W_{\pi N} \lesssim 1.6$ GeV because above this value the hadron finite size begins to be important (see section 6) . At first, it is possible to manipulate the FF proposed in those references to obtain forms very similar to Eq. 2.34. This FF can be seen as

$$F(\mathrm{k}, W_{\pi N}) = \frac{\left(\Lambda_{eff}\right)^2}{\left(\Lambda_{eff}\right)^2 + \mathrm{k}(\mathrm{W}_{\pi\mathrm{N}})^2}, \Lambda_{eff} = \Lambda \frac{\Lambda}{W_{\pi N} - W_{\pi N}^{th}}, \tag{2.36}$$

where we have a monopole FF with an effective cutoff diminishing with $W_{\pi N} - W_{\pi N}^{th}$, making that certain term "disappears" or contributes less in the amplitude since when $W_{\pi N}$ grows another resonance, not considered in

the amplitude, could be excited. Note that this FF affects also the on-shell contributions,i.e, the terms surviving in Eq. 2.32 and Eq. 2.33 when the $\mathcal{P}$ terms are dropped.

In resume, to get the full amplitudes in Eq. 2.32 we need to add FF taking into account the hadron extensions since as can be seen in $G_{TH}(\boldsymbol{k'}, W_{\pi N})$, we keep the $\pi$ and $N$ elemental character for any $W_{\pi N}$, and this makes the involved integral divergent. This entails to moderate the on shell amplitude $O^{\lambda}$ with this FF, which is not considered in the approach (2.30).

# Chapter 3

# DRESSING THE SPIN-3/2 PROPAGATOR

As resonances are unstables states with certain width, in this section we describe how to get this width from the decay of the resonance in certain channel and the different levels of approximation to dress them. The resonance mass $m$ and decay width $\Gamma$ are intrinsic properties of a resonance for which there are at least two commonly used definitions. One definition is obtained from the real and imaginary parts of the pole position $s_p \equiv m^2 - im\Gamma$ of the S-matrix amplitude; this complex pole is located at the value $s = s_p$, where $s$ is the square of the invariant mass of the decay products of the resonance. A different definition is provided by the mass parameter $m$ which is obtained from the renormalized propagator that includes the resummation of $\pi N$ self-energies computed from the field theory Lagrangian that describes the dynamics of the resonance; in this case, the corresponding energy-dependent decay width $\Gamma(s)$ is determined by the interactions of the resonance with other fields and the decay width is given by $\Gamma(m^2)$. In this section we will develop this last approach and hereafter, we will refer to these definitions as the pole and field-theoretic (FT) parameters of the resonance, respectively. We would like to remark that in order to account for the electromagnetic gauge invariance of the amplitude, when the spin$-3/2$ resonance participates in a radiative scattering the Ward identity Ref. [40],

$$i(p-p')_\alpha G_{\mu\nu}(p')\Gamma_{\alpha\nu\rho}G^{\rho\sigma}(p) = G^\sigma_\mu(p) - G^\sigma_\mu(p'), \tag{3.1}$$

where $\Gamma$ is the electromagnetic vertex, should be satisfied. As as we will see below in detail, the introduction of the width will be done through the replacement $m \to m - \frac{i\Gamma}{2}$. It can be easily proved that if this change is done only in the denominator of the propagator $G(p)$ or if the width $\Gamma = \Gamma(s)$ being not constant, these identities are violated by terms of order $\Gamma/m$. We will describe a different weak pion production process, but in consistence with the mentioned radiative one we should take care of this last observation and the departure of

this assumption will be discussed in each case. From the Chapter 1 we have seen that the unperturbed reduced propagator can be expressed in terms of (omitting indexes) projectors as (see appendix B)

$$G_0(p) \equiv G(p) = -\left[\frac{\not{p}+m}{p^2-m^2}P^{3/2} + 2/m^2(\not{p}+m)P_{11}^{1/2} + \sqrt{3}/m(P_{12}^{1/2}+P_{21}^{1/2})\right], \tag{3.2}$$

where the obtained spin projectors can also be expressed as

$$\begin{aligned}
(P^{3/2})^{\alpha\beta} &= g^{\alpha\beta} - \frac{2}{3}\frac{p^\alpha p^\beta}{p^2} - \frac{1}{3}\gamma^\alpha\gamma^\beta + \frac{1}{3p^2}(\gamma^\alpha p^\beta - \gamma^\beta p^\alpha)\not{p}, \\
(P_{11}^{1/2})^{\alpha\beta} &= \frac{1}{3}\gamma^\alpha\gamma^\beta - \frac{1}{3}\frac{p^\alpha p^\beta}{p^2} - \frac{1}{3p^2}(\gamma^\alpha p^\beta - \gamma^\beta p^\alpha)\not{p}, \\
(P_{22}^{1/2})^{\alpha\beta} &= \frac{p^\alpha p^\beta}{p^2}, \\
(P_{21}^{1/2})^{\mu\beta} &= -\sqrt{\frac{3}{p^2}}\frac{1}{3p^2}(-i\sigma^{\mu\alpha}p_\alpha)\not{p}p^\beta, \\
(P_{12}^{1/2})^{\mu\beta} &= \sqrt{\frac{3}{p^2}}\frac{1}{3p^2}(-i\sigma^{\beta\alpha}p_\alpha)\not{p}p^\mu,
\end{aligned} \tag{3.3}$$

with $\sigma^{\mu\nu} = i[\gamma^\mu,\gamma^\nu]/2$. Another useful form is obtained using the propagator expressions and after operating we get

$$\begin{aligned}
G_0^{\alpha\beta}(p) = \frac{\not{p}+m}{p^2-m^2}\Bigg\{ &-g_{\alpha\beta} + \frac{1}{3}\gamma^\alpha\gamma_\beta + \frac{1}{3m}(\gamma^\alpha p^\beta - \gamma^\beta p^\alpha) + \frac{2}{3m}p_\alpha p^\beta - \\
&\frac{2(p^2-m^2)}{3m^2}[\gamma^\alpha p^\beta - \gamma^\beta p^\alpha - (\not{p}+m)\gamma^\alpha\gamma^\beta]\Bigg\},
\end{aligned} \tag{3.4}$$

where $m$ is the bare mass of the spin$-3/2$ field and $p$ its $4-$momentum. The bare propagator being singular at $p^2 = m^2$ should be dressed by the inclusion of a self-energy ($\Sigma$) giving to it a width corresponding to an unstable particle. We will develop the dressing procedure for the $\Delta$-resonance which results to be dominant, but then we extend to another resonances. The self-energy (where usually only Born interaction terms are considered) could include the lowest order $pN$ one-loop contribution (Fig. 3.2 ) as well as other higher order $pN$ irreducible scattering non-pole (NP) terms Figs. 3.1(b) and 3.1(c) consistent with the $pN$ scattering amplitude.

If we focus on the 3.1(a) contribution (since the final $\pi N$ states concentrate rough all the decay ratio) for the $\Delta$ baryon, the corresponding interaction Lagrangian for the $\Delta \to N\pi$ decay is ($R$ matrixes were defined in

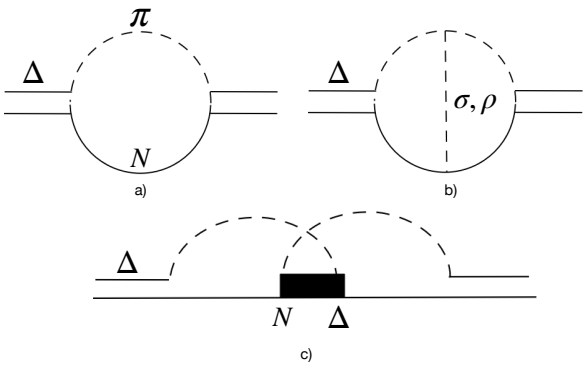


**Figure 3.1:** Self-energy possible contributions

chapter 1)

$$\mathcal{L}_{\Delta\pi N} = g\bar{\Psi}_\mu R(A)_{\beta\nu} R^{-1}(1/2(1-6Z/(1+4Z))^{\mu\beta}\bar{\psi}\partial\mathbf{\Phi}^\nu \cdot \boldsymbol{T}^\dagger\psi + hc., \tag{3.5}$$

while the reduced vertex (A-independent) is given by :

$$V_{\Delta\pi N} = -gk^\mu \times R^{-1}(1/2(1-6Z/(1+4Z))_{\mu\nu}, \tag{3.6}$$

where $g$ is the strong coupling with dimension of mass$^{-1}$ and $k$ denotes the $4-$momentum of the outgoing pion [41]. The factor depending on $A$ cancels with that of the propagator in Eq. 1.35 and the same structure will be assumed for the weak production resonant vertex. We adopt the value $Z = 1/2$ fixed in order to do not generate dynamics for the $\Psi_0$ component of the $\Delta$ field [42] (note that the time derivative of $\Psi_0$ does not appear in the wave equation 1.29).

The expression for the dressed propagator $G^{\mu\nu}(p)$ can be obtained by solving the Schwinger-Dyson equation that satisfied by the inverse propagators:

$$(iG^{-1})^{\mu\nu}(p) = (iG_0^{-1})^{\mu\nu}(p) - \Sigma^{\mu\nu}(p), \tag{3.7}$$

where $\Sigma^{\mu\nu}(p)$ denotes the self-energy correction of $\Delta$ as show in Fig. 3.2. In the following, we will consider only the absorptive (imaginary) parts of the self-energy correction, i.e. we will assume [43, 44] that the parameter $m$ represents the 'renormalized' mass of $\Delta$ (we place quotation marks as a reminder that the Lagrangian is not

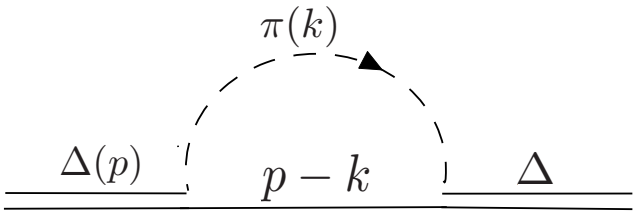


**Figure 3.2:** Self-energy correction to $\Delta$ propagator

renormalizable; only the absorptive corrections are finite in this case). If we denote by $p$ the $4-$momentum of $\Delta$ and compute the one-loop absorptive corrections by applying the cutting rules to Fig. 3.2, we obtain

$$\Sigma^{\mu\nu}_{\text{abs}}(p) = i\frac{g^2}{2(2\pi)^2}\int \frac{d^3\mathrm{k}}{2\mathrm{k}_0}\frac{1}{2\sqrt{p^2}}\delta\left(\mathrm{k}_0 + \frac{p^2+m_\pi^2-m_N^2}{2\sqrt{p^2}}\right)\theta(p^2-(m_N+m_\pi)^2)(\not{p}+\not{\mathrm{k}}+m_N)\mathrm{k}^\mu\mathrm{k}^\nu, \tag{3.8}$$

which, in terms of the new more proper basis of projection operators [45]

$$\begin{aligned}
(\mathcal{P}_{1,2})^{\alpha\beta} &= \Lambda^{\pm}(P^{3/2})^{\alpha\beta},\\
(\mathcal{P}_{3,4})^{\alpha\beta} &= \Lambda^{\pm}(P^{1/2}_{11})^{\alpha\beta},\\
(\mathcal{P}_{5,6})^{\alpha\beta} &= \Lambda^{\pm}(P^{1/2}_{22})^{\alpha\beta},\\
(\mathcal{P}_{7,8})^{\alpha\beta} &= \Lambda^{\pm}(P^{1/2}_{21})^{\alpha\beta},\\
(\mathcal{P}_{9,10})^{\alpha\beta} &= \Lambda^{\pm}(P^{1/2}_{12})^{\alpha\beta},
\end{aligned} \tag{3.9}$$

where $\Lambda^{\pm} = \frac{\sqrt{p^2}\pm\not{p}}{2\sqrt{p^2}}$, can be expressed as

$$\Sigma^{\mu\nu}_{\text{abs}}(p) = \sum_i \bar{J}_i(\mathcal{P}_i)^{\mu\nu}. \tag{3.10}$$

The coefficients $\bar{J}_i$ can be computed by introducing the Eq. 3.10 into Eq. 3.7 and solving using the projectors properties and the expression Eq. 3.2 for the unperturbed $G_0(p)$ propagator. Thus we obtain (we use $s = p^2$):

$$
\begin{aligned}
\bar{J}_1 = \bar{J}_3 &= -i\frac{g^2 I_0}{(2\pi)^2}\frac{1}{12s}\left[\frac{(\sqrt{s}+m_N)^2-m_\pi^2}{4\sqrt{s}}\right]\lambda(s,m_N^2,m_\pi^2),\\
\bar{J}_2 = \bar{J}_4 &= i\frac{g^2 I_0}{(2\pi)^2}\frac{1}{12s}\left[\frac{(\sqrt{s}-m_N)^2-m_\pi^2}{4\sqrt{s}}\right]\lambda(s,m_N^2,m_\pi^2),\\
\bar{J}_5 &= i\frac{g^2 I_0}{(2\pi)^2}\frac{1}{4s}(s-m_N^2+m_\pi^2)^2\left[\frac{(\sqrt{s}+m_N)^2-m_\pi^2}{4\sqrt{s}}\right],\\
\bar{J}_6 &= -i\frac{g^2 I_0}{(2\pi)^2}\frac{1}{4s}(s-m_N^2+m_\pi^2)^2\left[\frac{(\sqrt{s}-m_N)^2-m_\pi^2}{4\sqrt{s}}\right],\\
\bar{J}_7 &= \bar{J}_8 = \bar{J}_9 = \bar{J}_{10} = i\frac{g^2 I_0}{(2\pi)^2}\sqrt{\frac{3}{s}}\frac{1}{48s}(s-m_N^2+m_\pi^2)\lambda(s,m_N^2,m_\pi^2),
\end{aligned}
\tag{3.11}
$$

where $\lambda(x,y,z) = x^2+y^2+z^2-2xy-2xz-2yz$, and [45]:

$$
I_0 = \theta(s-(m_N+m_\pi)^2)\left(\frac{\pi}{2}\right)\frac{\lambda^{1/2}(s,m_N^2,m_\pi^2)}{s}
\tag{3.12}
$$

and by comparison with the result of [45], we obtain the closely related coefficients:

$$
\begin{aligned}
J_1 = J_3 &= -i\frac{g^2 I_0}{(2\pi)^2}\frac{m_N}{24s}\lambda(s,m_N^2,m_\pi^2),\\
J_2 = J_4 &= -i\frac{g^2 I_0}{(2\pi)^2}\frac{1}{48s^2}(s+m_N^2-m_\pi^2)\lambda(s,m_N^2,m_\pi^2),\\
J_5 &= i\frac{g^2 I_0}{(2\pi)^2}\frac{m_N}{8s}(s-m_N^2+m_\pi^2)^2,\\
J_6 &= i\frac{g^2 I_0}{(2\pi)^2}\frac{1}{16s^2}(s+m_N^2-m_\pi^2)(s-m_N^2+m_\pi^2)^2,\\
J_7 = J_9 &= i\frac{g^2 I_0}{(2\pi)^2}\sqrt{\frac{3}{s}}\frac{1}{48s}(s-m_N^2+m_\pi^2)\lambda(s,m_N^2,m_\pi^2),\\
J_8 = J_{10} &= 0,
\end{aligned}
\tag{3.13}
$$

which are defined from the relations: $\bar{J}_{2n-1} \equiv J_{2n-1} + \sqrt{s}J_{2n}$ and $\bar{J}_{2n} \equiv J_{2n-1} - \sqrt{s}J_{2n}$, for $n = 1,\ldots,5$. Finally by inserting the results shown in Eqs. 3.11−3.13 into Eq. 3.7 and Eq. 3.10, we obtain the following form of the *dressed propagator*:

$$
\begin{aligned}
G^{\alpha\beta}(p) = -\frac{1}{1-J_2}\Bigg\{ & \frac{\tilde{m}^2+\not{p}}{\tilde{m}^2-p^2}(\mathcal{P}^{3/2})^{\alpha\beta} + \frac{1}{2}\left[\frac{2\tilde{m}-2\sqrt{p^2}+A_+}{-\tilde{m}^2+X_+} + \frac{2\tilde{m}+2\sqrt{p^2}+A_-}{-\tilde{m}^2+X_-}\right](\mathcal{P}_{11}^{1/2})^{\alpha\beta} \\
& + \frac{1}{2\sqrt{p^2}}\left[-\frac{2\tilde{m}-2\sqrt{p^2}+A_+}{-\tilde{m}^2+X_+} + \frac{2\tilde{m}+2\sqrt{p^2}+A_-}{-\tilde{m}^2+X_-}\right]\not{p}(\mathcal{P}_{11}^{1/2})^{\alpha\beta} \\
+\frac{1}{2}\left[\frac{3\frac{J_3-\sqrt{p^2}J_4}{1-J_2}}{-\tilde{m}^2+X_+} + \frac{3\frac{J_3+\sqrt{p^2}J_4}{1-J_2}}{-\tilde{m}^2+X_+}\right](\mathcal{P}_{22}^{1/2})^{\alpha\beta} & + \frac{1}{2\sqrt{p^2}}\left[\frac{3\frac{J_3-\sqrt{p^2}J_4}{1-J_2}}{-\tilde{m}^2+X_+} - \frac{3\frac{J_3+\sqrt{p^2}J_4}{1-J_2}}{-\tilde{m}^2+X_+}\right]\not{p}(\mathcal{P}_{22}^{1/2})^{\alpha\beta} \\
& \frac{\sqrt{3}}{2}\left[\frac{\tilde{m}-\left(\frac{J_1+\sqrt{3}J_7}{1-J_2}\right)}{-\tilde{m}^2+X_+} - \frac{\tilde{m}-\left(\frac{J_1-\sqrt{3}J_7}{1-J_2}\right)}{-\tilde{m}^2+X_-}\right][(\mathcal{P}_{21}^{1/2})^{\alpha\beta}+(\mathcal{P}_{12}^{1/2})^{\alpha\beta}] \\
& \frac{\sqrt{3}}{2\sqrt{p^2}}\left[\frac{\tilde{m}-\left(\frac{J_1+\sqrt{3}J_7}{1-J_2}\right)}{-\tilde{m}^2+X_+} + \frac{\tilde{m}-\left(\frac{J_1-\sqrt{3}J_7}{1-J_2}\right)}{-\tilde{m}^2+X_-}\right]\not{p}[(\mathcal{P}_{21}^{1/2})^{\alpha\beta}-(\mathcal{P}_{12}^{1/2})^{\alpha\beta}]\Bigg\},
\end{aligned}
\tag{3.14}
$$

where are defined

$$
\begin{aligned}
X_\pm &\equiv \frac{2m(J_1+J_3\pm\sqrt{3}J_7\mp pJ_4)+2p(\mp J_3+pJ_4)+J_1^2}{(1-J_2)^2}, \\
A_\pm &\equiv \frac{3(J_5\pm pJ_6)-2(J_1\pm pJ_2)}{1-J_2}.
\end{aligned}
\tag{3.15}
$$

In equation 3.14 we have introduced the effective mass term:

$$
\begin{aligned}
\tilde{m} &= \frac{m+J_1}{1-J_2} \\
&= m+(J_1+\sqrt{s}J_2)+(m-\sqrt{s})J_2+O(g^4) \\
&\approx m-i\frac{\Gamma_\Delta(s)}{2}
\end{aligned}
\tag{3.16}
$$

where we have neglected terms of $O(g^4)$ and $O((m-\sqrt{s})g^2)$ in the last result, because these terms are expected to be very small in the resonance region $(\sqrt{s}\approx m)$. In equation 3.15 we have introduced the $\Delta\to N\pi$ energy-dependent decay width which is defined as

$$
\Gamma_\Delta(s) = \frac{g^2}{4\pi}\left(\frac{(\sqrt{s}+m_N)^2-m_\pi^2}{48s^{5/2}}\right)\lambda^{3/2}(s,m_N^2,m_\pi^2).
\tag{3.17}
$$

next, we define a renormalized propagator $iG_R^{\alpha\beta}$ as follows:

$$G^{\alpha\beta}(p) = (1-J_2)^{-1}[G_R^{\alpha\beta}(p)], \tag{3.18}$$

where the factor $(1-J_2)^{-1}$ can be absorbed as a component of the $\Delta$ wave function renormalization constant. Then after these approaches we obtain in terms of the old projectors,

$$G_R^{\alpha\beta}(p) = \frac{\tilde{m}+\not{p}}{\tilde{m}^2-p^2}(P^{3/2})^{\alpha\beta} - \frac{2}{\tilde{m}^2}(\tilde{m}+\not{p})(P_{11}^{1/2})^{\alpha\beta} - \frac{\sqrt{3}}{\tilde{m}}[(P_{21}^{1/2})^{\alpha\beta}+(P_{12}^{1/2})^{\alpha\beta}]. \tag{3.19}$$

A comparison of Eq. 3.19 and Eq. 3.2 show that the renormalized propagator has identical form to the bare propagator under the replacement $m \to \tilde{m} = m - i\Gamma_\Delta(s)/2$.

For the spin-$\frac{3}{2}$ resonances of negative parity (as the $N^*(1520)$ that has isospin $1/2$) we need to add $\gamma_5$ in Eq. 3.6 and now following the same procedure as above we get (we put $g = \frac{f_{\pi NR}}{m_\pi}$)

$$\Gamma_R(s)\times B_r \;=\; \frac{3\left(\frac{f_{\pi NR}}{m_\pi}\right)^2}{4\pi}\left(\frac{(\sqrt{s}-\pi m_N)^2-m_\pi^2}{48s^{5/2}}\right)\lambda^{\frac{3}{2}}(s,m_N^2,m_\pi^2), \tag{3.20}$$

where we have only a minus sign of difference regards the positive parity case and we have added a branching ratio factor $(B_r)$ since sometimes we have not a full decay into the $\pi N$ channel.

In the case of spin-$\frac{1}{2}$ resonances the unstable character introduced could also be introduced by the replacement

$$m_R \;\to\; m_R - i\frac{\Gamma_R(s)}{2}, \tag{3.21}$$

into the unperturbed propagator without changing its structure, and similar to the nucleon one. This width $\Gamma_R$ is obtained by considering the pion-nucleon loop contribution to the self energy [23] and reads

$$\Gamma_R(s)\times B_r \;=\; \frac{3}{4\pi}\left(\frac{f_{\pi NR}}{m_\pi}\right)^2(m_R+\pi m_N)^2\left(\frac{(\sqrt{s}-\pi m_N)^2-m_\pi^2}{4s^{3/2}}\right)\lambda^{\frac{1}{2}}(s,m_N^2,m_\pi^2),. \tag{3.22}$$

being $\pi = \pm$ the parity.

As mentioned above in this section, for the spin $3/2$ resonances (a similar discussion would be valid for the

$1/2$ case) when one introduces energy dependent widths in presence of radiative contributions, in order to fulfill the ward identities we need to add vertex corrections. Then the propagator given in Eq. 3.14 with the width in Eqs. 3.17 or Eqs. 3.20, or the usual spin $1/2$ propagator with 3.22, should be used including vertex corrections in the $\gamma R\gamma$ vertex. In order to overcome this problem it was adopted the complex mass scheme approach (CMS), what was introduced for another process previously [39] and we resume here.

If one analyzes the formal scattering T-matrix theory, see the last part in section 2, for the final $\pi N$ pair in both elastic scattering or pion photoproduction, or weak pion it is mandatory that the $R\pi N$ vertex should be also dressed as the propagator by the $\pi N$ rescattering through non-pole amplitudes ($K_{NP}$ in the first term of Eq. 2.32). This makes also the vertex $s-$dependent, or in other words we get an effective coupling constant $g(s) \equiv \frac{f_{\pi NR}(s)}{m_\pi}$, due to the decay mediated by the intermediate $\pi N-$propagator. The widths given in Eq. (3.17) or Eq. 3.20 grow with energy as $s^{3/2}$ while in the formal massless limit, the widths of the $W$ boson and $\rho$ meson grow as $s^{1/2}$ [39]. This different behavior can be easily understood because in the massless limit the decay width behaves as $\Gamma(s) = \tilde{g}^2 s^x$ ; therefore, for dimensionless couplings, $(W, \rho, x = 1/2)$, while for the $3/2-$resonance $x = 3/2$, because its coupling $g$ has (mass)$^{-1}$units.

Therefore, if we assume that the $R\pi N$ coupling behaves as $f_{\pi NR}(s) = \frac{\kappa f^0_{R\pi N}}{\sqrt{s}}$, being $f^0_{R\pi N}$ the bare $R\pi N$ coupling constant and $\kappa$ a constant of dimension MeV to fit, when the $R$ resonance is off its mass shell (now $\kappa$ is dimensionless and constant), we get that $\Gamma_R(s)$ grows with energy in a similar way as the $W$ boson and $\rho$ meson decay widths. We express as

$$\Gamma_R(s) \;=\; \frac{\sqrt{s}}{m_R}\Gamma_R^{CMS} = \left(1 + \frac{\sqrt{s} - m_R}{m_R}\right)\Gamma_R^{CMS},\; \Gamma_R^{CMS} = \frac{\kappa^2 (\frac{f^0_{\pi NR}}{m_\pi})^2}{192\pi} m_R. \tag{3.23}$$

In this case, we can remove the energy dependence in the complex mass introduced in Eq. 3.14 and Eq. 3.20 by using a proper redefinition of the mass and decay width (see [39]). Note, that $\Gamma_R^{CMS} = \Gamma_R(m_R)$, $m_R$ and $\kappa$ is a parameters to fit, and the propagator in this approach is obtained from Eq. 3.16 with the replacement $m_R \to m_R - i\Gamma_R^{CMS}/2$ and the Ward identity is satisfied, since we get a global factor $(1 + i\Gamma_R^{CMS}/m_R)^{-1}$ which is also present in the corrected radiative vertex in the same approach.

Another approach commonly used [23], is to fix $\sqrt{s} \approx m_R$ in Eqs. 3.14, (3.20) or (3.22) and to use the experimental values for $m_R$ and $\Gamma_R$ times $B_r$, and get $f_{R\pi N}$. We use this method to fix parameters in the resonances within the second region. Some another models, adopt the energy dependent width and is introduced through the replacement Eq. 3.21 but only in the denominator the propagator Eq. 3.16, which as mentioned above violates electromagnetic gauge invariance in the radiative case, without considering vertex corrections.

We hope that this violation will be of minor importance here since at least in the case of $3/2$ resonance the vector weak component is obtained from electromagnetic self-gauge invariant vertexes. We will consider this approach only for the sake of comparing with the mentioned works.

# Chapter 4

# NEUTRINO-NUCLEON SCATTERING WITH ONE-PION PRODUCTION. $\Delta$ RESONANCE and BACKGROUND

In this section we will show how to built the amplitude from the $\Delta$ resonance plus non resonant terms that are also important since can interfere with the resonant amplitude. Then, in the next chapters, we will repeat this scheme to include the second resonance region. In the early days before the discovery of quarks, hadrons, including pions and nucleons, were considered elementary and their dynamics was extensively studied through their reactions. Fig. 4.1 shows one example of such investigations. One immediately notes a rich structure in their behavior and many resonances have been identified. Today, they are recognized as superpositions of excited energy levels of quark composites. But discovery does not happen in a day. Given this kind of data, it is necessary to isolate levels, identify their properties and classify them to make a Mendeleev periodic table of hadrons. Namely, finding regularities among the many levels is the first step in reaching a deeper understanding of the structure. This is the process called hadron spectroscopy. Before launching a systematic investigation, we pick out the most conspicuous resonance at $m_{_\Delta} = 1232$ MeV, which used to be called the $P_{33}$ resonance. This is the main source of pions neutrino scattering since, when excited, it decays rough $99\%$ in $\pi N$ states.

Existence and properties of most $N$ and $\Delta$ resonances listed in the PDG ([46]) were derived from partial wave analyses of $\pi N$ elastic and charge exchange scattering data (Fig. 4.1). These resonances are also studied through Neutrino-Nucleon scattering, which is the spirit of this work. The Table 4.1 shows some properties of the $\Delta$ resonance and the resonances belonging to what we know as the second region of resonances and his representation in partial waves.

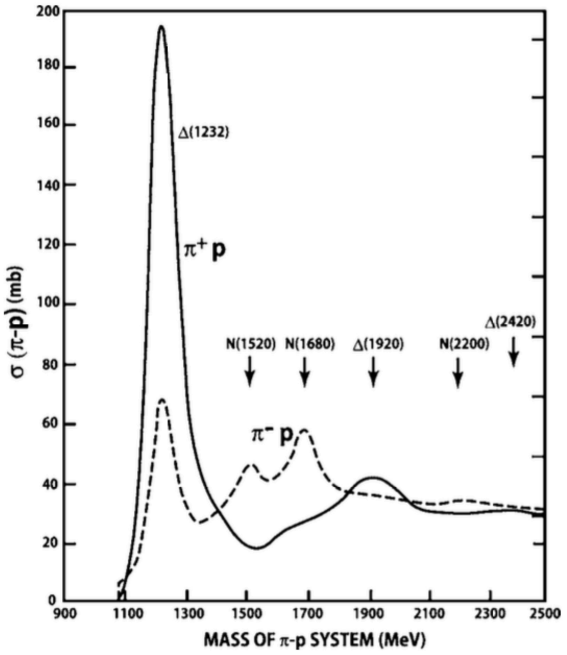


**Figure 4.1:** Resonance structure of low energy $\pi^{\pm} - p$ scattering data. $N$ for $I = 1/2$ and $\Delta = 3/2$ resonances. The number in parenthesis is its mass value. S, P, D, E, F, G and H stand for the $L = 0$, 1, 2, 3, 4 and 5 states. $D_{15}$ means $L = 2$, $I = 1/2$, $J = 5/2$. Some resonances are overlaps of two or more states. N(1680) may be an overlap of N(1675) $D_{15}$ and N(1680) $F_{15}$. Similarly, $\Delta(1930)$ $D_{35}$. N(2200) may also be an overlap of N(2190) $G_{17}$ and N(2200) $H_{19}$ [32].

We will use effective Lagrangian models taking into account the consistent hints mentioned in the previous chapters and apply the algebra of isospin symmetry to show the contribution for each channel [32]. In addition we must add other contributions to the background that do not come from resonance decay that could interfere with the resonance contribution at the amplitude level.

The CC interaction (we do not analyzed NC since the data is very scarce and by the reason mentioned in the introduction) between a neutrino and a hadron is obtained from the weak Lagrangian

$$\mathcal{L}_{CC} = \frac{-g}{2\sqrt{2}}\left(J^{\mu}_{lCC}W_{\mu} + J^{\mu}_{hCC}W_{\mu}\sqrt{2}\left(\boldsymbol{\tau} \text{ or } \boldsymbol{T}^{\dagger}\right)\cdot\boldsymbol{W}^{*} + h.c.\right), \tag{4.1}$$

where the isospin operators $\boldsymbol{\tau}$, $\boldsymbol{T}^{\dagger}$ and the isospin wave functions for the bosons $\boldsymbol{W}_{\pm}$ (equal to the pion ones) will be defined in the next section. The lepton and hadron charge current are

$$\begin{aligned} J^{\mu}_{lCC} &= \sum_{l}\bar{\psi}_{l}\gamma^{\mu}(1-\gamma_5)\psi_{\nu_l}, \\ J^{\mu}_{hCC} &= \bar{\psi}_{h'}(V^{\mu} - A^{\mu})\psi_{h}, \end{aligned}$$

| $\mathbf{\Delta(1232)}$ or $P_{33}$ $\quad I(J^P) = \frac{3}{2}\left(\frac{3}{2}^+\right)$ | |
|---|---|
| Breit-Wigner mass (mixed charges) $= 1230$ to $1234$ $(\approx 1232)$ MeV | |
| Breit-Wigner full width (mixed charges) $= 114$ to $120$ $(\approx 117)$ MeV | |
| $\Delta(1232)$ Decay modes | Fraction $(\Gamma_i/\Gamma)$ |
| $N\pi$ | $99,4\%$ |
| $N\gamma$ | $0,55-0,65\%$ |

| $\mathbf{N(1440)}$ or $P_{11}$ $\quad I(J^P) = \frac{1}{2}\left(\frac{1}{2}^+\right)$ | |
|---|---|
| Breit-Wigner mass (mixed charges) $= 1410$ to $1470$ $(\approx 1440)$ MeV | |
| Breit-Wigner full width (mixed charges) $= 250$ to $450$ $(\approx 350)$ MeV | |
| $N(1440)$ Decay modes | Fraction $(\Gamma_i/\Gamma)$ |
| $N\pi$ | $55-75\%$ |
| $N\eta$ | $< 1\%$ |
| $N\pi\pi$ | $17-50\%$ |

| $\mathbf{N(1520)}$ or $D_{13}$ $\quad I(J^P) = \frac{1}{2}\left(\frac{3}{2}^-\right)$ | |
|---|---|
| Breit-Wigner mass (mixed charges) $= 1510$ to $1520$ $(\approx 1515)$ MeV | |
| Breit-Wigner full width (mixed charges) $= 100$ to $120$ $(\approx 110)$ MeV | |
| $N(1520)$ Decay modes | Fraction $(\Gamma_i/\Gamma)$ |
| $N\pi$ | $55-65\%$ |
| $N\eta$ | $0,07-0,09\%$ |
| $N\pi\pi$ | $25-35\%$ |

| $\mathbf{N(1535)}$ or $S_{11}$ $\quad I(J^P) = \frac{1}{2}\left(\frac{1}{2}^-\right)$ | |
|---|---|
| Breit-Wigner mass (mixed charges) $= 1515$ to $1545$ $(\approx 1530)$ MeV | |
| Breit-Wigner full width (mixed charges) $= 125$ to $175$ $(\approx 150)$ MeV | |
| $N(1535)$ Decay modes | Fraction $(\Gamma_i/\Gamma)$ |
| $N\pi$ | $32-52\%$ |
| $N\eta$ | $30-55\%$ |
| $N\pi\pi$ | $3-14\%$ |

**Table 4.1:** Baryon resonances and main decay channels of $\Delta$ and second region resonances.

where $\psi_h$ represents the field of the incoming nucleon and $\bar{\psi}'_h$ represents the outgoing hadron, which can be a fermion with spin 1/2 or 3/2 In this work we assume the convention of $q = p_l - p_\nu$ outgoing from the hadronic vertex. It is well know that the baryonic currents $J^\lambda_{hi}$ have a vector-axial structure ($J^\lambda_{hi} \equiv V^\lambda_i - A^\lambda_i$). In term of of the vector current, the electromagnetic one is written as $J^\lambda_{\text{elec}} = V^\lambda_{\text{isoscalar}} + V^\lambda_3$ ($V^\lambda_3 = \tau_3 \frac{\gamma^\lambda}{2}$ for a nucleon or $V^\lambda T^\dagger_3$ for the $\Delta$) and the weak vector CC ($\tau_3, T^\dagger_3 \to \tau_\pm, T^\dagger_\pm$) as $V^\lambda_\pm \equiv \mp(V^\lambda_1 \pm iV^\lambda_2) = \sqrt{2}\,\boldsymbol{V}\cdot\boldsymbol{W}_\pm$.

The total cross section for weak production of single pions in terms of the $\nu N$ center mass (CM) variables

will be calculated from

$$\sigma(E_\nu^{\mathsf{CM}}) = \frac{m_\nu m_N^2}{(2\pi)^4 E_\nu^{\mathsf{CM}}\sqrt{s}} \int_{E_\mu^-}^{E_\mu^+} dE_\mu^{\mathsf{CM}} \int_{E_\pi^-}^{E_\pi^+} dE_\pi^{\mathsf{CM}} \int_{-1}^{+1} d\cos\theta \int_0^{2\pi} d\eta \frac{1}{16} \sum_{\text{spin}} |\mathcal{M}|^2, \tag{4.2}$$

where $\sqrt{s} = E_\nu^{\mathsf{CM}} + E_N^{\mathsf{CM}}$, the angular variable come from the integration elements $d\omega_\mu = d\cos\theta d\phi$ and $d\omega_\pi = d\xi d\eta$ ($d\phi$ integrations gives a factor $2\pi$ and $\cos\xi$ is fixed by energy conservation) and

$$\begin{aligned} E_\mu^- &= m_\mu, \qquad\qquad E_\mu^+ = \frac{s + m_\mu^2 - (m_N + m_\pi)^2}{2(E_\nu^{\mathsf{CM}} + E_N^{\mathsf{CM}})}, \\ E_\pi^\pm &= \frac{(\sqrt{2} - E_\mu^{\mathsf{CM}})(s - 2\sqrt{s}E_\mu^{\mathsf{CM}} - \Delta^2) \pm A\sqrt{(E_\mu^{\mathsf{CM}})^2 - m_\mu^2}}{2(s - 2\sqrt{s}E_\mu^{\mathsf{CM}} + m_\mu^2)}, \end{aligned} \tag{4.3}$$

with $A = \sqrt{(s - 2\sqrt{s}E_\mu^{\mathsf{CM}} - \Delta^2)^2 - 4m_\pi^2(s - 2\sqrt{s}E_\mu^{\mathsf{CM}} + m_\mu^2)}$, $\Delta^2 = m_N^2 - m_\mu^2 - m_\pi^2$. The neutrino energy CM energy is related with the laboratory one as $E_\nu^{\mathsf{CM}} = \frac{m_N E_\nu^{\mathsf{Lab}}}{\sqrt{2E_\nu^{\mathsf{Lab}} m_N + m_N^2}}$.

The differential cross section is computed from [47]

$$\frac{d\sigma}{dQ^2} = \frac{m_\mu m_N^2}{2(2\pi)^4 (E_\nu^{\mathsf{CM}})^2 \sqrt{s}} \int_{E_\mu^-}^{E_\mu^+} \frac{dE_\mu^{\mathsf{CM}}}{\sqrt{(E_\mu^{\mathsf{CM}}) - m_\mu^2}} \int_{E_\pi^-}^{E_\pi^+} dE_\pi^{\mathsf{CM}} \int_0^{2\pi} d\eta \frac{1}{16} \sum_{\text{spin}} |\mathcal{M}|^2 \tag{4.4}$$

where now $E_\mu^- = (Q^2 + m_\mu^2)/4E_\nu^{\mathsf{CM}} + m_\mu^2 E_\nu^{\mathsf{CM}}/(Q^2 + m_\mu^2)$ for a fixed value of $Q^2$. Finally, in order to compare with the experimental results, we calculated the neutrinos flux average cross section

$$\frac{d\langle\sigma\rangle}{dQ^2} = \frac{\int_{E_\nu^{\min}}^{E_\nu^{\max}} \frac{d\sigma(E_\nu)}{dQ^2} \phi(E_\nu) dE_\nu}{\int_{E_\nu^{\min}}^{E_\nu^{\max}} \phi(E_\nu) dE_\nu}, \tag{4.5}$$

where $\phi(E_\nu)$ is the flux of neutrinos corresponding to each experiment.

## 4.1 $\Delta(1232)$ RESONANCE

Several models have been developed to evaluate the $\Delta$ contribution to the corresponding cross section for the $1\pi-$production in neutrino$-$nucleon scattering. Some works treat inconsistently the vertex and the propagator of the $\Delta$ resonance, the free lagrangian density $\mathcal{L}(A)$ (kinetic term), $\mathcal{L}_{\pi N\Delta}(A,Z),\ \mathcal{L}_{WN\Delta}(A,Z)$ are invariant under the contact transformations on the field $\Psi^{\mu}_{\Delta}$ , and the amplitude built with them should be $A-$independent.

The difference between all models stems mainly from the treatment of the interaction vertexes and the propagator used to describe the $\Delta$ resonance and from the consideration (or not) of the background and it's interference with the resonant contribution. Here, we propose an effective Lagrangian model for the calculation of one pion production cross section. The formalism used is fully consistent from the point of view of contact transformations, and extends to weak pion production case the model used to treat elastic and radiative $\pi^{+}p$ scattering and pion-photoproduction. The $N$, $\Delta$, $\pi$, $\rho$, and $\omega$ degree of freedom and their interactions are introduced by preserving covariance and electromagnetic gauge invariance when the finite width of the $\Delta$ resonance is considered. We will adopt $Z=1/2$ for the interactions terms and the reduced $A-$independent Feynman rules for propagators and vertexes, in this way as explained in Chapter 1 there is not trace of $A$ in the amplitude. First of all we review the propagator and Lagrangians from where vertexes are obtained.

The $\Delta$ propagator is given by

$$G_{\alpha\beta}(p)=\frac{\not{p}+m_{\Delta}}{p^2-m_{\Delta}^2}\left\{-g_{\alpha\beta}+\frac{1}{3}\gamma_{\alpha}\gamma_{\beta}+\frac{1}{3m_{\Delta}}(\gamma_{\alpha}p_{\beta}-\gamma_{\beta}p_{\alpha})+\frac{2}{3m_{\Delta}^2}p_{\alpha}p_{\beta}-\right.$$
$$\left.\frac{2(p^2-m_{\Delta}^2)}{3m_{\Delta}^2}[\gamma_{\alpha}p_{\beta}-\gamma_{\beta}p_{\alpha}-(\not{p}+m_{\Delta})\gamma_{\alpha}\gamma_{\beta}]\right\}, \tag{4.6}$$

where the unstable character of the $\Delta$ will be introduced by the replacement [43]

$$m_{\Delta}\rightarrow m_{\Delta}-i\frac{\Gamma_{\Delta}}{2} \tag{4.7}$$

what is called CMS ($\Gamma_{\Delta}\equiv\Gamma_{\Delta}^{CMS}$) and is an approximation of the perturbed propagator developed in the previous section, valid for the resonance region. For the strong $\Delta\rightarrow\pi N$ (or $\Delta\pi N$) interaction Lagrangians $(\mathcal{L}_{\Delta\pi N})$ we have (with disexcitement and excitation $\Delta$ vertex shown)

$$\mathcal{L}_{\Delta\pi N}(x) \;=\; \frac{f_{\Delta\pi N}}{m_{\pi}}\bar{\psi}\partial\mathbf{\Phi}(x)^{\mu *}\cdot\boldsymbol{T}\Psi_{\mu}(x)+\frac{f_{\Delta\pi N}}{m_{\pi}}\bar{\Psi}_{\mu}(x)\bar{\psi}\partial\mathbf{\Phi}^{\mu}(x)\cdot\boldsymbol{T}^{\dagger}\psi(x), \tag{4.8}$$

where $\mathbf{T}^\dagger$ is the $N \to \Delta$ isospin excitation operator. This Lagrangian enables definition of the $\Delta \to \pi N$ vertex

$$\hat{\Gamma}_{\Delta\pi N} = - \frac{f_{\pi N\Delta}}{m_\pi} k^\mu \left( \chi^\dagger \boldsymbol{\phi}^* \cdot \boldsymbol{T} \Delta \right) \tag{4.9}$$

where we use the prescription $\hat{\Gamma} = i\mathcal{L}$ , $\partial^\mu \phi = -ik^\mu \phi$ and $i \times propagator$, in the amplitudes. Note the isospin wave functions

$$\chi(1/2) = \begin{pmatrix} 1 \\ 0 \end{pmatrix}, \quad \chi(-1/2) = \begin{pmatrix} 0 \\ 1 \end{pmatrix}$$

$$\boldsymbol{\phi}_{\pi^-} = \frac{1}{\sqrt{2}} \begin{pmatrix} 1 & -i & 0 \end{pmatrix}, \quad \boldsymbol{\phi}_{\pi^+} = \frac{-1}{\sqrt{2}} \begin{pmatrix} 1 & i & 0 \end{pmatrix}, \quad \boldsymbol{\phi}_{\pi^0} = \begin{pmatrix} 0 & 0 & 1 \end{pmatrix},$$

$$\Delta(3/2) = \begin{pmatrix} 1 \\ 0 \\ 0 \\ 0 \end{pmatrix}, \Delta(1/2) = \begin{pmatrix} 0 \\ 1 \\ 0 \\ 0 \end{pmatrix} \quad , \quad \Delta(-1/2) = \begin{pmatrix} 0 \\ 0 \\ 1 \\ 0 \end{pmatrix}, \Delta(-3/2) = \begin{pmatrix} 0 \\ 0 \\ 0 \\ 1 \end{pmatrix}$$

and the operators (shown in Appendix C) $\boldsymbol{\tau}$ ( or $\boldsymbol{T}$) $= (\tau_x, \tau_y, \tau_z)$ and $\tau_\pm = \mp \frac{1}{\sqrt{2}} (\tau_x \pm \tau_y) = \boldsymbol{\tau} \cdot \boldsymbol{\phi}_{\pi^\pm}$. The weak interaction Lagrangian $\hat{\mathcal{L}}_{WN\Delta}$ (compatible with the free $\hat{\mathcal{L}}_\Delta$) and strong interacting Lagrangian $\hat{\mathcal{L}}_{\Delta\pi N}$ that make possible also a definition of the weak $\Delta$ excitation $\mathcal{W}^{\beta\lambda}$ vertex, is [43, 33]

$$\hat{\mathcal{L}}_{WN\Delta}(x) = \bar{\Psi}^\mu(x) R_{\mu\alpha}(A) R^{-1\alpha\beta} (1/2(1 - 6Z/(1+4Z))(\hat{W}^V_\beta + \hat{W}^A_\beta)(\boldsymbol{T}^\dagger \cdot \boldsymbol{W}^*)\psi(x) + \text{h.c.}, \tag{4.10}$$

with the same reduced $\mathcal{W}^V_{\mu\nu}$ obtained vector vertex $\Delta-$production as in pion photo- [43] and electroproduction [49] reads

$$\hat{\mathcal{W}}^V_{\mu\nu}(p_\Delta, q, p) = \sqrt{2}[(G_M(Q^2) - G_E(Q^2))K^M_{\nu\mu} + G_E(Q^2)K^E_{\nu\mu} + G_C(Q^2)K^C_{\nu\mu}]\Delta^* \boldsymbol{W}^* \cdot \boldsymbol{T}^\dagger \psi, \tag{4.11}$$

being $Q^2 = -q^2 = -m_\ell + 2E_\ell E_\nu (p_\ell / E_\ell \cos\theta_{\nu\ell}) > 0$ and where the $\sqrt{2}$ factor from $\sqrt{2}\boldsymbol{T} \cdot \boldsymbol{W}$ was shifted into

the vertex $\hat{\mathcal{W}}^V$, being $K^M_{\nu\mu}$, $K^E_{\nu\mu}$, $K^C_{\nu\mu}$ are defined as [48]

$$
\begin{aligned}
K^M_{\nu\mu} &= -K^M(Q^2)\varepsilon_{\nu\mu\alpha\beta}\frac{(p+p_\Delta)^\alpha}{2}q^\beta,\; K^M(Q^2) = \frac{3(m_N+m_\Delta)}{2m_N((m_N+m_\Delta)^2+Q^2)} \\
K^E_{\nu\mu} &= \frac{4K^M(Q^2)}{((m_\Delta-m_N)^2+Q^2)}\varepsilon_{\nu\lambda\alpha\beta}\frac{(p+p_\Delta)^\alpha}{2}q^\beta\epsilon^\lambda_{\mu\gamma\delta}p^\gamma_\Delta q^\delta i\gamma_5 \\
K^C_{\nu\mu} &= \frac{2K^M(Q^2)}{((m_\Delta-m_N)^2+Q^2)}q_\nu[Q^2\frac{(p+p_\Delta)_\mu}{2}+q\cdot\frac{(p+p_\Delta)}{2}q_\mu]i\gamma_5.
\end{aligned}
\tag{4.12}
$$

For the reduced axial contribution we use the model given in Refs. [49, 50], which is compatible with $\hat{\mathcal{W}}^V_{\nu\mu}$ (it could be, in principle, obtained by using $-\hat{\mathcal{W}}^V_{\nu\mu}\gamma_5$) and reads

$$
\begin{aligned}
\hat{\mathcal{W}}^A_{\nu\mu}(p_\Delta,q,p) = -i\Bigg[ & -D_1(Q^2)g_{\nu\mu}+\frac{D_2(Q^2)}{m_N^2}(p+p_\Delta)^\alpha(g_{\nu\mu}q_\alpha-q_\nu g_{\alpha\nu})- \\
& \frac{D_3(Q^2)}{m_N^2}p_\nu q_\mu + i\frac{D_4(Q^2)}{m_N^2}\varepsilon_{\mu\nu\alpha\beta}(p+p_\Delta)^\alpha q^\beta\gamma_5\Bigg]\Delta^*\boldsymbol{W}^*\boldsymbol{T}^\dagger\psi,
\end{aligned}
\tag{4.13}
$$

here for the $\Delta$ resonance the $\sqrt{2}$ is incorporated in the $D_i(0)$ form factors. The $G_i(Q^2)$ and $D_i(Q^2)$ form factors will also be described below. Usually, some authors drop out the second term within square brackets of the $\Delta$ propagator from Eq. (4.6), this is usually wrong named Rarita- Schwinger propagator. This procedure introduces inconsistencies since this propagator corresponds to $A=-1$ , but we need the *full* propagator together with the above $\hat{\Gamma}_{\Delta\pi N}, \hat{\mathcal{W}}_{\nu\mu}$ reduced vertexes.

In this chapter we analyze as a first step the charged current (CC) modes of three process

$$
\nu p \to \mu^- p\pi^+, \quad \nu n \to \mu^- n\pi^+, \quad \nu n \to \mu^- p\pi^0,
\tag{4.14}
$$

then we will extend to the antineutrinos in the results. The tree-level amplitudes are shown schematically in Fig. 4.2. Clearly, all the Feynman graphs do not necessarily contribute to each of the process in Eq. 4.14. We have a background (B) contribution built from nucleon Born terms (Fig. 4.2(a)-(b)), the meson exchange amplitudes (Figs. 4.2(c)-(f))and the $\Delta$-crossed term (Fig. 4.2(g)); the genuine resonant contribution (R) coming from the $\Delta$-pole amplitude is shown in Fig. 4.2(h). The sum of all these terms give rise to the total amplitude which can

be separated into a background and a resonant contribution as

$$\mathcal{M} = \mathcal{M}_{\mathsf{B}} + \mathcal{M}_{\mathsf{R}}$$

where using the Lagrangians and propagators for resonant and non resonant contributions plus the Eq. 4.1 lead to

$$\mathcal{M}_i = \frac{ig^2}{\left(2\sqrt{2}\right)^2}\bar{u}(p_\mu)(-)i\gamma^\lambda(1-\gamma_5)u(p_\nu)\frac{ig_{\lambda\lambda'}}{m_W^2}V_{ud}\bar{u}(p')O_i^{\lambda'}(p,p',q)u(p), \quad i = \mathsf{B},\mathsf{R}, \tag{4.15}$$

being $\frac{g_{\lambda\lambda'}}{m_W}$ is the $W$ boson propagator in the high mass limit, where $\frac{g^2}{\left(2\sqrt{2}\right)^2} = \frac{G_F^2}{\sqrt{2}}$ ,spin and isospin indexes are omitted, $G_F$ =1.16637$\times 10^{-5}$ GeV$^{-2}$, $|V_{ud}|$ =0.9740, and the 4-momenta are defined as

$$p = (E_N, \mathbf{p}), \quad p_\nu = (E_\nu, \mathbf{p}_\nu), \quad p_\mu = (E_\mu, \mathbf{p}_\mu), \quad \mathsf{k} = (E_\pi, \mathbf{k}), \quad p' = (E_{N'}, \mathbf{p}'),$$

with $E_i = \sqrt{|\mathbf{p}_i|^2 + m_i^2}$($|\mathbf{v}_i| = \frac{|\mathbf{p}_i|}{E_i}$ and we set $m_\nu = 0$).

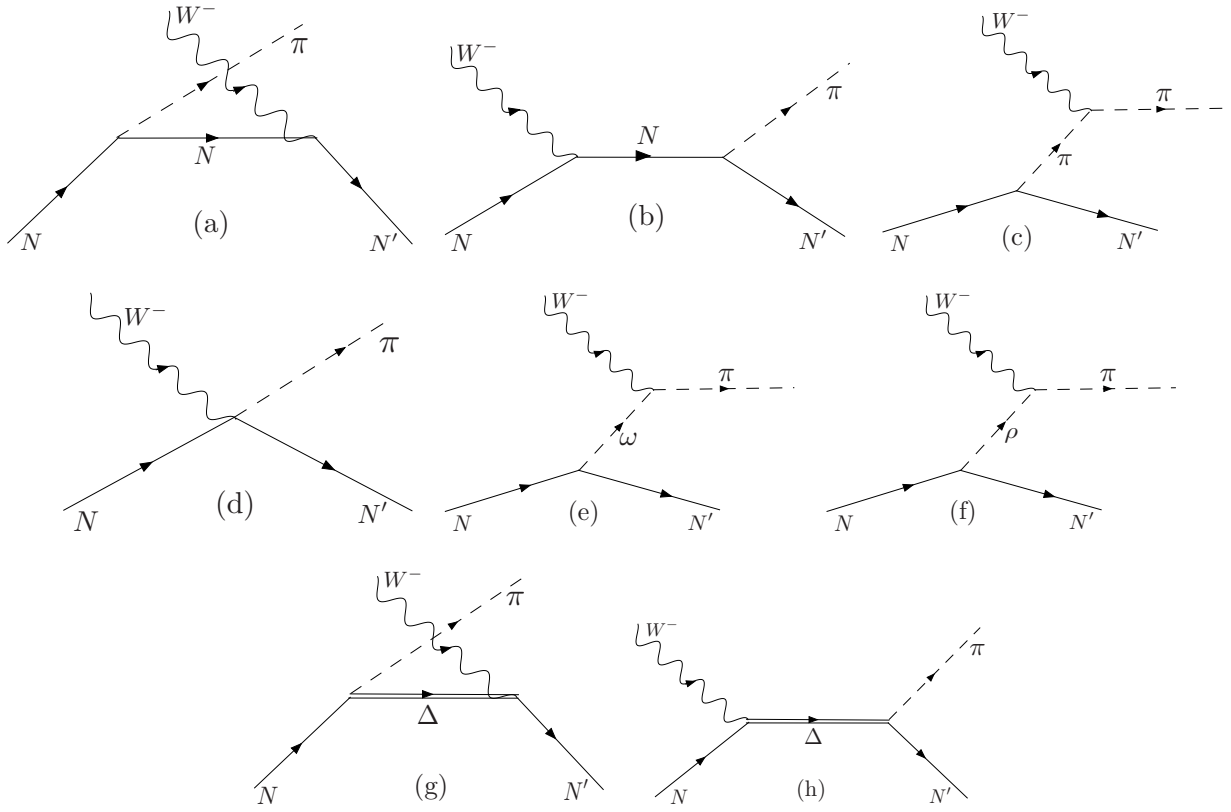


**Figure 4.2:** Contributions to the scattering amplitude for the process $\nu N \to \mu N'\pi$. Fig (a)-(f) is the background (B) contribution. Fig (h) is a Resonantcontribution (R)

The conserved vector current (CVC) hypothesis allow to relate the isovector pieces of these both vector currents. In the same way it is also possible to get information on the effective $WM \to \pi'$ (with $M \equiv \pi, \omega$) and the contact $NW\pi \to N'\pi'$ vector vertexes. Here the FF are again obtained assuming CVC from the electromagnetic $\gamma M \to \pi'$and $N\gamma\pi \to N'\pi'$ vertexes obtained through the corresponding effective interaction Lagrangians, making the replacement $(\mathbf{\Phi}_\pi^{'*} \times \mathbf{\Phi}_\pi)_3 \to \mp[(\mathbf{\Phi}_\pi^{'*} \times \mathbf{\Phi}_\pi)_1 \pm i(\mathbf{\Phi}^{'*} \times \mathbf{\Phi}_\pi)_2] = \sqrt{2}(\mathbf{\Phi}_\pi^{'*} \times \mathbf{\Phi}_\pi)\pm = \sqrt{2}(\mathbf{\Phi}_\pi^{'*} \times \mathbf{\Phi}_\pi) \cdot \boldsymbol{W}\pm$ (the same is valid for the contact vertex changing $\Phi_\pi \to \tau$) for$M = \pi$ or $\Phi'_{\pi_3} \to \sqrt{2}\mathbf{\Phi}'_\pi \cdot \boldsymbol{W}\pm$ for $M = \omega$. In this way, the Born and $\omega$-exchange contributions ($\rho$-exchange contributions do not contribute to $V$ since the $\rho - \pi$ is isoscalar) can be obtained from the usual strong [51] ($\mathcal{L}_{NN\omega}(x)$ is built from $\mathcal{L}_{NN\rho}(x)$ change $\rho_\mu(x) \to \omega_\mu(x)$ and $\tau \to 1$) and electromagnetic interaction Lagrangians [33, 52]. For the axial currents we adopt the Lagrangians of Refs. [49, 50] based on standard effective methods and spin-parity arguments. These Lagrangians and related propagators are shown in Appendix D. We get

$$
\begin{aligned}
O_{\mathrm{B}}^{\lambda}(p,p',q) = -i\frac{1}{2}\left[F_1^V(Q^2)\gamma^\lambda - i\frac{F_2^V(Q^2)}{2m_N}\sigma^{\lambda\nu}q_\nu - F^A(Q^2)\gamma^\lambda\gamma_5\right] i\frac{\not p' + \not q + m_N}{(p'+q)^2 - m_N}\frac{g_{\pi NN}}{2m_N}\times \\
\gamma_5(\not p - \not p' - \not q)\sqrt{2}\mathcal{T}_1(m_t, m_{t'}) + \frac{g_{\pi NN}}{2m_N}\gamma_5(\not p - \not p' - \not q) i\frac{\not p - \not q + m_N}{(p-q)^2 - m_N^2} \\
(-i)\frac{1}{2}\left[F_1^V(Q^2)\gamma^\lambda - i\frac{F_2^V(Q^2)}{2m_N}\sigma^{\lambda\nu}q_\nu - F^A(Q^2)\gamma^\lambda\gamma_5\right]\sqrt{2}\mathcal{T}_2(m_t, m_{t'}) - iF_1^V(Q^2)(2p - 2p' - q)^\lambda \times \\
\frac{i}{(p-p')^2 - m_\pi^2}\frac{g_{\pi NN}}{2m_N}\gamma_5(\not p - \not p')\sqrt{2}\mathcal{T}_3(m_t, m_{t'}) + \frac{g_{\pi NN}}{2m_N}F_1^V(Q^2)\gamma_5\gamma^\lambda\sqrt{2}\mathcal{T}_4(m_t, m_{t'}) \\
+ i\frac{g_{\omega\pi V}}{m_\pi}F_1^V(Q^2)\epsilon^{\lambda\alpha\beta\delta}q_\alpha(p-p')_\beta i\frac{-g_{\delta\epsilon}}{(p-p')^2 - m_\omega^2}(-i)\frac{g_{\omega NN}}{2}\left[\gamma^\varepsilon - i\frac{\kappa_\omega}{2m_N}\sigma^{\varepsilon\kappa}(p-p')_\kappa\right]\times \\
\sqrt{2}\mathcal{T}_5(m_t, m_{t'}) + f_{\rho\pi A}F^A(Q^2) i\frac{-g^{\lambda\mu}}{(p-p')^2 - m_\rho^2}(-i)\frac{g_{\rho NN}}{2}\left[\gamma_\mu - i\frac{\kappa_\rho}{2m_N}\sigma_{\mu\kappa}(p-p')^\kappa\right]\sqrt{2}\mathcal{T}_6(m_t, m_{t'}) \\
+ (-)\overline{\hat{\mathcal{W}}^{\lambda\alpha}(p_\Delta, -q, p')} iG_{\alpha\beta}(p_\Delta = p' + q)(-)\frac{f_{\pi N\Delta}}{m_\pi}(p - p' - q)^\beta\mathcal{T}_7(m_t, m_{t'}),
\end{aligned}
\tag{4.16}
$$

$$
O_{\mathrm{R}}^{\lambda}(p,p',q) = -\frac{f_{\pi N\Delta}}{m_\pi}(p - p' - q)^\alpha iG_{\alpha\beta}(p_\Delta = p - q)\hat{\mathcal{W}}^{\beta\lambda}(p_\Delta, q, p)\mathcal{T}_8(m_t, m_{t'}),
\tag{4.17}
$$

where $\overline{\hat{\mathcal{W}}} = \gamma_0\hat{\mathcal{W}}^\dagger\gamma_0$ and note that for the $\Delta \to \pi N$ vertex $-\gamma_0(-\mathrm{k}_\mu)^\dagger\gamma_0 = \mathrm{k}_\mu$, where $q = p_\mu - p_\nu$ is the momentum transferred by leptons and $Q^2 \equiv -q^2$. In order to built the cross vertexes we use the rule $\Gamma^c_{\mu\nu} = -\gamma_0\Gamma^\dagger_{\nu\mu}(-q)\gamma_0$, that differs from other works since we use the convention $i\mathcal{L}$ and not $\mathcal{L}$ to get the vertexes. Note that in the cross term in spite of using the h.c. term the mesons or bosons are still outgoing, for that we

need to make $-q$. Here we have defined the isospin matrix elements for each channel in Eq. 4.14 respectively

$$\begin{aligned}
\mathcal{T}_1(m_t,m_{t'}) &= \chi^\dagger(m_{t'})(\boldsymbol{\tau}\cdot\mathbf{W}^*)(\boldsymbol{\tau}\cdot\boldsymbol{\Phi}^*_\pi)\chi(m_t) = -2,0,-\sqrt{2}\\
\mathcal{T}_2(m_t,m_{t'}) &= \chi^\dagger(m_{t'})(\boldsymbol{\tau}\cdot\boldsymbol{\Phi}^*_\pi)(\boldsymbol{\tau}\cdot\mathbf{W}^*)\chi(m_t) = 0,-2,\sqrt{2}\\
\mathcal{T}_3(m_t,m_{t'}) &= -i\chi^\dagger(m_{t'})[(\boldsymbol{\Phi}^*_\pi\times\boldsymbol{\Phi}_{\pi'})\cdot\mathbf{W}^*](\boldsymbol{\tau}\cdot\boldsymbol{\Phi}^*_{\pi'})\chi(m_{t'}) = 1,-1,\sqrt{2}\\
\mathcal{T}_4(m_t,m_{t'}) &= i\chi^\dagger(m_{t'})[(\boldsymbol{\Phi}^*_\pi\times\boldsymbol{\tau})\cdot\mathbf{W}^*]\chi(m_t) = -1,1,-\sqrt{2}\\
\mathcal{T}_5(m_t,m_{t'}) &= \chi^\dagger(m_{t'})(\boldsymbol{\Phi}^*_\pi\cdot\mathbf{W}^*)\chi(m_t) = -1,-1,0\\
\mathcal{T}_6(m_t,m_{t'}) &= i\chi^\dagger(m_{t'})[(\boldsymbol{\Phi}^*_\pi\times\boldsymbol{\rho})\cdot\mathbf{W}^*](\boldsymbol{\tau}\cdot\boldsymbol{\rho}^*)\chi(m_t) = -1,1,-\sqrt{2}\\
\mathcal{T}_7(m_t,m_{t'}) &= \chi^\dagger(m_{t'})(\mathbf{T}\cdot\mathbf{W}^*)(\mathbf{T}^\dagger\cdot\boldsymbol{\Phi}^*_\pi)\chi(m_t) = -1/3,-1,\sqrt{2}/3\\
\mathcal{T}_8(m_t,m_{t'}) &= \chi^\dagger(m_{t'})(\mathbf{T}\cdot\boldsymbol{\Phi}^*_\pi)(\mathbf{T}^\dagger\cdot\mathbf{W}^*)\chi(m_t) = -1,-1/3,-\sqrt{2}/3
\end{aligned} \tag{4.18}$$

whit $m_t$ and $m_{t'}$ being the isospin projections of the initial and final state nucleons, respectively and the isospin 1/2 to isospin 3/2 transition operator $\mathbf{T}$ is a 2 $\times$ 4 matrix defined by the matrix element of its components $\mathbf{T}_\lambda$ =( $-1$, 0, $+1$) (see appendix C). The $N \to$ B weak vector currents (B = $N'$ or $\Delta$) above are obtained from electromagnetic transitions in photo-production ($\gamma N \to B$), by assuming CVC hypothesis. In addition to the terms shown in the Eq. (4.16), we include the so-called pion-pole amplitudes (i.e., an intermediate pion is introduced in the $W$ propagation line).

The coupling constant we use are the values from pion-nucleon scattering and analysis of photoproduction and electroproduction of pions. For the strong couplings of nucleons we take $g^2_{\pi NN}/4\pi = 14$,(note that $\frac{f}{m_\pi} = \frac{g}{2m_N}$) $g^2_{\rho NN}/4\pi = 2.9$, $\kappa_\rho = 3.7$, $g_{\omega NN} = 3g_{\rho NN}$ and $\kappa_\omega = -0.12$ [51] with the usually adopted masses for involved hadrons [27]. The coupling of nucleon $\rho$ and $\omega$ mesons were obtained by assuming the vector dominance model. For the $\Delta$ mass width and $\pi N$ coupling constant we assume consistently values obtained previously from fitting to the $\pi^+ p$ scattering data [51], namely: $f^2_{N\pi\Delta}/4\pi = 0.317 \pm 0.003$, $m_\Delta = 1211.7 \pm 0.4$ MeV and $\Gamma_\Delta = 92.2 \pm 0.4$ MeV.

In the weak sector the vector coupling constant are fixed by assuming the CVC hypothesis bot for B an R amplitudes. As usual, for the axial currents we exploit the PCAC hypothesis and Golderberg-Treiman relations. For the nucleon Born and meson exchange contributions we adopt $g_V = 1$, $g_{\omega\pi\gamma} = g_{\omega\pi V} = 0.324e$ [33], while for the axial couplings we assume $g_A = 1.26$ (PCAC values) and $f_{\rho\pi A} = \frac{m^2_\rho}{(93\text{MeV})g_{\rho NN}}$ [49]. For the FF we adopt

the usual Sachs dipole model for the vector current [49, 53] and also a dipole FF for the axial part [49]:

$$F_1^V(Q^2) = \frac{g_V}{1+t}\left[G_E^p(Q^2) - G_E^n(Q^2) + t(G_M^p(Q^2) - G_M^n(Q^2))\right],$$
$$F_2^V(Q^2) = \frac{g_V}{1+t}\left[G_M^p(Q^2) - G_M^n(Q^2) - (G_E^p(Q^2) - G_E^n(Q^2))\right],$$
$$F^A(Q^2) = \frac{g_A}{(1+Q^2/M_A^2)^2}, \quad M_A = 1.032\text{GeV}, \tag{4.19}$$

where $t = Q^2/4m_N^2$ and

$$G_E^p(Q^2) = \frac{1}{1+\kappa_p}G_M^p(Q^2) = \frac{1}{\kappa_n}G_M^n(Q^2) = \frac{1}{1+Q^2/M_V^2}, \quad G_E^n(Q^2) = 0,$$

with $M_V^2 = 0.71$ GeV$^2$, $\kappa_p = 1.79$, $\kappa_n = -1.91$. In the case of the contribution involving the $W\pi\pi$ vertex (third term in Eq. 4.16) we adopt the same $F_V^1(Q^2)$ as in the other Born terms (first, second and fourth terms in Eq. 4.16) since these together should form a gauge invariant amplitude in the electromagnetic radiative case.

For the vector $\Delta$ contribution to the B and R amplitude we use the effective (empirical) values $G_M(0) = 2.97$, $G_E(0) = 0.055$ and $G_C(0) = \frac{2m_\Delta}{m_N - m_\Delta}G_E(0)$ fixed from photo and electroproduction reactions [33, 54]. We call these "effective" values, as discussed in Ref. [33], because they correspond to the bare ones $G_i^0(0)$ (usually related with QM) *renormalized* through the decay of a $\pi N$ state coming from the B amplitude into a $\Delta$ (FSI). In Ref. [33] we also get the bare $G_{E,M}^0(0)$ values by introducing dynamically the FSI by an explicit evaluation of the rescatering amplitudes and show that the effective values, which are obtained through a fitting procedure, can be in fact interpreted as the "dressed" ones. For the FF we adopt

$$G_i(Q^2) = G_i(0)(1 - Q^2/M_V^2)^{-2}(1 + aQ^2)e^{-bQ^2}, \tag{4.20}$$

with $a = 0.154/(\text{GeV}/c)^2$ and $b = 0.166/(\text{GeV}/c)^2$, for $i = M$, $E$, $C$, which corresponds also to Sachs dipole model times a corrections factor already used in electroproduction calculations [54]. The axial FF at $Q^2 = 0$, $F_\Delta(0) \equiv D_i(0)$, $i = 1,4$, are obtained by comparing the non-relativistic limit of $\bar{u}_\Delta^\nu \mathcal{W}_{\nu\mu}^A u$ in the $\Delta$ rest frame ($p_\Delta = (m_\Delta, \mathbf{0})$, $p = (E_N(\mathbf{q}), -\mathbf{q})$ with the non-relativistic QM [54, 50]. $D_4(Q^2) = 0$ since we will not take into account the contribution of the $\Delta$ deformation to the axial current. The $Q^2$ dependence of $D_i$ is taken to be the same as in vector case with a different parameter in the dipole factor, i.e.

$$D_i(Q^2) \quad = \quad D_i(0)F(Q^2), \text{ for } i=1,2, \quad ,D_3(Q^2) = D_3(0)F(Q^2)\frac{m_N^2}{Q^2+M_\pi^2}, \tag{4.21}$$

with $M_A = 1.02$ GeV and $F(Q^2) = (1+Q^2/M_A^2)^{-2}(1+aQ^2)e^{-bQ^2}$. Here

$$D_1(0) = \frac{6g_A}{5}\frac{m_N+m_\Delta}{2m_N F(-(m_\Delta-m_N)^2)}, D_2(0) = -D_1(0)\frac{m_N^2}{(m_N+m_\Delta)^2}, D_3(0) = D_1(0)\frac{2m_N^3}{(m_N+m_\Delta)m_\pi^2},$$

where $F(-(m_\Delta-m_N)^2)$ in the denominator comes from the fact that we scale $D_i(Q^2=-q^2)$ from the time-like point $q_0^2=(m_\Delta-m_N)^2$ to $q^2=0$ through $F(Q^2)$. Then, as in the case of pion photoproduction , we will consider $D_1(0)$ as a free (effective or empirical) parameter to be fitted from the experimental data for $d\sigma/dQ^2$ and including the final state interactions (FSI) effects. From this fit we get $D_1(0)=2.35$, $C_5=1.35$ with $\chi^2/dof = 0.71$, and results are shown with full lines in the Fig. (2) of Ref. [47].

# Chapter 5

# SECOND REGION OF RESONANCES

In order to investigate the reanalyzed data of [19] for ANL and BNL, we need to go to energies around 1.7 GeV (they use this cutoff) and thus to extend the model that assumes only the $\Delta$ as in the previous chapter. For this reason we will included the so called second resonance region that encloses the $N^*(1440)$,$N^*(1535)$ and $N^*(1520)$ resonances. Since it is not easy to achieve a systematic analysis as was done for the $\Delta$ [51], we will adopt parameters values for these resonances from other works, changing vertex parametrization when necessary in order to treat the $3/2$-resonances on the same footing. Also we will explain in detail the different approaches in including the width.

## 5.1 $N^*(1440)$ RESONANCE

The $N^*(1440$ MeV)($P_{11}$) resonance has a spin-1/2, isospin-1/2 and positive parity. For the resonances of spin 1/2 the parametrization of the hadronic vertex is more simple than spin 3/2 resonances and is similar to the parametrization for the $\nu N \to N'$ vertex depending on the parity.

The propagator of $P_{11}$ is given by:

$$S_{P_{11}}(p) = \frac{\not{p} + m_{P_{11}}}{p^2 - m_{P_{11}}^2 + i\Gamma_{P_{11}} m_{P_{11}}}, \tag{5.1}$$

where the same CMS prescription $m_{P_{11}} \to m_{P_{11}} - i\frac{\Gamma_{P_{11}}}{2}$ is followed. The $P_{11} \to N\pi$ strong coupling is described by the Lagrangian [23]:

$$\mathcal{L}_{P_{11}\pi N} = \frac{f_{P_{11}\pi N}}{m_\pi} \left(\bar{\Psi}_{P_{11}} \gamma^\mu \gamma_5 \boldsymbol{\tau} \Psi_N\right) \cdot \partial_\mu \boldsymbol{\Phi}_\pi + \frac{f_{P_{11}\pi N}}{m_\pi} \partial_\mu \boldsymbol{\Phi}_\pi^* \cdot \left(\bar{\Psi}_N \gamma^\mu \gamma_5 \boldsymbol{\tau} \Psi_{P_{11}}\right), \tag{5.2}$$

where $\mathcal{L}_{P_{11}\pi N}$ is similar to the $\mathcal{L}_{N\pi N}$ . From the Lagrangian Eq. 5.2, we can deduce the $P_{11}\pi N$ vertex:

$$\frac{f_{P_{11}\pi N}}{m_\pi}\gamma_5 \not{k}(\mathbf{\Phi}^*_\pi \cdot \boldsymbol{\tau}), \tag{5.3}$$

where k is the pion outgoing momentum, and corresponds to the same $\pi-$production vertex that in the second term of Eq. 4.16.

For the W$NP_{11}$ vertex as we outgoing boson, make $q \to -q$ in the hadronic vertex of Ref. [22], and the matrix element of $P_{11}$ resonance production can be written as:

$$\Gamma^\lambda_{WNP_{11}} = -i\frac{1}{2}\left[\frac{g_{1V}}{(m_{P_{11}}+m_N)^2}(Q^2\gamma^\lambda + \not{q}q^\lambda) - \frac{g_{2V}}{(m_{P_{11}}+m_N)}i\sigma^{\lambda\nu}q_\nu - g_{1A}\gamma^\lambda\gamma_5 + \frac{g_{3A}}{m_N}q^\lambda\gamma^5\right] \times \sqrt{2}\boldsymbol{\tau}\cdot\boldsymbol{W}^*, \tag{5.4}$$

where the kinematics factors are scaled by $m_{P_{11}}+m_N$ in order to make each term together the coupling constant dimensionless. Here $\chi_{P_{11}}(\pm 1/2)$ is equal to the nucleon ones. Note the similarity of Eq. 5.4 with the second term of Eq. 4.16 that is for nucleons. The term with $g_{3A}$ is called pion-pole term and gives de contribution where the $W$ boson decays in a pion and then interacts with the nucleon. This can be obtained replacing the axial contribution $A^\lambda$ by $A^\lambda + q^\mu qA/(Q^2+m_\pi^2)$ (see $g_{3A}$ below). Then, one assumes the resonance on shell and evaluates $(\bar{u}^*)\not{q}\gamma_5 u = -\bar{u}^*(m^*+m_N)u$ . Note that $q = p - p^*$ for out going $q$ in the direct contribution. This procedure is also assumed for the contributions of nucleons in Eq. 4.16.The form factors for $WNN^*(1440)$ vertex are obtained from the connection between electromagnetic resonance and the helicity amplitudes.The helicity amplitudes describe the nucleon-resonances transition depending on the polarization of the incoming photon and the spins of the baryons [22]. For non-zero $Q^2$, data on helicity amplitudes for the $N^*(1440)$ are available only for the proton [22], where it is assumed that the isovector contribution on the neutrino production is given as $g_i^V = -2g_i^p$.

The PCAC hipothesys allows us to relate the two form factors and fix their values at $Q^2 = 0$:

$$g_{1A}(Q^2) = \frac{0.51}{(1+Q^2/M_A^2)^2(1+Q^2/3M_A^2)} \tag{5.5}$$

$$g_{3A}(Q^2) = 0.51\frac{(m_{P_{11}}+m_N)}{Q^2+m_\pi^2}m_N \tag{5.6}$$

$$g_{1V}(Q^2) = \frac{4.6}{(1+Q^2/M_V^2)^2(1+Q^2/4.3M_V^2)} \quad , \quad g_{2V}(Q^2) = \frac{1.52}{(1+Q^2/M_V^2)^2}(2.8\ln(1+Q^2/\text{GeV}^2)-1). \tag{5.7}$$

With $M_V = 0.84$ and $M_A = 1.05$ . Note that the signs of $g_{1V}(Q^2), g_{2V}(Q^2), g_{1A}(Q^2)$ are the same that for $F_{1V}(Q^2), F_{2V}(Q^2), F_A(Q^2)$ in Eq. 4.19 in spite we have different form factors. The coupling $f_{P_{11}\pi N}$ can be obtained of the partial decay width ($P_{11} \to \pi N$) according to:

$$\Gamma_{P_{11}\to\pi N} = \frac{I_{P_{11}}}{4\pi}\left(\frac{f_{P_{11}\pi N}}{m_\pi}\right)^2 (m_{P_{11}}+m_N)^2 \frac{E_N - m_N}{m_{P_{11}}}|\mathbf{q}_{\text{c.m}}|, \tag{5.8}$$

where $|\mathbf{q}_{\text{c.m}}|$ is the momentum of the outgoing pion in the rest frame of the resonance

$$|\mathbf{q}_{\text{c.m}}| = \frac{\sqrt{(m_R^2 - m_\pi^2 - m_N^2)^2 - 4m_\pi^2 m_N^2}}{2m_R}, \tag{5.9}$$

being $I_R = 3$ for isospin $1/2$ resonances, and $E_N$ is the energy of the outgoing nucleon in the rest frame that can be found as:

$$E_N = \frac{m_R^2 + m_N^2 - m_\pi^2}{2m_R}. \tag{5.10}$$

The expression Eq. 5.8 can be obtained from Eq. 3.22 fixing $\sqrt{s} = m_{P_{11}}$ and this should correspond and the $\Gamma_{P_{11}}^{CMS}$ of the 3/2 resonances. The coupling $f$ can be determinate from the Eq. 5.8 where the width $\Gamma_{\text{P}_{11}\to\pi N} \approx 0.69 \times 391$ MeV $= 269.79$ MeV [23] since the branding ratio in N$\pi$ is between 55% and 75%. With this the coupling constant is calculate using the Eq. 5.9 and Eq. 5.10 and have value of $f_{\text{P}_{11}\pi N} = 0.412$. With this, the contribution to the amplitude should be

$$\begin{aligned}
&O^{\lambda}_{RP_{11}}(p,p',q) + O^{\lambda}_{BP_{11}}(p,p',q) = \bar{u}(p'm')\frac{f_{\text{P}_{11}\pi N}}{m_\pi}\gamma_5(\not{p}-\not{p}'-\not{q})iS_{\text{P}_{11}}(p-q)(-i)\frac{1}{2}\left[\frac{g_{1V}}{(m_{P_{11}}+m_N)^2}(Q^2\gamma^\lambda + \not{q}q^\lambda)\right. \\
&\left. - \frac{g_{2V}}{(m_{P_{11}}+m_N)}i\sigma^{\lambda\nu}q_\nu - g_{1A}\gamma^\lambda\gamma_5 + \frac{g_{3A}}{m_N}q^\lambda\gamma^5\right]u(p,m)\sqrt{2}\mathcal{T}_{10} + \\
&+ \bar{u}(p'm')(-i)\frac{1}{2}\left[\frac{g_{1V}}{(m_{P_{11}}+m_N)^2}(Q^2\gamma^\lambda + \not{q}q^\lambda) - \frac{g_{2V}}{(m_{P_{11}}+m_N)}i\sigma^{\lambda\nu}q_\nu - g_{1A}\gamma^\lambda\gamma_5 + \frac{g_{3A}}{m_N}q^\lambda\gamma^5\right] \\
&\times iS_{\text{P}_{11}}(p+q)(-)\frac{f_{\text{P}_{11}\pi N}}{m_\pi}\gamma_5(\not{p}-\not{p}'-\not{q})u(p,m)\sqrt{2}\mathcal{T}_9
\end{aligned} \tag{5.11}$$

being

$$\mathcal{T}_9 = \chi(m_t')(\mathbf{W}^* \cdot \boldsymbol{\tau})(\boldsymbol{\Phi}^* \cdot \tau)\chi(m_t)$$

and

$$\mathcal{T}_{10} = \chi(m_t')(\boldsymbol{\Phi}^* \cdot \boldsymbol{\tau})(\mathbf{W}^* \cdot \boldsymbol{\tau})\chi(m_t)$$

for pole a cross contributions respectively.

$$\mathcal{T}_{10} \quad = 0, -2, \sqrt{2} \quad , \mathcal{T}_9 = -2, 0, -\sqrt{2}, \tag{5.12}$$

equal to $\mathcal{T}_1$ and $\mathcal{T}_2$ respectively. For the cross contribution, that is a background, the width of the resonance should be done zero. The contributions in Eq.5.11 should be added to those obtained in Eqs.4.16

## 5.2 $N^*(1520)$ RESONANCE

The ($D_{13}$) resonance has a spin$-3/2$, Isospin$-1/2$ and negative parity. The propagator is the same as the $\Delta$ Eq. 4.6 but changing $m_\Delta \to m_{D_{13}}$ and making $m_{D_{13}} \to m_{D_{13}} - i\frac{\Gamma^{N\pi}_{D_{13}}}{2}$ where $\Gamma_{D_{13}} = \Gamma^{N\pi}_{D_{13}} + \Gamma^{\Delta\pi}_{D_{13}} = 115$.MeV from PDG (Particle data Group).

The strong Lagrangian is given by [23]:

$$\mathcal{L}_{D_{13}\pi N} = \frac{f_{D_{13}\pi N}}{m_\pi}\bar{\Psi}_\mu \gamma_5 \partial^\mu \boldsymbol{\Phi}_\pi \cdot \boldsymbol{\tau}\Psi - \frac{f_{D_{13}\pi N}}{m_\pi}\bar{\Psi}\partial^\mu \boldsymbol{\Phi}^*_\pi \cdot \boldsymbol{\tau}\gamma_5 \Psi_\mu, \tag{5.13}$$

where $\Psi_\mu$ is a Rarita - Schwinger field for the spin$-3/2$ but isospin $1/2$. Note that is the same Lagrangian that for $\Delta$ but with $\gamma_5$ inserted. From this Lagrangian we derive the vertex factor using $i\mathcal{L}(\partial^\mu \boldsymbol{\Phi}^*_\pi \to ik^\mu)$ in the last term

$$\hat{\Gamma}_{D_{13}N\pi} = \frac{f_{D_{13}\pi N}}{m_\pi}\mathrm{k}_\mu \gamma_5 \times \boldsymbol{\Phi}^*_\pi \cdot \boldsymbol{\tau} \tag{5.14}$$

where the $\mathrm{k}_\mu$ is the pion momentum. Again isospin wave functions are the same as for nucleons. Clearly, the $s$-contribution in the channel $\mathrm{D}^{\pm}_{13} \to p\pi^+$ is forbidden due the charge conservation.

The coupling constant $\frac{f_{D_{13}\pi N}}{m_\pi}$ can be calculated from the partial decay width as (replace $\sqrt{s} = m_{D_{13}}$ in Eq.3.20)

$$\Gamma_{D_{13}\to\pi N} = \frac{3}{12\pi}\left(\frac{f_{D_{13}\pi N}}{m_\pi}\right)^2 \frac{E_N - m_N}{m_{D_{13}}}|\mathbf{q}_{\mathrm{c.m}}|^3, \tag{5.15}$$

where $|\mathbf{q}_{\mathrm{c.m}}|$ and $E_N$ are given by

$$\begin{aligned} |\boldsymbol{q}_{cm}| &= \frac{\sqrt{\left(m_{D_{13}}^2 - m_\pi^2 - m_N^2\right) - 4m_\pi^2 m_N^2}}{2m_{D_{13}}} \\ E_N &= \frac{m_{D_{13}}^2 - m_\pi^2 + m_N^2}{2m_{D_{13}}}, \end{aligned}$$

and which should correspond to $\Gamma_{D_{13}}^{CMS}$. For $E_N$ =1.044 GeV, $|\mathbf{q}_{\mathrm{c.m}}|$=0.45 GeV and using the partial width $0.55 \times 115$ MeV [46] the $\frac{f_{D_{13}\pi N}}{m_\pi}$ constant coupling can be calculated giving $11.29$ GeV$^{-1}$ and $\frac{f_{D_{13}\pi N}^2}{4\pi}$ =0.2.

The electromagnetic vector form factors can be expressed in the so called parity conserving parametrization which is related with the other called Sachs one, that we assume for the $\Delta$. This terms can be written in terms of the Sachs form factors. We will assume similar vertex than for $\Delta$ times $\gamma_5$ , then transform to parity conserving an compare with Ref. [55] and fix our parameters from this comparison. We use

$$\mathcal{W}_{\nu\mu} = \mathcal{V}_{\nu\mu} + \mathcal{A}_{\nu\mu}, \tag{5.16}$$

$$\mathcal{V}_{\nu\mu}(p_{\mathrm{D}_{13}}, q, p) = [(G_M(Q^2) - G_E(Q^2))K_{\nu\mu}^M + G_E(Q^2)K_{\nu\mu}^E + G_C(Q^2)K_{\nu\mu}^C]\gamma_5 \frac{\sqrt{2}}{2} D_{13}^\dagger \boldsymbol{W}^* \cdot \boldsymbol{\tau}\psi \tag{5.17}$$

The $Q^2-$dependence of form factors is assumed to be equal to the $\Delta$ in Eq. 4.20 and Eq. 4.21. The Lorentz tensor structure is:

$$\begin{aligned} K_{\nu\mu}^M &= -K^M(Q^2)\varepsilon_{\nu\mu\alpha\beta}\frac{(p + p_{\mathrm{D}_{13}})^\alpha}{2}q^\beta \\ K_{\nu\mu}^E &= \frac{4}{(m_{\mathrm{D}_{13}} - m_N)^2 + Q^2}K^M(Q^2)\varepsilon_{\nu\lambda\alpha\beta}\frac{(p + p_{\mathrm{D}_{13}})^\alpha}{2}q^\beta \varepsilon_{\mu\gamma\delta}^\lambda p_{D_{13}}^\gamma q^\delta i\gamma_5 \\ K_{\nu\mu}^C &= \frac{2}{(m_{\mathrm{D}_{13}} - m_N)^2 + Q^2}K^M(Q^2)q_\nu\left[Q^2\frac{(p + p_{\mathrm{D}_{13}})_\mu}{2} + q\cdot\frac{p + p_{\mathrm{D}_{13}}}{2}q_\nu\right] i\gamma_5, \end{aligned} \tag{5.18}$$

with $K^M(Q^2) = \frac{3(m_N+m_{\mathrm{D}_{13}})}{2m_N(m_N+m_{\mathrm{D}_{13}})^2+Q^2}$.

Now, $\mathcal{V}^V_{\nu\mu}$ can be expressed in the so-called "normal parity" (NP) decomposition making use of non-trivial relation

$$-i\varepsilon_{\alpha\beta\mu\nu}a^\mu b^{nu}\gamma_5 = (\not{a}\not{b} - a\cdot b)i\sigma_{\alpha\beta} + \not{b}(\gamma_\alpha a_\beta - \gamma_\beta a_\alpha) - \not{a}(\gamma_\alpha b_\beta - \gamma_\beta b_\alpha) + (a_\alpha b_\beta - a_\beta b_\alpha), \tag{5.19}$$

and some on-shell considerations we get a simplified version of $\mathcal{V}^V_{\nu\mu}$ [55],

$$\begin{aligned}\mathcal{V}_{\nu\mu}(p_{\mathrm{D}_{13}},q,p) = i\Bigg\{ & -(G_M(Q^2)-G_E(Q^2))m_{\mathrm{D}_{13}}K_M(Q^2)H_{3\nu\mu} \\ & + \left[G_M(Q^2)-G_E(Q^2)+2\frac{2G_E(Q^2)(q\cdot p_{\mathrm{D}_{13}})-G_C(Q^2)Q^2}{(m_{\mathrm{D}_{13}}-m_N)^2+Q^2}\right]K_M(Q^2)H_{4\nu\mu} - \\ & \left[2\frac{2G_E(Q^2)m^2_{\mathrm{D}_{13}}+(p_{\mathrm{D}_{13}}\cdot q)G_C(Q^2)}{(m_{\mathrm{D}_{13}}-m_N)^2+Q^2}\right]K_M(Q^2)H_{6\nu\mu}\Bigg\},\end{aligned} \tag{5.20}$$

we have omitted isospin contributions and where

$$\begin{aligned} H_3^{\nu\mu}(p,p_{\mathrm{D}_{13}},q) &= g^{\nu\mu}\not{q} - q^\nu\gamma^\mu, \\ H_4^{\nu\mu}(p,p_{\mathrm{D}_{13}},q) &= g^{\nu\mu}q\cdot p_{\mathrm{D}_{13}} - q^\nu p^\mu_{\mathrm{D}_{13}}, \\ H_5^{\nu\mu}(p,p_{\mathrm{D}_{13}},q) &= g^{\nu\mu}q\cdot p - q^\nu p^\nu, \\ H_6^{\nu\mu}(p,p_{\mathrm{D}_{13}},q) &= g^{\nu\mu}q^2 - q^\nu p^\nu. \end{aligned} \tag{5.21}$$

Note tha the $H_5^{\nu\mu}$ tensor does not contribute to Eq. 5.20, but it will appear in others expression. The Lorentz tensor are independent of taking $p = p_{\mathrm{D}_{13}} \pm q$, + sign corresponds to the $\mathrm{D}_{13}$-pole contribution and $-$ sign to the cross-$\mathrm{D}_{13}$ term, which is clear since $\varepsilon_{\nu\mu\alpha\beta}q^\alpha q^\beta = 0$. Thus, the Eq. 5.20 is valid in both cases, but the specific value of $q\cdot p_{\mathrm{D}_{13}}$ depends on the particular contribution to the amplitudes $\left(q\cdot p_{\mathrm{D}_{13}} = \pm\frac{m_N^2+Q^2-m^2_{\mathrm{D}_{13}}}{2}\right)$. If we set on the $\mathrm{D}_{13}-$pole contribution and replace $p = p_{\mathrm{D}_{13}} + q$ we can write Eq. 5.20 as

$$\mathcal{V}^V_{\nu\mu}(p_{\mathrm{D}_{13}},q,p = p_{\mathrm{D}_{13}}+q) = i\Gamma^V_{\nu\mu}(p_{\mathrm{D}_{13}},q),$$

$$\Gamma^V_{\nu\mu}(p_{D_{13}},q)=\left[-\frac{C_3^V(Q^2)}{m_N}H_{3\nu\mu}-\frac{C_4^V(Q^2)}{m_N^2}H_{4\nu\mu}-\frac{C_5^V(Q^2)}{m_N^2}H_{5\nu\mu}+\frac{C_6^V(Q^2)}{m_N^2}H_{6\nu\mu}\right], \tag{5.22}$$

where we have the new Form Factors:

$$\begin{aligned}
C_3^V(Q^2)&=\frac{m_{D_{13}}}{m_N}R_M\left[G_M(0)-G_E(0)\right]F^V(Q^2)\\
C_4^V(Q^2)&=-R_M\left[G_M(0)-\frac{3m_{D_{13}}}{m_{D_{13}}-m_N}G_E(0)\right]F^V(Q^2)\\
C_5^V(Q^2)&=0\\
C_6^V(Q^2)&=-R_M\frac{2m_{D_{13}}}{m_{D_{13}}-m_N}G_E(0)F^V(Q^2),
\end{aligned} \tag{5.23}$$

being $R_M=\frac{3}{2}\frac{m_N}{m_{D_{13}}+m_N}$ and $F^V(Q^2)=\left(1+\frac{Q^2}{(m_N+m_{D_{13}})^2}\right)^{-1}G^V(Q^2)$. Note that $\Gamma^V_{\nu\mu}(p_{D_{13}},q)$ coincides with eq.(30) and (31) in Ref. [23] making $q\to -q$. For the axial part we get multiplying by $\gamma_5$ the $\Delta$ vertex (now we explicitly put $\sqrt{2}$ in the axial vertex)

$$\begin{aligned}
\mathcal{A}_{\nu\mu}(p_{D_{13}},q) &= i\left[D_1(Q^2)g_{\nu\mu}-\frac{D_2(Q^2)}{m_N^2}(p+p_{D_{13}})^\alpha(g_{\mu\nu}q_\alpha-q_\nu g_{\mu\alpha})\right.\\
&+ \left.\frac{D_3(Q^2)}{m_N^2}q_\mu p_\nu\right]\gamma_5\frac{\sqrt{2}}{2}D^\dagger_{13}\boldsymbol{W}^*\cdot\boldsymbol{\tau}\psi
\end{aligned}$$

where $D_4(Q^2)=0$ as before and rearranging we get (omitting again isospin factors)

$$\begin{aligned}
\mathcal{A}_{\nu\mu}(p_{D_{13}},q)&=\sqrt{2}i\left[\left(D_1(Q^2)\pm\frac{D_2(Q^2)Q^2}{m_N^2}\right)g_{\nu\mu}-\frac{2D_2}{m_N^2}H_{4\nu\mu}\right.\\
&\left.\pm\frac{D_3(Q^2)+D_2(Q^2)}{m_N^2}q_\nu q_\mu\right]\gamma_5 \qquad (5.24)\\
&=i\Gamma^A_{\mu\nu}\\
\Gamma^A_{\mu\nu}&=\left[C_5^A g_{\nu\mu}-\frac{C_4^A}{m_N^2}g^{\mu\nu}H_{4\nu\mu}+\frac{C_6^A}{m_N^2}H_{6\mu\nu}\right]\gamma_5. \qquad (5.25)
\end{aligned}$$

We have for the pole contribution ("$+$" sign in previous equation, with "$-$" we use for the cross contribution). Note that this last coincides with eq.(32 ) from Ref. [23] making $q \to -q$. By comparison we get

$$\begin{aligned} D_1 \pm D_2 \frac{Q^2}{m_N^2} &= C_5^A, \\ -\frac{2D_2}{m_N^2} &= -\frac{C_4^A}{m_N^2}, \\ C_A^3 &= 0, \\ \pm\frac{D_3 + D_2}{m_N^2} &= \frac{C_A^6}{m_N^2}. \end{aligned} \tag{5.26}$$

Choosing the values reported for the vector couplings for $Q^2 = 0$ in Ref. [23], we have for the vector part

$$\begin{aligned} -2.98 &= \frac{3}{2}\frac{1.52}{0.94+1.52}(G_M - G_E), \\ 4.21 &= \frac{-3}{2}\left(G_M - \frac{4.56}{1.52-0.94}G_E\right)\frac{0.94}{0.94+1.52}, \end{aligned} \tag{5.27}$$

where $G_E = 0.6$, $G_M = -2.62$, while for $\Delta\, G_{_M}(0) = 2.97, G_{_E}(0) = 0.055$, the change in $G_M$ is consistente with the change of $C_3^V$ between both resonances (see Ref. [22]). If we use $C^A$ values of Ref. [22] we get $G_E = -0.26$ and $G_M = -4.67$. For the axial couplings (we fix for the pole case) we have

$$\begin{aligned} D_1(0) &= -2.15, \\ D_2(0) &= 0, \\ D_3(0) &= -2.15\frac{m_N^2}{m_\pi^2} = -2.15\frac{m_N^2}{m_\pi^2}. \end{aligned} \tag{5.28}$$

while for $\Delta\, D_1(0) = 2.35$, this is consistent also with the change in $C_A^5$ [22]. The additional contribution from this resonance to Eq. 4.16 will be

$$O^{\lambda}_{RD_{13}}(p,p',q)+O^{\lambda}_{BD_{13}}(p,p',q)= \tag{5.29}$$
$$\frac{1}{2}\frac{f_{D_{13}\pi N}}{m_\pi}\gamma_5(p-p'-q)^{\alpha}iG_{\alpha\beta}(p_{D_{13}}=p-q)(\mathcal{V}_{\beta\lambda}+\mathcal{A}_{\beta\lambda})(p_{\mathrm{D}_{13}},q,p)\sqrt{2}\mathcal{T}_{12}(m_t,m_{t'})$$
$$+\frac{1}{2}\overline{(\mathcal{V}_{\beta\lambda}+\mathcal{A}_{\beta\lambda})}(p_{\mathrm{D}_{13}},-q,p')iG_{\alpha\beta}(p_{D_{13}}=p'+q)\frac{f_{D_{13}\pi N}}{m_\pi}\gamma_5(p-p'-q)^{\beta}\sqrt{2}\mathcal{T}_{11}(m_t,m_{t'}),$$

Since $-\gamma_0(-\mathrm{k}_\mu\gamma_5)^\dagger\gamma_0=-\mathrm{k}_\mu\gamma_5$ note additionally that $\overline{W(-q)\gamma_5}=\gamma_5\overline{W(-q)}=-\gamma_5 W_{\mathrm{cross}}$then $(W(q))\gamma_5=-\gamma_5 W_{\mathrm{cross}}(q)$ and for this case $-W_{\mathrm{cross}}\gamma_5$, where the isospin coefficients are:

$$\mathcal{T}_{11}(m_t,m_{t'})=\chi^\dagger(m_{t'})(\boldsymbol{\tau}\cdot\mathbf{W}^*)(\boldsymbol{\tau}\cdot\boldsymbol{\Phi}^*_\pi)\chi(m_t)$$

and

$$\mathcal{T}_{12}(m_t,m_{t'})=\chi^\dagger(m_{t'})(\boldsymbol{\tau}\cdot\boldsymbol{\Phi}^*_\pi)(\boldsymbol{\tau}\cdot\mathbf{W}^*)\chi(m_t)$$

with value

$$\mathcal{T}_{12}\quad=0,-2,\sqrt{2}\quad,\mathcal{T}_{11}=-2,0,-\sqrt{2}.$$

## 5.3 $N^*(1535)$ RESONANCE

This resonance $N^*(1535)$ is of negative parity and spin, isospin $1/2$ and has a branching-ratio of decaying 0.51 in $N\pi$ states. Its propagator corresponds to the half-spin fermion with the same complex mass scheme prescription

$$S_{11}(p)=\frac{\not{p}+m_{\mathrm{S}_{11}}}{p^2-m^2_{S_{11}}+im_{\mathrm{S}_{11}}\Gamma_{\mathrm{S}_{11}}}. \tag{5.30}$$

The $\pi NS_{11}$ coupling is described for the strong Lagrangian

$$\mathcal{L}_{\pi NS_{11}}=\frac{f_{S_{11}\pi N}}{m_\pi}\bar{\Psi}_{S_{11}}\gamma^\mu\partial_\mu\boldsymbol{\Phi}_\pi\cdot\boldsymbol{\tau}\psi+\frac{f_{S_{11}\pi N}}{m_\pi}\bar{\psi}\partial_\mu\boldsymbol{\Phi}^*_\pi\cdot\boldsymbol{\tau}\gamma^\mu\Psi_{S_{11}}, \tag{5.31}$$

which corresponds to that of $P_{11}$ resonance by $\gamma_5$. From this lagrangian we deduce the $S_{11}\pi N$ vertex as

$$-\frac{f_{S_{11}\pi N}}{m_\pi}\not{k}(\boldsymbol{\Phi}^*_\pi\cdot\boldsymbol{\tau}), \tag{5.32}$$

The coupling $f_{S_{11}\pi N}$ can be obtained from the same procedure as in the $N^*(1440)$ case and from Ref. [23], we get a value $f_{S_{11}\pi N} = 0.17$.

For the $WNS_{11}$ vertex we assume (is obtained from Eq. 5.4 times $\gamma_5$ or from Ref. [22]

$$\Gamma^{\lambda}_{WNS_{11}} = -i\frac{1}{2}\left[\frac{g_{1V}}{(m_{S_{11}}+m_N)^2}(Q^2\gamma^{\lambda}+\not{q}q^{\lambda})\gamma_5 - \frac{g_{2V}}{(m_{S_{11}}+m_N)}i\sigma^{\lambda\nu}q_{\nu}\gamma_5 - g_{1A}\gamma^{\lambda}+\frac{g_{3A}}{m_N}q^{\lambda}\right]\sqrt{2}\boldsymbol{\tau}\cdot\boldsymbol{W}^*, \quad (5.33)$$

where

$$\begin{aligned}
g_{1V} &= \frac{4.0}{(1+Q^2/M_V^2)^2(1+Q^2/1.2M_V^2)}(7.2\ln(1+Q^2/\mathrm{GeV}^2)+1),\\
g_{2V} &= \frac{1.68}{(1+Q^2/M_V^2)^2}(0.11\ln(1+Q^2/\mathrm{GeV}^2)),\\
g_{1A} &= \frac{0.21}{(1+Q^2/M_A^2)^2(1+Q^2/3M_A^2)},\\
g_{3A} &= \frac{0.21(m_{S_{11}}-m_N)m_N}{Q^2+m_\pi^2}.
\end{aligned} \quad (5.34)$$

the contribution to the amplitude that should be added to those obtained in Eq.4.16, will be

$$O^{\lambda}_{RS_{11}}(p,p',q)+O^{\lambda}_{BS_{11}}(p,p',q) = \bar{u}(p'm')(-)\frac{f_{S_{11}\pi N}}{m_\pi}(\not{p}-\not{p}'-\not{q})iS_{S_{11}}(p-q)(-i)\frac{1}{2}\left[\frac{g_{1V}}{(m_{S_{11}}+m_N)^2}(Q^2\gamma^{\lambda}+\not{q}q^{\lambda})\right. \quad (5.35)$$

$$\left.-\frac{g_{2V}}{(m_{S_{11}}+m_N)}i\sigma^{\lambda\nu}q_{\nu}-g_{1A}\gamma^{\lambda}\gamma_5+\frac{g_{3A}}{m_N}q^{\lambda}\gamma^5\right]\gamma_5 u(p,m)\sqrt{2}\mathcal{T}_{14}+$$

$$+\bar{u}(p'm')(-i)\frac{1}{2}\gamma_5\left[\frac{g_{1V}}{(m_{S_{11}}+m_N)^2}(Q^2\gamma^{\lambda}+\not{q}q^{\lambda})-\frac{g_{2V}}{(m_{S_{11}}+m_N)}i\sigma^{\lambda\nu}q_{\nu}-g_{1A}\gamma^{\lambda}\gamma_5+\frac{g_{3A}}{m_N}q^{\lambda}\gamma^5\right]$$

$$\times iS_{S_{11}}(p+q)(-)\frac{f_{S_{11}\pi N}}{m_\pi}(\not{p}-\not{p}'-\not{q})u(p,m)\sqrt{2}\mathcal{T}_{13},$$

where $\mathcal{T}_{13,14}$ are equal to $\mathcal{T}_{9,10}$ in Eq. 5.12. Note that $-\gamma_0(-)(\not{k})^{\dagger}\gamma_0 = -\not{k}$.

# Chapter 6

# RESULTS

In this section we resume the results obtained with our formalism for the total and differential $1\pi-$production cross section and compare them with the old bubble chamber ANL, BNL data and also with the reanalyzed ones. In addition we apart in some cases from the CMS approach in order to simulate the results obtained in other works with the purpose of discuss the effects of the adopted inconsistencies on the calculations.

## 6.1 FORMAL ISSUES

We firstly consider in the amplitude contributions from the $\Delta$ pole and cross terms, the nucleon pole and cross terms, and contact, pion in flight and rho ($\rho$) plus omega ($\omega$) exchange terms as shown in Eqs. 4.16 and 4.17. Then, we add the contributions of the second resonance region enlarging the final $M_{\pi N}$ invariant mass in order to see the effect of more energetic resonances to the cross section. We will add the amplitude of Eqs.( 5.11, 5.29 and 5.35).

We begin discussing a formal issue referred to spin $3/2$ resonances and the introduction of FF. It would be useful to repeat here the Eq. 3.2 , where $\Delta$ propagator is written in a different way without using the projectors, that is

$$
\begin{aligned}
G^{\mu\nu}(p) &= \frac{\not{p}+m_{\Delta}}{p^2-m_{\Delta}^2}\left\{-g_{\mu\nu}+\frac{1}{3}\gamma_{\mu}\gamma_{\nu}+\frac{2}{3m_{\Delta}^2}p^{\mu}p^{\nu}-\frac{1}{3m_{\Delta}}(p^{\mu}\gamma^{\nu}-\gamma^{\mu}p^{\nu})\right. \\
&- \left.\frac{2\left(i\not{p}-m_{\Delta}\right)}{3m_{\Delta}^2}\left[-(p^{\mu}\gamma^{\nu}-\gamma^{\mu}p^{\nu})+\left(\not{p}+m_{\Delta}\right)\gamma_{\mu}\gamma_{\nu}\right]\right\} \\
&= \frac{\not{p}+m_{\Delta}}{p^2-m_{\Delta}^2}\left[-g_{\mu\nu}+\frac{1}{3}\gamma_{\mu}\gamma_{\nu}+\frac{2}{3m_{\Delta}^2}p^{\mu}p^{\nu}-\frac{1}{3m_{\Delta}}(p^{\mu}\gamma^{\nu}-\gamma^{\mu}p^{\nu})\right] \\
&- \frac{2}{3m_{\Delta}^2}\left[\left(\not{p}+m_{\Delta}\right)\gamma_{\mu}\gamma_{\nu}-(p^{\mu}\gamma^{\nu}-\gamma^{\mu}p^{\nu})\right]. \qquad (6.1)
\end{aligned}
$$

Note that the form Eq. 6.1 corresponds to the reduced propagator (see chapter 1) and should be used with the corresponding interaction reduced vertexes to get $A-$independent amplitudes. On the other hand if one takes $A=-1$ in Eq. 1.37 to get a simplified form, only the first term of Eq. 6.1 appears and the term in brackets sometimes it is called (Wrongly) on shell $3/2$ projector (see Eq. 3.3). Nevertheless, for the reduced and any value of $A$, $1/2$ off-shell propagation is always present. This is not private of the $3/2$ field, also in the massive vector meson propagator we have present an off-shell lower spin $0$ component [56]. As can be seen from the Eq. 6.1, the propagator has a contribution with a pole at $p^2=m_{\Delta}^2$ and another that is not singular. When the value $A=-1$ is adopted this last term is not present, nevertheless now the reduced interaction vertexes should not be used and need to be modified.

The other formal point is how to fix $Z$ in the interaction vertex's. We concentrate for example in the strong $\Delta\pi N$ decay vertex that quit generally has a contact transformation invariant form (see Eq.(1.39) and [57])

$$
\hat{\Gamma}^{\alpha}_{\Delta\pi N} \quad \times \quad R^{\mu}_{\alpha}\left(\frac{1}{2}(1+4Z)A+Z\right), \qquad (6.2)
$$

where $\hat{\Gamma}^{\alpha}_{\Delta\pi N}$ was defined in Eq. 4.9 and where $Z$ is arbitrary and independent of $A$. Now we point to the question of the true degrees of freedom of the spin $3/2$ field, and remember that this it belong to a constrained quantum field theory. Observe that in the free RS Lagrangian Eq. 1.31, there is no term containing $\dot{\Psi}_0$. So, the equation of motion for it is a true constraint, and $\Psi_0$ has no dynamics. It is necessary then that interactions do not change that fact, and as it is shown in [42] this is fulfilled for the value $Z=1/2$ . The same conclusion was obtained in the original work of Nath [58] where through other method the same value was obtained. Then, we adopt this value for our interactions. This election will be the same for the $D_{13}$ that is a spin $3/2$ resonance.

In spite of this analysis some authors try to get both, the simpler versions for $3/2$ propagator using $A=-1$ and vertexes with $\frac{1}{2}(1+4Z)A+Z=0$. This can be read in two different manners. First, if they are adopting the same $Z=1/2$ value (generally this is not discussed clearly), we could conclude that there is an inconsistence since they are adopting a value $A=-1$ for the propagator while $A=-1/3$ to get $\frac{1}{2}(1+4Z)A+Z=0$, violating the independence of the amplitude with $A$. Or second, they are thinking, but not expressing it, the different choice $Z=-1/2$ and using $A=-1$ in both propagator and vertexes. Nevertheless, this $Z$ value does not avoid the dynamics of $\Psi_0$ in the vertex Eq. 6.2. En each case, model dependencies are introduced. We fell important to mention these shortcomings, because sometimes results are presented without taking into account these formal issues and are only qualified by its proximity to the experimental data.

Up to now many studies have been achieved around the region $M_{\pi N}\sim m_{\Delta}=1232$ MeV and with the approach for the $\Delta$ propagator assuming a constant width Eq. 3.23 into Eq. 3.19 (CMS approach), or with an energy dependent width as in Eqs. 3.17 replaced only in the denominator $p^2-m_{\Delta}^2$, violating thus the ward identities . The $\Delta$ contribution is supplemented by adding the background terms mentioned above and shown in Figs 4.2(a)-(g). The resulting model was compared with CC$1\pi$ or NC$1\pi$ data subject to the invariant mass constraints $M_{\pi N}<$ 1.4 and $M_{\pi N}<$1.5 GeV, in accordance with experimental data respectively [59, 60, 61]. In addition, in Ref.[62] , the replacement $\mathcal{L}_{\Delta\pi N}\rightarrow\mathcal{L}_{\Delta\pi N}+c\mathcal{L}_C$ is proposed with $\mathcal{L}_C$ describing contact terms without the $\Delta$ field, with adjusting the low-energy constant $c$ to get a better fitting. The addition of contact terms is based on the argumentation that within the ChPT framework, the equivalence between different Lagrangians is at less of low energy constants, to be adjusted, terms. In Ref. [59, 60] the $\Delta\pi N$ vertex was chosen consistently with the assumed form for the $\Delta$ propagator, from the point of view of the contact transformations mentioned above, and reduced Feynman rules were used. In Ref. [61, 24], this was not the case and the inconsistence mentioned above respect different $A$-choices is present and also they use an energy dependent width with the consequence already mentioned. Referring the procedure followed in Ref. [62], we fell that is arbitrary and prefer the inclusion of higher derivative Lagrangians terms with new couplings constants [42, 63].

In the present thesis work we wish to built a model to describe the region of higher $M_{\pi N}$ invariant masses and thus, we are faced to the following difficulties:

**(i)** Far away the $\Delta$ resonance region, the approach for the $\Delta$ resonant propagator 3.19 plus the fixed width $\Gamma_{\Delta}^{CMS}$ in *all* places, cannot be very good as shown for $\pi N$ scattering [59].

**(ii)** At high $\pi N$ invariant mass the finite size effects of hadrons become relevant [35]. These effects can be taken into account empirically by introducing appropriate form factors. They are meant to model the deviations from the *pointlike* couplings we use in all the Lagrangians employed to built the amplitudes,

due to the quark structure of hadrons as was shown in the section 2.2. In addition, rescattering of the final $\pi N$ pair should be important.

**(iii)** At higher energies, other more energetic resonances should be included in the scattering amplitude. In this thesis work we occupated of the so named second resonance region which includes the $N^*(1440)(P_{11})$, $N^*(1520)(D_{13})$, $N^*(1535)(S_{11})$ resonances. As it will be discussed later, the contribution of heavier resonances does not warranty a better agreement with data unless the amplitudes are added coherently and interferences of all contributions are properly taken into account.

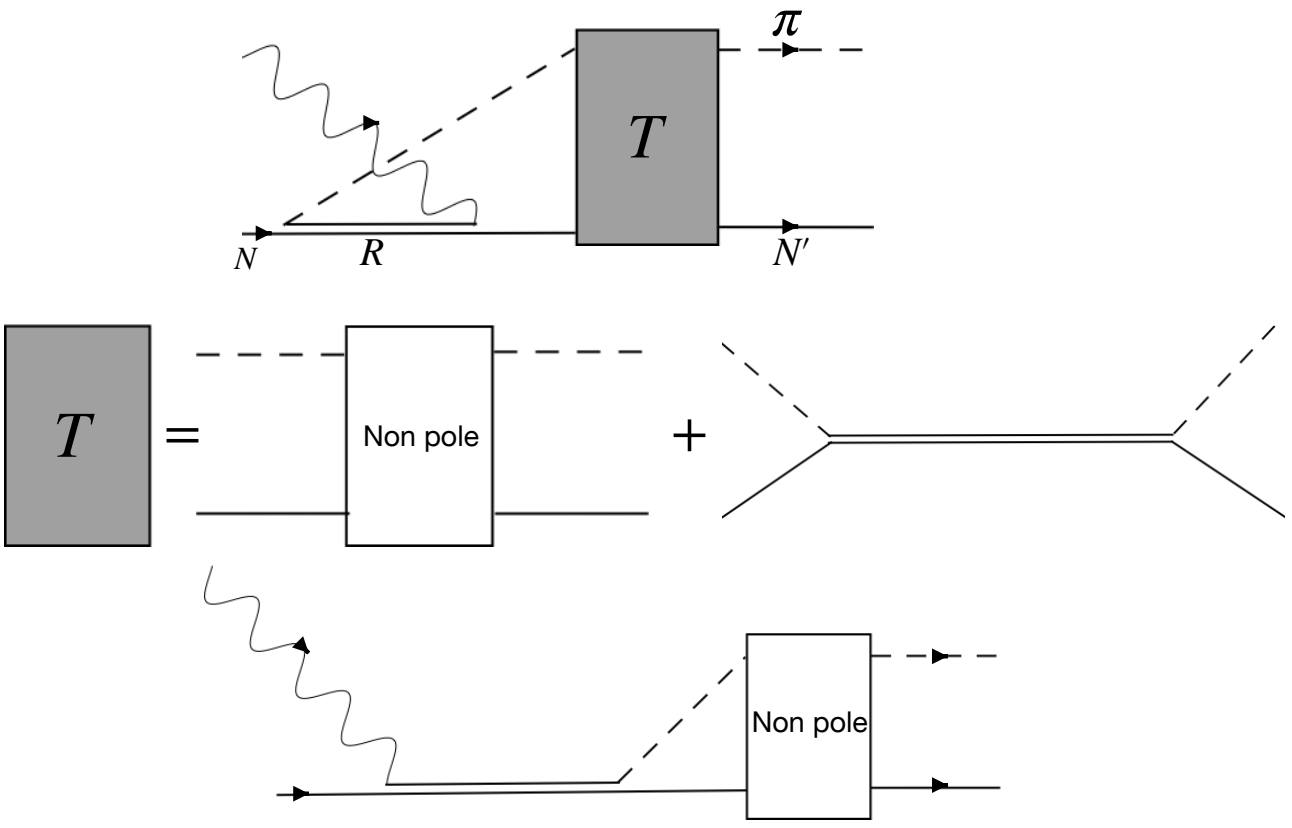


**Figure 6.1:** Rescattering of the Δ cross contribution

As mentioned in chapter 3, the use of a constant width via the CMS approach ensures electromagnetic gauge invariance in the simplest way in the presence of an unstable particle. If the width of the resonance is energy-dependent, the electromagnetic Ward identity involving the propagator and the radiative vertex may be broken by terms of order $\Gamma_\Delta/m_\Delta$ if vertex corrections are not taken into account. We have also violations of the Ward identiy if the width is only replaced in the denominator of the resonance.

Nevertheless, when final $M_{\pi N}$ invariant mass grows the CMS approach falls in reproduced for example $\pi N$ elastic scattering [59], then we needed to go ahead implementing more sophisticated approaches as using an

energy dependent width or the exact form of the $\Delta$ propagator, in order to describe the $\pi N$ elastic scattering data. But now the corresponding vertex corrections should be also included, that is not a trivial task. Now in weak pion production we deal with similar problems. The resonance width has its origin in the self energy as shown in chapter 3, which only dresses and includes rescattering in the resonant term shown in Fig. 4.2(h). This effect can be included to different approximation degrees. Through a constant width, introducing an energy dependent width and considering the effects of this dressing in the structure of the propagator that leads to the form in Eq.3.14. The improvement in the approximation in treating the rescattering of the $\pi N$ pair, regularize the tree label (singular) resonant contribution by summing an infinite series of graphs. The cross term in Fig.4.2(g) is not affected by this dressing and as we will see the enlarging effect of the $3/2$ propagator caused by the second term in Eq.(6.1)) cannot be corrected by a self energy. Still more, the final $\pi N$ pairs in the all background contributions in Fig. 4.2(a),(c),(d),(e),(f) (known as non resonant) to the amplitud could be of course rescattered, exciting or not resonances, this changing and softening without doubt its tree behavior. This is schematized in Fig.(6.1) for the resonance contributions.

To avoid model dependencies coming from the introduction of arbitrary FF at each interaction vertex (which violates gauge invariance without vertex corrections), we will introduce a global form factor in the decay amplitude as described in section 2. As we are including resonances until around $M_{\pi N} \sim 1.6$ GeV, taking into account the width of the most energetic considered one($S_{11}(1535)$ MeV), we will only light on this FF above this energy. In this way, we also correct the amplitude for excitation of more energetic resonances not considered in our model since we also wish describe experimental data without $M_{\pi N}$ cuts. Guided by a previous proper description on NC1$\pi$ data obtained by the CERN Gargamelle experiment without applying cuts in the neutrino energies, we adopt for the final $\pi N$ pair a FF [60] (we have shown this FF in section 2 but repeat here for completeness)

$$F(k) \;=\; \frac{\Lambda^4}{\Lambda^4 + k^2 (M_{\pi N} - M_{\pi N}^{th})^2 \theta(M_{\pi N} - 1.6 \text{ GeV})} \tag{6.3}$$

where $k \equiv |\mathbf{p}_\pi(M_{\pi N})| = |-\mathbf{p}_N(M_{\pi N})| = [(M_{\pi N}^2 - m_N^2 - m_\pi^2)^2 - 4 m_N^2 m_\pi^2)]^{1/2}/2M_{\pi N}$ is the momentum of the emitted pion in the $\pi N$ CM frame, and $M_{\pi N}^{th} = m_N + m_\pi$. We will adopt $\Lambda = 600$ MeV as we done previously for neutral currents in Ref. [60].

This FF is expected to correct in an effective way the behavior of the theoretical $d\sigma/dM_{\pi N}$ distribution at higher values of the $\pi N$ invariant-mass. Since the excitation of heavier resonances lying above the second region in the $\pi N$ channel is expected to occur at higher values of $M_{\pi N}$, their effects in the $\pi N$ invariant mass

are more important above this resonance region and only modifies slightly the mass distribution in the included resonance region. Note that we are including explicitly, at difference of Ref.[60], resonances with energies in the $1.4-1.6$ GeV and for this we will light on $F(k)$ above the second region energy. These physical reasons justify our choice for the modulation factor of the resonance amplitude by means of Eq. 6.3. As it can be realized, Eq. (6.3) can be seen as a monopole hadronic FF, that takes into account the finite size of hadrons, with an energy-dependent cutoff $\Lambda_{\text{eff}} = -\Lambda^2/(M_{\pi N} - M_{\pi N}^{th})$ only for $M_{\pi N} > 1.6$ GeV (see the $\theta$ function in Eq. 6.3) since below that energy ($1.6$ GeV) the description of weak pion production in the channels Eq. 4.14 are done acceptably using the CMS approach without FF as will show immediately. At the same time as $\Lambda_{\text{eff}} = f(M_{\pi N})$ , we are correcting the behavior of the amplitude with the growing of $M_{\pi N}$ . It is important to mention that the form Eq. 6.3, was used satisfactorily in the description of the pion photoproduction reaction [33] as a regularization FF to include final state interactions. In the case of pion photoproduction we have seen that a value of $\Lambda = 0.7$ GeV properly accounts for the $\pi N$ intermediate state contributions to the loop integrals present in the rescattering amplitudes, which at the same time enables to get consistent values for the dressed $G_M$ and $G_E$ FF fitted from experimental data. We take for consistence the same value of $\Lambda = 600$ MeV for all the channel. A more evolved analysis would lead to different values, since experimental data on $d\sigma/dM_{\pi N}$ depends on the specific channel. Nevertheless, by simplicity we adopt a common value for all channels. Finally the using of a global FF preserves gauge invariance.

## 6.1 TOTAL CROSS SECTION

### 6.2.1 NEUTRINOS

Remember how the cross section is defined

$$d\sigma \;=\; \frac{\#events\ detected\ in\ d\Omega/sec}{\#incidents\ \nu/area\ sec \qquad \#scattering\ centers}, \tag{6.4}$$

where the amount $F(E_\nu) = (\#incidents\ \nu \equiv N_\nu)\ in\ (E_\nu, E_\nu + \Delta E_\nu)/\Delta E_\nu area\ sec$ is know as neutrino flux. Nevertheless in long base line (LBL) experiments within the detector, an effective volume $V_F$ where the interaction of the neutrinos with the protons (because the reaction $\nu p \to \mu^- p\pi^+$is use for calibration) is considered and called fiducial volume. Then, we can consider that for a given geometry assumed for $V_F$ we have that $F(E_\nu)V_F = N_\nu d(E_\nu)$, where $d$ is the distance traveled by all the neutrinos of energy $E_\nu$ called pathlength per second and energy unit . When we divide both sides by the number of protons $N_p$ found by these neutrinos we find $F(E_\nu) = \frac{N_\nu d(E_\nu)/N_p}{\rho_p}$ and reads $F(E_\nu) \equiv \frac{l(E_\nu)}{\rho_p}$. As in Eq. 6.4 we have a ratio of rates we considered $l(E_\nu)$

in units of cm/GeV proton and as $\rho_p$ , the proton density, is a fixed property of the detector for example in ANL they use as unit of flux cm/GeV proton. Nevertheless, when cross section is calculated the factor $1/\rho_p$ should be considered. This flux (normalyzed by the total flux and thus adimentional) is shown in the Figs. 6.2 for the experiments BNL [64] and ANL [65] respectively. We analyze the total cross section calculated in Eq.4.2 and the

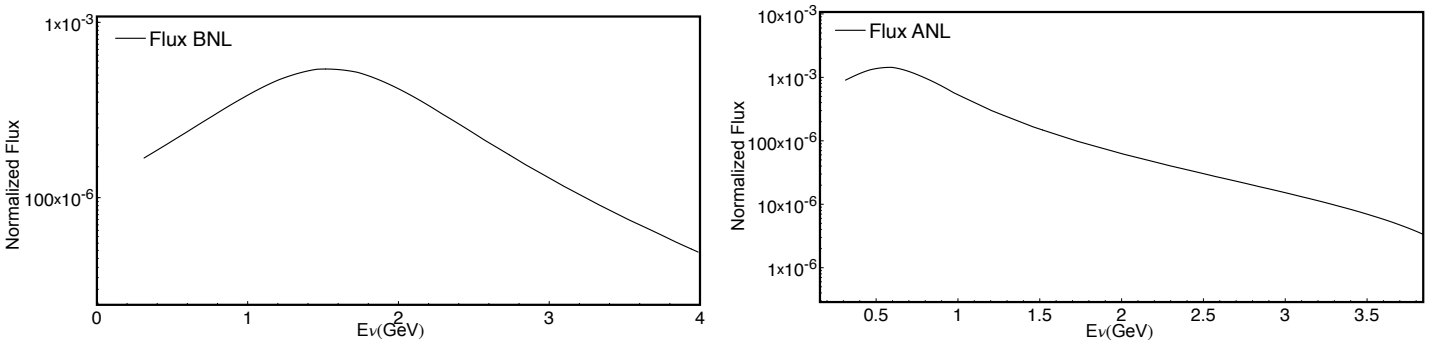


**Figure 6.2:** Neutrino fluxes

total amplitud built as explained at the beginning of the chapter. We first compare our theoretical results with the data obtained in the ANL experiment [65] which shows results for three regimes of events $M_{\pi N} < 1.4, 1.6$ GeV and no cut of this invariant mass. The data to be considered are obtained by the ratio between the distribution of events/Gev measured in each channel, that are considered integrated in $\Omega$ in Ref. [65] and the ANL flux $F(E_\nu)$ [66] as defined above. Note that the cross section is normally given in units of $10^{-38}$ cm$^2$ while in the experiment it is measured in Events per GeV units, then if we compare with the results for $\sigma(E_\nu)$ reported in that reference we can get the conversion factor which enclose the amount $1/\rho_p$ that is proper for the experiment. Then, this factor enables us to calculate the differential cross section $d\sigma/dQ^2$ from the corresponding event distribution.

Firstly, in Fig. 6.3 we compare our results within the CMS approach, that was used previuosly to obtain the $\Delta$ strong and weak parameters [47, 51, 33], without and with the second resonance energy region contribution(with constants widths also in Eq. 5.1 and Eq. 5.30) included, for $M_{\pi N} < 1.4$ GeV. As can be seen the effect of adding the second resonance region depends on the considered channel. If we considered a fixed energy $E_\nu = 3.0,\ 1.5,\ 1.5$ GeV for the mentioned channels in Eq. 4.14 respectively, one can see that the contribution of the second resonance region is correspondingly $4\%, 17\%$ and $10\%$ , approaching data and the theoretical cross sections. Note that in spite of the cut in $M_{\pi N}$, the tails of the resonances generated by the finite width give an appreciable contribution and the interference between them is also important. Analyzing the individual contributions of the $P_{11}, D_{13}$ and $S_{11}$ resonances on can notice that the main contribution comes from the $D_{13}$ being the other contribution less that $1\%$. All isospin factors for the mentioned three resonances for the resonant

(direct) and background ( cross) amplitudes read

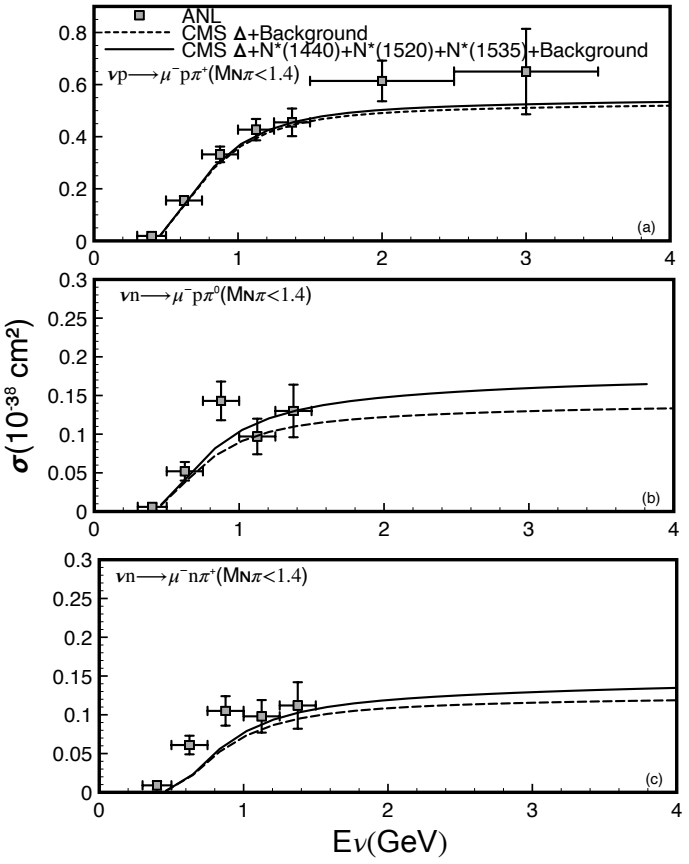


**Figure 6.3:** Total $\nu N$ cross section as function of the neutrino energy for different channel. Results with only the $\Delta$ and $\Delta+$ second region resonances plus the corresponding background in each case are shown for a cut $M_{\pi N} < 1.4$ GeV. Data are taken from Ref. [65]. The Figure show the three channels of interest for the single pion production, where (a) $\nu p \to \nu^- p\pi^+$ process, (b) $\nu n \to \nu^- p\pi^0$ process, (c) $\nu n \to \nu^- n\pi^+$ process.

$$\begin{aligned} \tau_R &= 0, \sqrt{2}, -2 \\ \tau_B &= -2, -\sqrt{2}, 0, \end{aligned} \tag{6.5}$$

and thus this explain why the contribution for the first channel is small and comes from background terms. For the second channel we have the main contribution since there are contributions of both the direct and cross terms and interference between of them, while the last one we have only the direct contribution.

In addition, Also, one might ask why the contributions from the second resonance region are, apart from the cutting in invariant mass effect, lower than the $\Delta+$ background contributions. This can be understood form the Eq. 4.2 that for certain value of the neutrino energy $E_\nu$ in the Lab and $\nu N$ CM systems $E_\nu^{CM}\sqrt{s} = E_\nu m_N$, being

the limits in the cross section integrals fixed. This means that for a given final $\mu\pi N'$ state and amplitudes of the same order of magnitude in the second resonance region regards the $\Delta$ one, the kinematical cross section factor $\frac{1}{E_\nu}$ favors smaller neutrinos energies and thus lowest energy contributions. For example if we take the final muon at rest $P_R^2 = (E_\nu + m_N - m_\mu)^2$ and thus $P_\Delta^2 = (1232)^2$ MeV$^2$ with $(m_N E_\nu)^{-1} \approx 7$ while $P_{D_{13}}^2 = (1520)^2$ MeV$^2$ and $(m_N E_\nu)^{-1} \approx 1.5$. Then, in spite strong and weak coupling constants would be of the same order, the $\Delta$ contribution is favored by the neutrino kinematical factor and because the propagator peak at each resonance energy. This explain the different size of the resonances contribution.

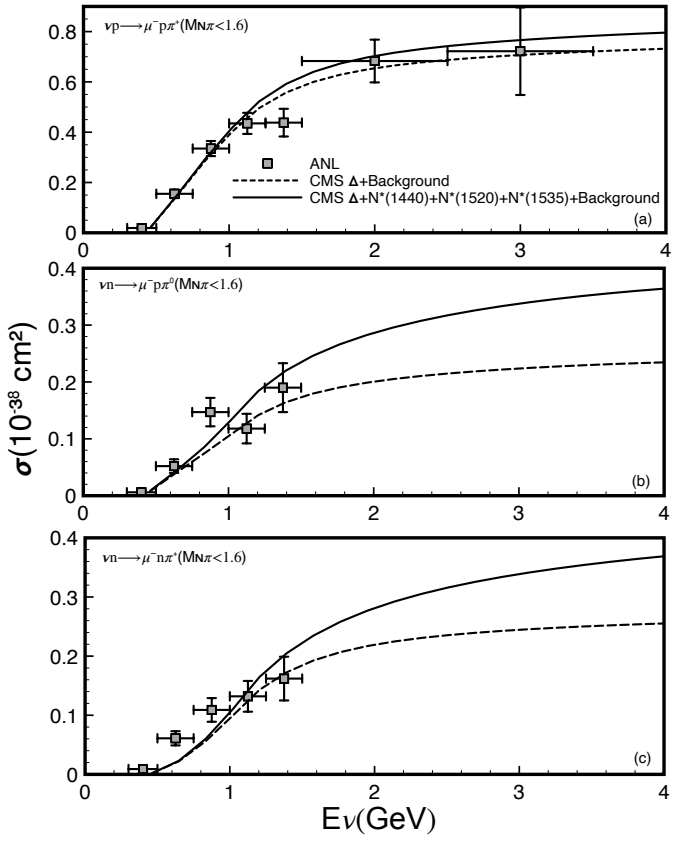


**Figure 6.4:** Total $\nu N$ cross section as function of the neutrino energy for different channel. Results with only the $\Delta$ and $\Delta$ + second region resonances plus the corresponding background in each case are shown for a cut $M_{\pi N} < 1.6$ GeV. Data are taken form Ref. [65]. The Figure show the three channels of interest for the single pion production, where (a) $\nu p \to \nu^- p\pi^+$ process, (b) $\nu n \to \nu^- p\pi^0$ process, (c) $\nu n \to \nu^- n\pi^+$process.

Now we go to the cut $M_{\pi N} < 1.6$ GeV where the second resonance region is fully included. As can be seen from the Fig. 6.4 the contribution of resonances in this region is more important and necessary in order to improve the coincidence with data. In spite we are not fitting any of the parameters in the model, if one

evaluates the $\chi^2/dof$ amount defined as:

$$\frac{\chi^2}{dof} = \sum_i \frac{\frac{(\sigma^i_{\text{exp}} - \sigma^i_{\text{calc}})^2}{\epsilon_i^2}}{dof},$$

where, $\epsilon$ is the error, $dof =$ data number and $i = 1, \ldots,$ data, it can be used to qualify the different approaches. For example for the calculations in Fig. 6.4 the full line is closer than the dotted one in all the centroids (specially in the (b) and (c) channels what are the most sensible to the resonance-background interference), it is evident the $\chi^2/dof$ it will be better for the calculations that include the second resonance region. A numerical estimates lead to values $\chi^2/dof = 0.11(0.11), 0.10(0.25), 0.10(0.2)$ for each channels from above to below in the Figure and for the amplitude including (not including) second resonance region. In spite the difference It is small the improvement it is clear for the last two channels where the background-resonance interference it is more important. This will be totally evident in the calculations without cuts that will be shown in the Fig. 6.6.

Until this moment we kept within the CMS approach, the most simple to treat all the resonances together the Born terms of the non-resonant backgrounds, that also enables to keep electromagnetic gauge invariance. Nevertheless, the data of Ref. [65] contains also results without energy cuts and also all results in Ref. [64] are reported without events exclusion. For this we need to extend the model to higher energies.

Before discussing a final calculations without cut, we will firstly analyze the behavior of the total cross section without adding any FF. When total cross section is calculated without a FF we get the results in Fig.6.5. The full lines corresponds to the CMS approach with constant width, and as can be seen the calculated values are well above the data. It is clear the increasing of the cross section above $1.6$ GeV, this perhaps the absence of more energetic resonances to interfere in the model, and also from the lack of validity of the tree level approach. Then, we keep the same propagators structure (Eq. 6.1, Eq. 5.1 and Eq. 5.30) and enable an energy dependent widths Eq. 3.17, Eq. 3.20 and Eq. 3.22 but only in the denominator of the resonances, that is more realistic regards the description of the self energy but with the observations done regards the violation of the electromagnetic gauge invariance made above. This approach is assumed for several works. As can be seen from the dashed lines the behavior is improved in the first channel where the direct resonance contribution (that is the dressed by the self energy) contributes appreciably due to the isospin coefficients. Finally within the CMS approach, we exclude the off-shell contribution in Eq. 6.1 for the $3/2$ resonances, and as can be seen the theoretical results fall bellow the experimental data (in the first channel below BNL data) as shown in the dotted lines. This should be the results obtained if one uses an inconsistent spin $3/2$ model, regards $A-$independence of amplitudes, as mentioned above. All this indicates that it is necessary to use a FF if we wish to keep us within

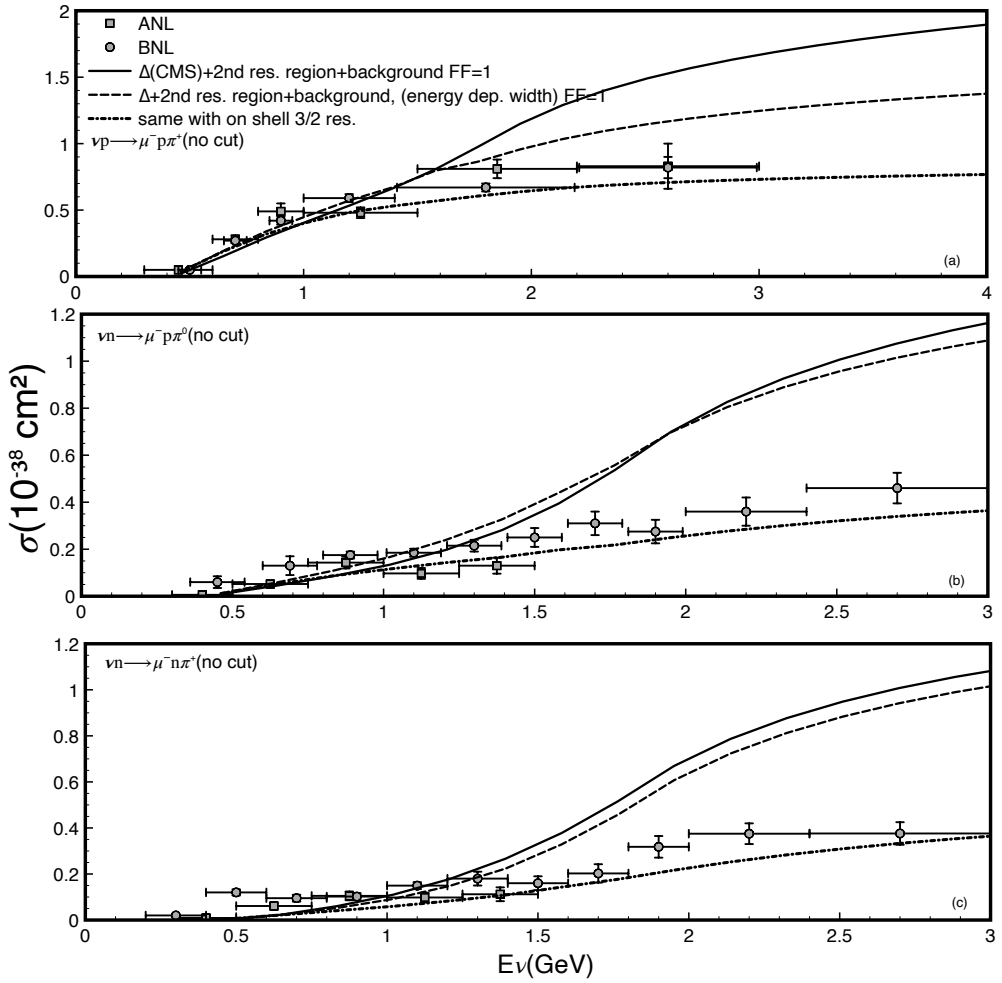


**Figure 6.5:** Results within CMS with FF=1. Total $\nu N$ cross section as function of the neutrino energy for different channel. The Figure show the three channels of interest for the single pion production, where (a) $\nu p \to \nu^- p\pi^+$ process, (b) $\nu n \to \nu^- p\pi^0$ process, (c) $\nu n \to \nu^- n\pi^+$process.

a consistent treatment.

Now, that we have established the necessity of a FF to work within a spin $3/2$ consistent model we discuss with more detail the calculations without cuts. As we will see in the Fig. 6.5 the models used to treat the $3/2$ propagator leads to different results, not losing sight that only the CMS preserves electromagnetic gauge invariance. First we use the CMS approach with a constant width, second keeping the same propagators structure but with the energy dependent widths only in the denominators. Finally we change to the exact propagator given in Eq. 3.14 only for the $\Delta$ resonance with the same energy dependent width, without affecting the other resonances (more energetic and less important). The global FF Eq. 6.3 will affect the full amplitude as explained above. Results are shown in Figs. 6.6. As can be seen, the tendency of increasing the cross section by the second resonant contribution is persistent and the results that better reproduce the data is still the CMS approach. If we calculate the $\chi^2/dof$ throughs out, we get the same conclusions in the Fig. 6.4, it is clear that

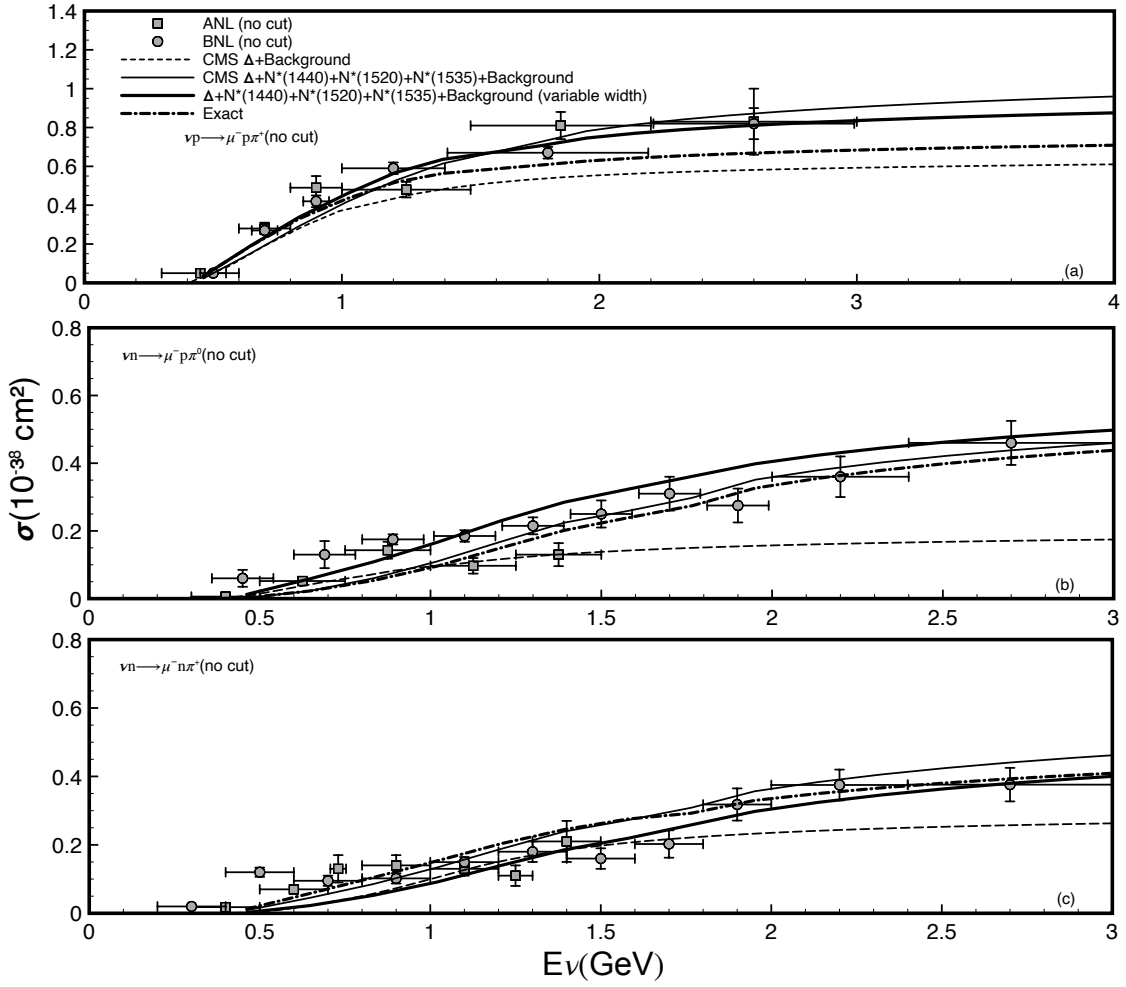


**Figure 6.6:** Total $\nu N$ cross section as function of the neutrino energy for a no cut in $M_{\pi N}$ for the three channels of interest for the single pion production. We also show here results within the CMS, variable width, and exact approach for the $\Delta$ with energy dependent width, where for the pannels (a) $\nu p \to \nu^- p\pi^+$ process, (b) $\nu n \to \nu^- p\pi^0$ process, (c) $\nu n \to \nu^- n\pi^+$process.

the CMS approach has a better global approximation for the data centroids and the results in this case is for ANL data $0.4(0.90)$, $1.1(1.1)$, $1.0(1.3)$ for the three channels mentioned above and the CMS (variable width) approaches, and for the BNL data $0.6(0.9)$, $0.7(0.4)$, $0.8(1.0)$ respectively.

In order to understand why the CMS gives the better results we note what follows.The exact propagator is obtained from a solution of the Schwinger–Dyson equation, if we do not make any approximation to the solution we get the exact propagator. In the same way the $T-$matrix and amplitude for the weak pion production process should be obtained form the relativistic Bethe-Salpeter equation. If one do so, rescattering contributions should emerge and using adequate regularizing FF we would to get an ‘’exact” total amplitude valid to all order. Nevertheless we use a background at tree label that does not consider the rescattering and that is an approximation. In this way, the CMS constant width approach is more consistent with the approach implemented for the total

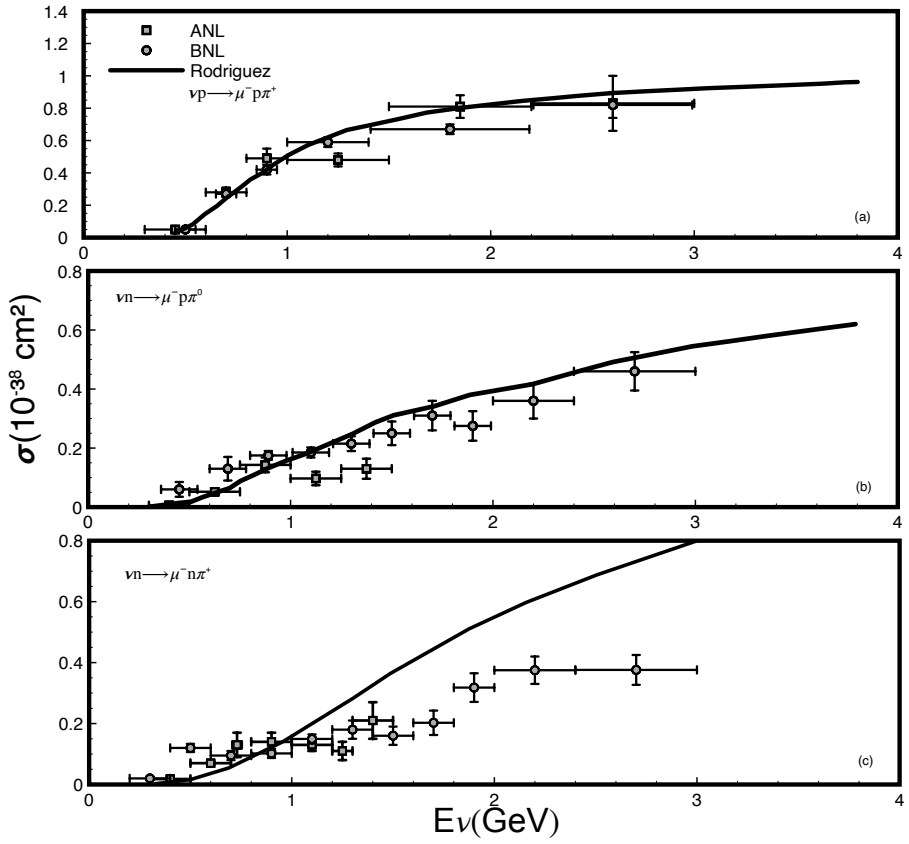


**Figure 6.7:** GENIE prediction [19] for the three single pion production channels of interest, and is compared to the corrected ANL and BNL data, where for the pannels (a) $\nu p \to \nu^- p\pi^+$ process, (b) $\nu n \to \nu^- p\pi^0$ process, (c) $\nu n \to \nu^- n\pi^+$process .

amplitude. When we enable an energy dependent width we see a change that depends on the channel diminishing the results in the main one (first panel of Fig. 6.6 ) and growing and diminishing in the other two (second an third panels of Fig. 6.6 ). The parameters used for the $\Delta$ resonance $(f_{\pi N\Delta}, m_\Delta, \Gamma_\Delta, G_E, G_M, C_A^5)$ have been fitted using the CMS approach with a constant width, and thus if one wish to use another approach a new fitting should be done. This could explain why the best approach to data is done with the simpler CMS model, which is the only fully consistent approach that enable to satisfy the Ward identities in the electromagnetic case. In another works it is possible that the inconsistency in the use of the Feynman rules for the $3/2$ resonances plus the inconsistence in using energy dependent widths compensate at the moment of get results. So, when one only looks for the proximity to the data in the results, it is possible to get coincidence with inconsistent models. We have analyzed if Figs. 6.5 and 6.6 the effects of these inconsistencies. In addition, is evident that the FF taken from NC pion productions also works very well here.

Finally In Fig. 6.7, and for the sake of comparison, we show the result reported in [19], where It is clear of the Figure that the nominal GENIE prediction cannot describe all of the pion production channels well for

the reanalyzed datasets. We can check that for the total cross section in the three above mentioned channels we get for ANL $0.4(1.13)$, $1.1(0.34)$, $1.0(2.6)$ and for BNL $0.6(1.9)$, $0.7(0.8)$, $0.8(5.2)$ results for the $\chi^2/dof$ within the CMS (Genie) models, what support that our model is working overall better.

### 6.2.2 ANTINEUTRINOS

Now, in order to follow probing our model we wish to calculate the antineutrinos total cross section. We have two differences regards the neutrinos case. Firstly, the interactions of neutrinos with hadrons is not the same that for antineutrinos. We have a sign of difference in the lepton current contraction that makes a different coupling with the hadron ones. Then, the interaction with neutrinos is different from antineutrinos due the use of spinors for antiparticles in Eq. 4.14 and has nothing to do with the well-known CP violation. Secondly, in the experiment we have the detector of an admixture of heavy freon $CF_3Br$ that was exposed to the CERN PS antineutrino beam (peaked at $E_{\bar{\nu}} \sim 1.5$ GeV). It is informed that we have $0.44\%$ on neutrons and $0.55\%$ of protons, and since our calculations were for free nucleons we weight out results with this percentages depending on the channel. Firstly we only show results within the CMS approach with all resonances for a cutoff $W_\pi N \equiv M_\pi N = 1.4$ GeV, and we can be seen that the data is well reproduced but barely bellow the center of error bars. Secondly, we show results without cuts and with the global FF. In the second Figure we have the CMS with only the $\Delta$ and the $\Delta$ plus the other resonances, showing an appreciable difference. Adding the energy dependent width we get an improvement [67], but at the expense of a violation of electromagnetic gauge invariance. Our results compared with the data are shown in Figs. 6.8 and 6.9.

## 6.2 DIFFERENTIAL CROSS SECTION

Now, as for the fitting of the $\Delta$ parameters [47] the flux averaged differential cross section $< d\sigma/dQ^2 >$ it is used, we show the results within our model and compare with the more recent experimental data where ANL and BNL old results are reanalyzed and put in accordance [19]. In that reference results are shown for the event $Q^2$ distribution in units of Events/GeV$^2$ for Both ANL and BNL experiments. As our results are given in $10^{-38}$ cm$^2$/GeV$^2$ we use the same conversion factor found in the total cross section calculation to compare with the data. These data are reported without cuts. We first compare with ANL results that were originally measured without cuts and this comparison is shown in Fig. 6.10. We show calculations within, the CMS approach and omit the Exact one since as mentioned above, a readjusting of the full set of the $\Delta$ parameters should be necessary [59], while for the energy dependent width approach this reffiting though necessary it shouldn't be crucial since we are keeping the same structure of the CMS propagator but with the width's replacement only

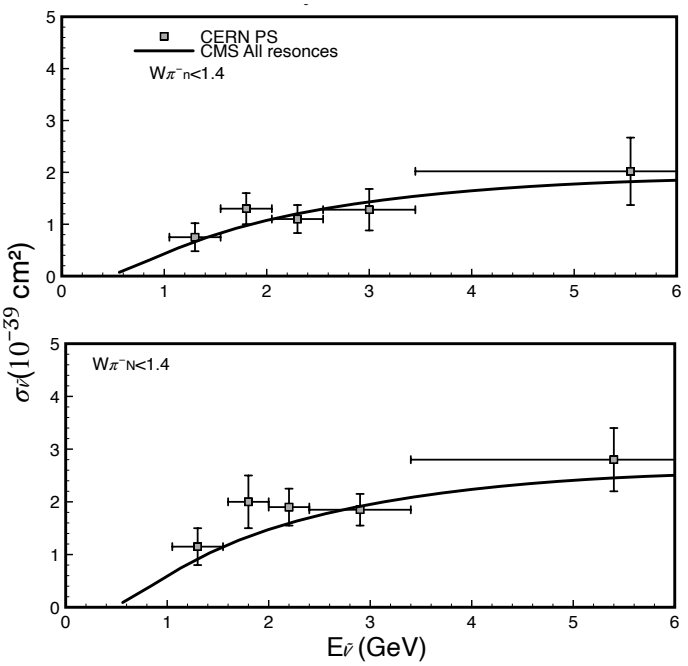


**Figure 6.8:** Antineutrino's total cross sections with a cut in 1.4 GeV for the $\bar{\nu}n \to \mu^+ n\pi^-$ and that leadding to a final $N\pi^-$ final state.

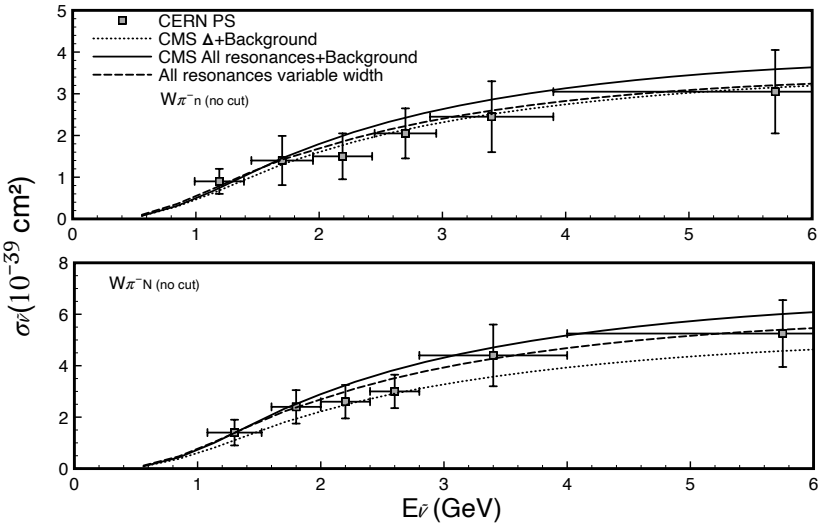


**Figure 6.9:** Antineutrino's total cross sections for the $\bar{\nu}n \to \mu^+ n\pi^-$ and that leadding to a final $N\pi^-$ final state without energy cut.

in denominators. As can be seen, results within the constant width CMS are acceptable in the three channels, remember we are not doing any fit (the fixing of $C_A^5$was done previuolsy [47] using the ANL data with cuts $M_{\pi N} < 1.4$ GeV [65]). If we compare with Genie results [19], as before for the total cross section, we get

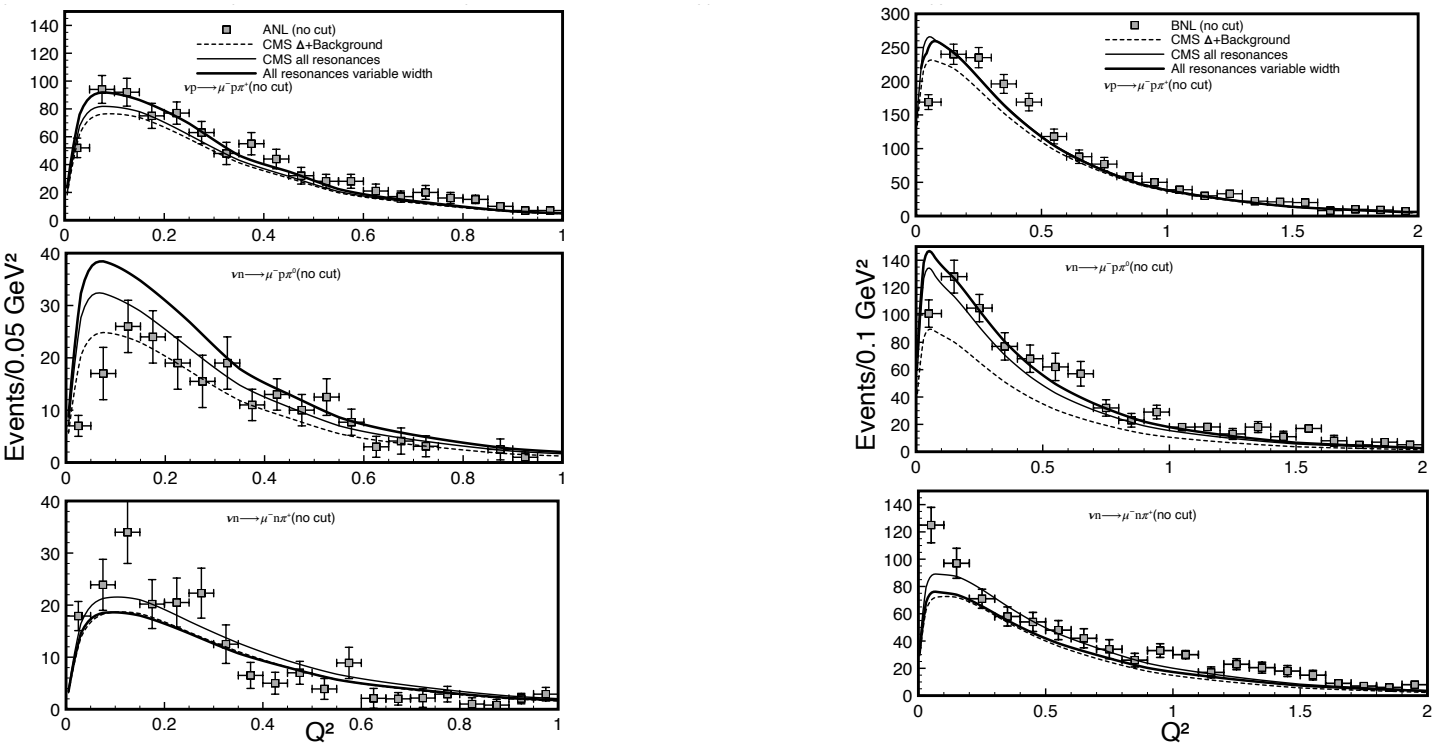


**Figure 6.10:** Differential cross section without cuts in the final $M_{\pi N}$ invariant mass. On the left we have the results for the ANL experiment and on the right for the BNL experiment. Results within the constant width CMS approach for the $\Delta + B$ and $\Delta + P_{11} + D_{13} + S_{11} + B$ amplitudes are considered. Also results for the last amplitude with energy dependent width is shown. Data are taken from Ref. [64].

better global reproduction of data.The using of energy dependent width enlarges the first and second channels theoretical results and diminishes those for the third one, this leads to a worse coincidence with data in an amount depending on the considered experiment ANL or BNL. Remember that this is an inconsistent approach used by several works.

## 6.1 CONCLUSIONS

Along this thesis work we have tackled the description of weak pion production within consistent effective models from the point of view of the treatment of resonances described by spin $3/2$ fields. In addition, we have discussed as to include resonances in the second energy region and, how to treat the structure of hadrons when $M_{\pi N}$ grows and the effect of more energetic resonances not included in the model.

We showed how to get the exact dressed propagator for a spin $3/2$ resonance including only the $\pi N$ loop in the self energy. From this, we can generate different approaches that have each one certain advantages and shortcomings. The complex mass scheme (CMS) where this approach is equivalent to the replacement $m_R \to m_R - \frac{i}{2}\Gamma_R^{CMS}$ (with constant values for the mass and width) in the unperturbed propagator of the resonance $R$ in *all places*. It is obtained keeping terms until $g^2 = \left(\frac{f_{\pi N\Delta}}{m_\pi}\right)^2$ in the coefficients of the exact propagator and evaluate the width as $\Gamma_R(\sqrt{s} \approx m_R)$. We use this approach also for the spin$-1/2$ resonances. This means that the effect of the self energy on the spin $\left\{\frac{1}{2}, \frac{3}{2}\right\}$ mathematical structure is not affected and that the resonance width is assumed constant. This approach has the advantage that with it is is possible fulfill the Ward identities that relates propagators and vertexes for radiation from a resonance, and thus this enables to keep gauge invariance. In a next step, we kept the same structure of the propagator but enabling the energy dependence in the width but only in the denominators, an approach very used in several works and that violates gauge invariance. Finally we probe the effects of using the exact structure of the propagator for the $\Delta$ (the most important) with the energy dependent width, nevertheless in this case a readjustment of the $\Delta$ parameters should be done.

In all the mentioned approaches we have respected the consistence between vertexes and propagators regards the contact transformations, for the spin $3/2$ field. It is important to note that for the first time the parametrization of Sachs was used for the $D_{13}$ resonance, where the $G_E(Q^2=0), G_M(Q^2=0), C_5^A(Q^2=0)$ values where obtained by comparison with the usually adopted parity conserving parametrization.

Firstly, we achieved the comparison with the data of the ANL experiment in the region of $M_{\pi N} < 1.4, 1.6$ GeV, where we have worked within the CMS approach without FF. From the results including and not including resonances in the second resonance region, we conclude that in spite that the fitting of $C_5^A$ is not affected to explain the data, in this region they should be included. Moreover, in the case $M_{\pi N} < 1.4$ one can think why ? This second resonance region influences due to the tail of the resonances that have their centroids out of this region but contribute through the interference effects with the $\Delta$ and backgrounds. Finally, to make the calculations with no cuts we show the need of using a common FF that was also successfully used in pion photo-

production NC and calculations [33, 60]. This FF takes into account the hadron structure of the final $\pi N'$pair and the rescattering into both nonresonant terms and more energetic resonances. In this case in addition to the CMS approach we show results with the energy dependent width (replaced only in the denominator) and the exact propagator with energy dependent width. In order to define which of the different approaches works properly, taking into account the mentioned problems with the last two approaches and because many works use the second one. You would think that the exact approach would be the best, however the constant width CMS works best.. This could be because the $\Delta$ parameters were obtained with this prescription and because is the full consistent approach enabling gauge invariance. In addition, the exact approach introduces a more complex structure for the propagator who takes into account in the more realistic way the rescattering through intermediate $\pi N$ loops of the direct $\Delta$ amplitude. Nevertheless, neither the cross term nor the other background contributions are dressed as should be, in a T-matrix calculation (that is out of the scope of this thesis work) generating a not consistent treatment of all remaining contributions that are introduced at tree level. For this it seems better to conserve the simpler CMS and introduce the common FF.

Then results for the flux averages cross section $\left\langle \frac{d\sigma}{dQ^2} \right\rangle$ and total cross section for antineutrinos where reported.

Now, we analyze the quality of our results and compare with other calculations putting emphasis in the obtained advantages and differences, objects of this thesis work. As can be seen from a general view, our model meets consistency with respect to contact transformations in the $3/2$ field reproduce better the ANL data than other inconsistent models including the second resonance region [20]. In addition, in that reference it seems that the cross resonance contributions are omitted for the $\nu p \to \mu^- \pi^+ p$ channel. It is true that the direct contribution of isospin $1/2$ resonances cannot contribute to a $3/2$ isospin amplitude but the cross terms do contribute, note the isospin factor for this channel that is not zero in Eq. 6.5. A last shortcoming to mention is that for nonresonant backgrounds Figs 4.2(a)-(f) an arbitrary cutoff of $M_{\pi N} < 1.2$ GeV is applied changing artificially the behavior of these contributions independently from the rest of terms. This is done for all the presented regimes $M_{\pi N} < 1.4, 1.6$ GeV and no cut. Note that we can reproduce very well the first two energy ranges without the necessity of any special cutting, all contributions are calculated with the same $M_{\pi N}$ cutting, while for the uncutted case we include a *common FF.* In addition, we note that in Ref. [20] the antineutrino results are not reproduced, while within our model the accordance with the data is very well in all the energy region where the data is reported. Finally in that reference differential cross section is not reported.

On the other hand in GENIE simulation [19], single pion production is separated into resonant and non-resonant terms, with interference terms between them neglected, as also interferences between resonances

are neglected in the calculation. The resonant component (RES) is a modified version of the RS model [26]. In the original RS model, the production and subsequent decay of 18 nucleon resonances with invariant masses $W \leq 2.0$ GeV are considered. In GENIE, only 16 resonances are included, based on the recommendation of the Particle Data Group [27]. In this work they make the assumption that interactions on deuterium can be treated as interactions on quasi-free nucleons which are only loosely bound together, and so neglect FSI effects. In GENIE, there are a number of systematic parameters which can be varied to change the single pion production model. Resonant axial mass ($M_A^{RES}$) resonant normalization (RES norm) non-resonant normalization (DIS norm), and normalization of the axial form factor ($F^A(0)$). The total GENIE prediction is the incoherent sum of the RES and DIS contributions, where interference terms have been neglected. GENIE cannot describe all of the pion production channels well for the reanalyzed data sets. For example, the data of the $\nu_\mu n \to \mu^- p\pi^0, \nu_\mu n \to \mu^- n\pi^+$ channels are very similar, but there are large differences between the nominal GENIE predictions for these channels. The non-resonant component of the GENIE prediction, which contributes strongly to these channels, appears to be too large. Nevertheless, within our model these two channels are described properly without cuts, within the same regime presented by GENIE.

Finally, it can be seen from Fig. 3 of Ref. [19], where neutrino energy distribution is shown, that the nominal GENIE prediction fails to describe the low-$Q^2$ data well for some channels. We also note that the GENIE uncertainties are larger than the data suggests, and they may be reduced by tuning the GENIE model to the ANL and BNL data. Nevertheless, within our model the low $Q^2$ distribution seem to be right.

In resume we have described with a fully relativistic and consistent model from the point of view of contact transformation and gauge invariance, which includes interference between resonances and resonances with background contributions, total cross sections and averaging differential cross sections in different $M_{\pi N}$ ranges without new fitting but those done for the $\Delta$ resonances in the low cutting $M_{\pi N} < 1.4$ GeV one for neutrinos. Also, the antineutrino cross section was calculated. Our results give a reasonable description of the experimental data, and better that other approach that lack in one or several conditions that we are assume in our approach. These results we published recently in Refs. [68, 69]. Some ideas of improvement could be mentioned

- Remember that the axial $\Delta$ parameter $C_5^A(0)$ was fitted for $M_{\pi N} < 1.4$ GeV with only the $\Delta$ resonance included. Perhaps a new fitting including the other resonances would be necessary.

- When the invariant mass $M_{\pi N}$ is enlarged one could add new resonances gradually and fitting the corresponding axial parameters for them as was done for the $\Delta$.

- The rescattering should be introduced through a T-matrix formalism.

- Higher order derivative terms in the $\pi NR$ vertexes could be included since they are important in elastic $\pi N$ scattering [63].

# References


[1] S. L Glashow, Nucl. Phys, 22, 579-588, 1961; S. Weimberg, Phys. Rev. Lett, 19, 1264- 1266, 1967; A Salam, 1969, Proc. of the 8th Nobel Symposium on Elementary Particle Theory, Relativistic Groups and Analyticity, Sweeden, 1968, edited by N. Svartholm, p. 367-377.

[2] Janet M. Conrad, William C. Louis, and Michael H. Shaevitz, Annu. Rev. Nucl. Part. Sci. 2013, 63 pages 45-67.

[3] F. Reines and C.L. Cowan, The neutrino, Nature 178 (1956)446.

[4] C. H. Llewellyn Smith, Phys. Rep., 3, 261, 1972.

[5] P. Renton, Electroweak Interactions: an Introduction to the Physics of Quarks and Leptons, Cambridge University Press, 1990.

[6] Janet M. Conrad, William C. Louis, and Michael H. Shaevitz, Annu. Rev. Nucl. Part. Sci. 2013, 63 pages 45-67.

[7] A. A. Aguilar-Arevalo et al. [The MiniBooNE Col- laboration], Phys. Rev. Lett. 98, 231801 (2007).

[8] 1. B.Eberly et al.,Phys. Rev. D 92(9), 092008(2015).

[9] T. Le et al., Phys. Lett. B 749,130(2015).

[10] A. Aguilar-Arevalo et al., Phys. Rev. D 83, 052007 (2011).

[11] J. T. Sobczyk, J. Z˙muda, Phys. Rev. C 91(4), 045501 (2015).

[12] 5. U. Mosel, Phys. Rev. C 91(6), 065501 (2015).

[13] K. Graczyk, D. Kielczewska, P. Przewlocki, J. Sobczyk, Phys. Rev.D 80, 093001 (2009).

[14] E. Hernandez, J. Nieves, M. Valverde, M. Vicente, Vacas. Phys.Rev. D 81, 085046 (2010).

[15] M. Ahn et al., Phys. Rev. Lett. 90, 041801 (2003).

[16] K. Abe et al., Phys. Rev. D 88, 032002 (2013).

[17] O. Lalakulich, U. Mosel, Phys. Rev. C 87, 014602 (2013).

[18] C. Wilkinson, P. Rodrigues, S. Cartwright, L. Thompson, K. McFarland, Phys. Rev. D 90(11), 112017 (2014).

[19] Philip Rodrigues, Callum Wilkinson,and ,Kevin McFarland, Eur. Phys. J. C (2016) 76:474.

[20] M. Rafi Alam, M. Sajjad Athar, S. Chauhan and S. K. SinghInternational Journal of Modern Physics E Vol. 25, No. 2 (2016) 1650010 .

[21] E. Hernandez, J. Nieves, M. Valverde, M. Vicente, Vacas. Phys. Rev. D 81, 085046 (2010).

[22] O. Lalakulich, E. A. Paschos, and G. Piranishvili, Phys. Rev. D 74,(2006), 014009 .

[23] T. Leitner, O. Buss, L. Alvarez-Ruso, and U. Mosel, Phys. Rev. C 79,(2009).

[24] O. Lalakulich, T. Leitner, O. Buss, and U. Mosel, Phys. Rev. D 82, 093001 (2010)

[25] C. Andreopoulos, A. Bell, D. Bhattacharya, F. Cavanna, J. Dobson et al., Nucl. Instrum. Methods A A614,87 (2010).

[26] D. Rein, L.M. Sehgal, Ann. Phys. 133(1), 79 (1981).

[27] Review of Particle Physics,W.-M. Yao, et al, J. Phys. G 33 (2006) 1.

[28] K. Abe, et al.(T2K Collaboration), Phys. Rev. D 91(7) (2015) 072010.

[29] Rarita W. and Schwinger J. 1941 Phys.Rev.60 61

[30] J. D. Bjorken and S. D. Drell, Relativistic quantum mechanics (McGraw-Hill, New York, 1964).

[31] Torleif Ericson and Wolfram Weise. Pions and Nuclei. Oxford Science Publications 1988.

[32] Yorikiyo Nagashima Volume 1: Quantum Field theory and Particles. WILEY-VCH Verlag GmbH & Co. KGaA, Weinheim. 2010

[33] A. Mariano. Phys. Lett. B (2007) 253; A. Mariano, J. Phys. G (2007) 1627.

[34] T. Melde,L. Canton and W. Plessas, PRL 102, 132002 (2009).

[35] T. Feuster and U. Mosel, Phys. Rev. C 58, 457 (1998).

[36] T. Sato and T.-S. H. Lee, Phys. Rev. C 54, (1996) 2660.

[37] B. C. Pearce and B.K. Jennings, NuclearPhysicsA528 (1991) 655-675.

[38] A. Mariano, C. Barbero and G. López Castro, Nuc.Phys. A 849 (2011) 218.

[39] G. López Castro and G. Toledo Sánchez, Phys. rev D, VOLUME **61**, 033007, (2000)

[40] M .El Amiria, G. Loópez Castro and and J. Pestieau, Nucl. Phys. **A543** (1992) 673-684.

[41] A. Mariano, C. Barbero and D. Badagnani,J. Phys. G: Nucl. Part. Phys. 39 (2012) 035005 (11pp).

[42] [9] D. Badagnani, A. Mariano, and C. Barbero, J. Phys. G: Nucl. Part. Phys. 44, 025001 (2017).

[43] M. El-Amiri, G. López Castro, J. Pestieau, Nucl. Phys. A 543 (1992) 673.

[44] Beuthe M, Gonzalez Felipe R, Lopez Castro G and Pestieau J 1997 *Nucl. Phys.* A **543** 673

[45] Kaloshin A E and lomov V P 2006 *Phys. At. Nucl.* **69** 189

[46] J. Beringer *et al*. (Particle Data Group), Phys. Rev. D **86**, 010001 (2012).

[47] C. Barbero, A. Mariano, G. Lopez Castro. Physics letters B 664 (2008) 70-77.

[48] H. F. Jones, M. D. Scadron, Ann. Phys. 81 (1973) 1.

[49] T. Sato, D. Uno, T.-S.H Lee, Phys. Rev. C 67 (2003) 065201.

[50] T. R. Hemmert, B.R Holstein, Phys. Rev. D 51 (1995) 158.

[51] G. Lopez Castro, A. Mariano, Nucl. Phys. A 697 (2001)440.

[52] S. Nozawa, T.-S.H. Lee, Phys. Rev. C (1996) 2660.

[53] G. L. Fogli, G. Nardoulli. Nucl. Phys. B 160 (1979) 116.

[54] T. Sato, T-S.H Lee, Phys. Rev. C 63 (2001) 055201

[55] C. Barbero, A. Mariano, G. Lopez Castro. Physics Letters B 728 (2014) 282-287.

[56] M. Bermerrouche, R. M. Davidson, and N. C. Mukhopadhyay, Phys. Rev. C 39, 2339 (1989).

[57] A. Mariano, D. Badagnani, C. Barbero, and E. Berrueta Martinez, Phys. Rev. C 100, 024001 (2019).

[58] Nath L M, Etemadi B. and Kimel J. D. 1971 Phys. Rev. D 3 2153.

[59] C. Barbero and A Mariano, J. Phys. G: Nucl. Part. Phys. 42 (2015) 105104.

[60] A. Mariano, C. Barbero and G. López Castro, Nuclear Physics A 849 (2011) 218–244.

[61] E. Hernández, J. Nieves and M. Valverde, Phys. Rev. D 76, 033005 (2007).

[62] E. Hernandez and J. Nieves, Phys. Rev. D **95**, 053007 (2017).

[63] A. Mariano, C. Barbero, D. Badagnani, and D.F. Tamayo Agudelo, sent to Phys.Lett.B.

[64] T. Kitagaki,et al., Phys. Rev. D **34**, 2554 (1986).

[65] G. M. Radecky, et. al, Phys. Rev. D **25,** 1161 (1982).

[66] S. J. Barish et al., Phys. Rev. D **16**, 3103 (1977).

[67] T. Bolognese, J. P. Engel, J.L Guyonnet and J.L. Riester, Phys. Lett. 81B (1979),393.

[68] D. F. Tamayo Agudelo, A. Mariano and D. E. Jaramillo Arango, Phys. Rev. D 105, 033008 (2022).

[69] D. F. Tamayo Agudelo, A. Mariano and D. E. Jaramillo Arango, Phys. Rev. D 106, 033002 (2022).

# Appendix A

# DIRAC EQUATION FOR $SPIN-3/2-$ FIELDS

In this appendix we will look for the relativistic equations satisfied by the Rarita-Schwinger field and equivalents forms, useful for future developments in the thesis. Also we get the constrains that filters on-shell the spin 3/2 component. For many years there has been interest in studying spin$-3/2$ fields in order to describe nucleon resonances with spin$> 1/2$ particles. In the latter case, Dirac Equation has been shown to provide a reasonable starting basis for such studies. The formalism for spin$-3/2$ particles allows investigating the $\Delta$ and $D_{13}$ resonance. The Dirac Equation can de generalized to describe a general spin$-m/2$ particle, where $m = \pm 1, \pm 2, \pm 3, \ldots$, etc and w get it for the $3/2$ case.

Firstly we get an equivalent form of (1.29) and we start with the relations

$$\epsilon^{\sigma\mu\nu\rho}\epsilon_{\sigma\alpha\beta\delta} = -\delta^{\mu}_{\alpha}\delta^{\nu}_{\beta}\delta^{\rho}_{\delta} - \delta^{\mu}_{\beta}\delta^{\nu}_{\delta}\delta^{\rho}_{\alpha} - \delta^{\mu}_{\delta}\delta^{\nu}_{\alpha}\delta^{\rho}_{\beta} + \delta^{\mu}_{\beta}\delta^{\nu}_{\alpha}\delta^{\rho}_{\delta} + \delta^{\mu}_{\alpha}\delta^{\nu}_{\delta}\delta^{\rho}_{\beta} + \delta^{\mu}_{\delta}\delta^{\nu}_{\beta}\delta^{\rho}_{\alpha}, \tag{A.1}$$

$$\gamma^5\gamma_\sigma = -\tfrac{i}{6}\epsilon_{\alpha\beta\delta\sigma}\gamma^\alpha\gamma^\beta\gamma^\delta \tag{A.2}$$

where we can get that

$$\begin{aligned}
\gamma^5\epsilon^{\mu\nu\sigma\rho}\gamma_\sigma &= (\gamma^5\gamma_\sigma)\epsilon^{\mu\nu\sigma\rho} = \frac{i}{6}\epsilon_{\alpha\beta\delta\sigma}\epsilon^{\mu\nu\rho\sigma}\gamma^\alpha\gamma^\beta\gamma\delta \\
&= \left(-\delta^{\mu}_{\alpha}\delta^{\nu}_{\beta}\delta^{\rho}_{\delta} - \delta^{\mu}_{\beta}\delta^{\nu}_{\delta}\delta^{\rho}_{\alpha} - \delta^{\mu}_{\delta}\delta^{\nu}_{\alpha}\delta^{\rho}_{\beta} + \delta^{\mu}_{\beta}\delta^{\nu}_{\alpha}\delta^{\rho}_{\delta} + \delta^{\mu}_{\alpha}\delta^{\nu}_{\delta}\delta^{\rho}_{\beta} + \delta^{\mu}_{\delta}\delta^{\nu}_{\beta}\delta^{\rho}_{\alpha}\right)\gamma^\alpha\gamma^\beta\gamma^\delta \\
&= \frac{i}{6}\left(-\gamma^\mu\gamma^\nu\gamma^\rho - \gamma^\rho\gamma^\mu\gamma^\nu - \gamma^\nu\gamma^\rho\gamma^\mu + \gamma^\mu\gamma^\nu\gamma^\rho + \gamma^\mu\gamma^\rho\gamma^\nu + \gamma^\rho\gamma^\nu\gamma^\mu\right),
\end{aligned} \tag{A.3}$$

and with the anti-commutator $\{\gamma^\mu\gamma^\nu\} = 2g^{\mu\nu} \longrightarrow \gamma^\mu\gamma^\nu + \gamma^\nu\gamma^\mu = 2g^{\mu\nu}$, we can simplify the last result as

$$\gamma^\rho\gamma^\mu\gamma^\nu = 2g^{\mu\nu}\gamma^\rho - \gamma^\rho\gamma^\nu\gamma^\mu$$
$$\gamma^\nu\gamma^\rho\gamma^\mu = 2g^{\nu\rho}\gamma^\mu - \gamma^\rho\gamma^\nu\gamma^\mu$$
$$\gamma^\nu\gamma^\mu\gamma^\rho = 2g^{\mu\nu}\gamma^\rho - \gamma^\mu\gamma^\nu\gamma^\rho$$
$$\gamma^\mu\gamma^\rho\gamma^\nu = 2g^{\rho\nu}\gamma^\mu - \gamma^\mu\gamma^\nu\gamma^\rho.$$

and replacing in A.2, we get:

$$\frac{i}{6}(-\gamma^\mu\gamma^\nu\gamma^\rho - 2g^{\mu\nu}\gamma^\rho + \gamma^\rho\gamma^\nu\gamma^\mu - 2g^{\nu\rho}\gamma^\mu + \gamma^\rho\gamma^\nu\gamma^\mu$$
$$+ 2g^{\mu\nu}\gamma^\rho - \gamma^\mu\gamma^\nu\gamma^\rho + 2g^{\rho\nu}\gamma^\mu - \gamma^\mu\gamma^\nu\gamma^\rho + \gamma^\rho\gamma^\nu\gamma^\mu)$$

$$\frac{i}{6}(3\gamma^\rho\gamma^\nu\gamma^\mu - 3\gamma^\mu\gamma^\nu\gamma^\rho) = \frac{i}{2}(\gamma^\rho\gamma^\nu\gamma^\mu - \gamma^\mu\gamma^\nu\gamma^\rho). \tag{A.4}$$

The mass term in (1.29) can be written using the relation for $\sigma^{\mu\nu}$ as,

$$\frac{1}{2}m(\gamma^\mu\gamma^\nu - \gamma^\nu\gamma^\mu). \tag{A.5}$$

and collecting the equations A.4 and A.5 in 1.29, we have:

$$i\gamma^{\mu\nu\rho}\partial_\nu\psi_\rho - m\gamma^{\mu\nu}\psi_\nu = 0. \tag{A.6}$$

We can get another more equivalent useful form expanding the operators $\gamma^{\rho\nu\mu}$ and $\gamma^{\mu\nu}$ , getting (in the mo-

menta space $i\partial_\nu \to p_\nu$)

$$\begin{aligned}
\frac{1}{2}p_\nu\left(\gamma^\rho\gamma^\nu\gamma^\mu-\gamma^\mu\gamma^\nu\gamma^\rho\right)\psi_\rho-m\frac{1}{2}\left(\gamma^\mu\gamma^\nu-\gamma^\nu\gamma^\mu\right)\psi_\rho&=0,\\
\frac{1}{2}p_\nu\left(2g^{\mu\nu}\gamma^\rho-\gamma^\mu\gamma^\nu\gamma^\rho-2g^{\rho\mu}\gamma^\nu+\gamma^\mu\gamma^\rho\gamma^\nu\right)\psi_\rho-m\frac{1}{2}\left(\gamma^\mu\gamma^\rho-2g^{\mu\rho}+\gamma^\mu\gamma^\rho\right)\psi_\rho&=0,\\
\frac{1}{2}p_\nu\left(2g^{\mu\nu}\gamma^\rho-\gamma^\mu\gamma^\nu\gamma^\rho-2g^{\rho\mu}\gamma^\nu+2g^{\rho\nu}\gamma^\mu-\gamma^\mu\gamma^\nu\gamma^\rho\right)\psi_\rho-m\frac{1}{2}\left(2\gamma^\mu\gamma^\rho-2g^{\mu\rho}\right)\psi_\rho&=0,\\
\frac{1}{2}p_\nu\left(2g^{\mu\nu}\gamma^\rho-2\gamma^\mu\gamma^\nu\gamma^\rho-2g^{\rho\mu}\gamma^\nu+2g^{\rho\nu}\gamma^\mu\right)\psi_\rho-m\left(\gamma^\mu\gamma^\rho-g^{\mu\rho}\right)\psi_\rho&=0,\\
\left(-\gamma^\mu p_\nu\gamma^\nu\gamma^\rho+\left(p_\nu g^{\mu\nu}\gamma^\rho-p_\nu g^{\rho\nu}\gamma^\mu\right)+p_\nu\gamma^\nu g^{\mu\rho}\right)\psi_\rho-m\left(\gamma^\mu\gamma^\rho-g^{\mu\rho}\right)\psi_\rho&=0.
\end{aligned}$$

and finally obtaining

$$\boxed{\left(\gamma^\mu\not{p}\gamma^\rho-\left(p^\mu\gamma^\rho+p^\rho\gamma^\mu\right)-\not{p}g^{\mu\rho}\right)\psi_\rho+m\left(\gamma^\mu\gamma^\rho+g^{\mu\rho}\right)\psi_\rho=0}. \tag{A.7}$$

The solution $\psi_\nu$ for the Rarita-schwinger equation A.6 must satisfy the constraint conditions 1.6 y 1.7 of the $3/2-$spin field, to get them pre multiplying for $\gamma_\rho$ the equation A.6

$$\gamma_\rho\left(i\gamma^{\mu\nu\rho}\partial_\nu\psi_\rho-m\gamma^{\mu\rho}\psi_\rho\right)=0,$$

and solving in the first term we get

$$\begin{aligned}
\gamma_\rho\gamma^{\rho\nu\mu} &= \frac{1}{2}\left(\gamma_\rho\gamma^\rho\gamma^\nu\gamma^\mu-\gamma_\rho\gamma^\mu\gamma^\nu\gamma^\rho\right),\\
&= \frac{1}{2}\left(\left(\gamma_\rho\right)^2\gamma^\nu\gamma^\mu-\gamma_\rho\gamma^\mu 2g^{\nu\rho}+\gamma_\rho 2g^{\mu\rho}\gamma^\nu-\gamma_\rho\gamma^\rho\gamma^\mu\gamma^\nu\right),\\
&= \frac{1}{2}\left(4\gamma^\nu\gamma^\mu-\gamma_\rho\gamma^\mu 2g^{\nu\rho}+\gamma_\rho\left(2g^{\mu\rho}\gamma^\nu\right)-\left(\gamma_\rho\right)^2\gamma^\mu\gamma^\nu\right),\\
&= \frac{1}{2}\left(4\gamma^\nu\gamma^\mu-2\gamma^\nu\gamma^\mu+2\gamma^\mu\gamma^\nu-4\gamma^\mu\gamma^\nu\right),\\
&= \frac{1}{2}\left(2\gamma^\nu\gamma^\mu-2\gamma^\mu\gamma^\nu\right),
\end{aligned}$$

$$\boxed{\gamma_\rho\gamma^{\rho\nu\mu}=2\gamma^{\nu\mu}} \tag{A.8}$$

and in the second one

$$\begin{aligned}\gamma_\rho\gamma^{\mu\rho} &= \frac{1}{2}(\gamma_\rho\gamma^\mu\gamma^\rho - \gamma_\rho\gamma^\rho\gamma^\mu),\\ &= \frac{1}{2}(\gamma_\rho 2g^{\mu\rho} - \gamma_\rho\gamma^\rho\gamma^\mu - \gamma_\rho\gamma^\rho\gamma^\mu),\\ &= \frac{1}{2}(2\gamma^\mu - 4\gamma^\mu - 4\gamma^\mu),\end{aligned}$$

$$\boxed{\gamma_\rho\gamma^{\mu\rho} = -3\gamma^\mu}, \tag{A.9}$$

then, we have that

$$\gamma_\mu\left(p_\nu\gamma^{\mu\nu\rho} - m\gamma^{\mu\rho}\right)\psi_\rho = 0,$$

which implies that:

$$2p_\nu\gamma^{\nu\rho}\psi_\rho + 3m\gamma^\rho\psi_\rho = 0. \tag{A.10}$$

Now, premultiplying by $p_\mu$ the equation A.6

$$p_\mu\left(p_\nu\gamma^{\mu\nu\rho} - m\gamma^{\mu\rho}\right)\psi_\rho = 0, \tag{A.11}$$

the first term in A.11 should be zero, since we have the product of a symmetric part with another anti-symmetric, from this

$$mp_\mu\gamma^{\mu\rho}\psi_\rho = 0, \tag{A.12}$$

for any value of $p^\mu$ which indicates that $\gamma^{\mu\rho}\psi_\rho = \gamma^\mu(\gamma^\rho\Psi_\rho - \Psi_\mu) = 0$ and thus we have that the only unique solutions is:

$$\gamma^\rho\psi_\rho = 0. \tag{A.13}$$

Used it again in A.12 leads us to

$$p^{\rho}\psi_{\rho} = 0. \tag{A.14}$$

Since the physical field satisfies the constraint conditions 1.6 and 1.7, then the Rarita-Schwinger equation 1.28 becomes the equation $(\not{p} - m)\psi^{\nu} = 0$.

Now Performing a contact transformation on the fields ,

$$\psi_{\rho} \rightarrow \psi^{'}_{\rho} = \psi_{\rho} + a\gamma_{\rho}\gamma_{\mu}\psi^{\mu}, \tag{A.15}$$

with $a$ an arbitrary parameter, a field which satisfies A.13 is not affected and also the new fields $\psi'_{\rho}$ satisfy the same constraints:

$$p_{\rho}\psi^{'\rho} = 0,$$
$$\gamma_{\rho}\psi^{'\rho} = 0,$$

and also the Dirac equation,

$$\left(\not{p} - m\right)\psi^{'\rho} = 0,$$

therefore the components of $spin - 3/2-$ of the fields $\psi$ y $\psi'$ match.

# Appendix B

# SPIN$-3/2$ PROPAGATOR STRUCTURE

To find the propagator associated with the Rarita-Schwinger field, the kinetic operator must be inverted $\Lambda_{\mu\nu}$. To do this, it is convenient to rewrite this operator as a function of the projection operators that obey a simple algebra. To construct the projection operators we start from the orthogonal vectors found in the chapter 1.

$$p_1^\mu = \frac{p^\mu}{|p|} = \hat{p}^\mu \tag{B.1}$$

$$p_2^\mu = \frac{1}{\sqrt{3}}\left(\gamma^\mu - \not{p}\frac{p^\mu}{|p|^2}\right), \tag{B.2}$$

replacing B.1 in B.2 we find,

$$p_2^\mu = \frac{1}{\sqrt{3}}\left(\gamma^\mu - \not{p}\frac{\hat{p}_1^\mu}{|p|}\right) \longrightarrow \gamma^\mu = \sqrt{3}p_2^\mu + \frac{\not{p}}{|p|}\hat{p}_1^\mu, \tag{B.3}$$

$$\gamma^\mu = \sqrt{3}p_2^\mu + \hat{\not{p}}p_1^\mu, \tag{B.4}$$

without indexes can be written as:

$$\gamma = \sqrt{3}p_2 + \hat{\not{p}}p_1, \tag{B.5}$$

in the same way for the operator

$$\Lambda^{\mu\rho} = \left(\not{p} - m\right) g^{\mu\rho} + \gamma^{\mu}\not{p}\gamma^{\rho} - \left(p^{\mu}\gamma^{\rho} + \gamma^{\mu}p^{\rho}\right) + m\gamma^{\mu}\gamma^{\rho}, \tag{B.6}$$

without indexes can be written as

$$\Lambda = \left(\not{p} - m\right) + \gamma\not{p}\gamma - \left(p\gamma + \gamma p\right) + m\gamma\gamma. \tag{B.7}$$

It can be shown that $p_2^{\mu}$ y $\not{p}$ anti-commute

$$\begin{aligned}
\{p_2^{\mu}, \not{p}\} &= \frac{1}{\sqrt{3}}\left\{\left(\gamma^{\mu} - \frac{\not{p}p^{\mu}}{|p|^2}\right), \not{p}\right\} = \frac{1}{\sqrt{3}}\left(\gamma^{\mu}\not{p} - \not{p}p^{\mu}\frac{\not{p}}{|p|^2} + \not{p}\gamma^{\mu} - \not{p}\not{p}\frac{p^{\mu}}{|p|^2}\right) \\
&= \frac{1}{\sqrt{3}}\left(\gamma^{\mu}\not{p} - \not{p}\not{p}\frac{p^{\mu}}{|p|^2} + \not{p}\gamma^{\mu} - \not{p}\not{p}\frac{p^{\mu}}{|p|^2}\right) = \frac{1}{\sqrt{3}}\left(\gamma^{\mu}\not{p}\not{p}\gamma^{\mu} - 2p_{\mu}\right) \\
&= \frac{1}{\sqrt{3}}\left(\{\gamma^{\mu}, \not{p}\} - 2p^{\mu}\right) = \frac{1}{\sqrt{3}}\left(\{\gamma^{\mu}, \gamma^{\nu}\}\, p_{\nu} - 2p^{\mu}\right) \\
&= \frac{1}{\sqrt{3}}\left(2g^{\mu\nu}p_{\nu} - 2p^{\mu}\right) \\
&= 0.
\end{aligned}$$

likewise the commutator $\hat{p}_1$ y $\not{p}$ it is null

$$\left[\hat{p}_1, \not{p}\right] = \left[\frac{p^{\mu}}{|p|}, \not{p}\right] = \frac{p^{\mu}}{|p|}\not{p} - \not{p}\frac{p^{\mu}}{|p|} = \frac{p^{\mu}}{|p|}\not{p} - \frac{p^{\mu}}{|p|}\not{p} = 0.$$

Using B.5, we found a way to $\gamma\not{p}\gamma$.

$$\begin{aligned}
\gamma\not{p}\gamma &= \left(\sqrt{3}p_2 + \hat{\not{p}}p_1\right)\not{p}\left(\sqrt{3}p_2 + \hat{\not{p}}p_1\right) \\
&= 3p_2\not{p}p_2 + \sqrt{3}p_2\not{p}\hat{\not{p}}p_1 + \sqrt{3}\hat{\not{p}}p_1\not{p}p_2 + \hat{\not{p}}p_1\not{p}\hat{\not{p}}p_1 \\
&= -3\not{p}p_2p_2 + \sqrt{3}|p|p_2p_1 + \sqrt{3}|p|p_1p_2 + \not{p}p_1p_1,
\end{aligned} \tag{B.8}$$

where was used that $\not{p}\hat{\not{p}} = \not{p}\frac{\not{p}}{|p|} = \frac{|p|^2}{|p|} = |p|$, $\hat{\not{p}}\hat{\not{p}} = \left(\hat{\not{p}}\right)^2 = 1$, $\left\{p_2, \not{p}\right\} = 0$. On the other hand we have the

projectors $\Lambda^{\pm}$

$$\Lambda^{\pm} = \frac{1 \pm \hat{\not{p}}}{2}, \tag{B.9}$$

$$\tag{B.10}$$

with the properties

$$\Lambda^{+} + \Lambda^{-} = 1 \tag{B.11}$$

$$\Lambda^{+} - \Lambda^{-} = \hat{\not{p}}. \tag{B.12}$$

They allow to define the new projectors:

$$P^{\pm}_{ij} = p_i \Lambda^{\pm} p_j; \tag{B.13}$$

which satisfy the algebra

$$P^{\epsilon}_{ij} P^{\epsilon'}_{k\ell} = \delta_{jk} \delta^{\epsilon\epsilon'} P^{\epsilon}_{i\ell}, \tag{B.14}$$

the linear combinations of these projectors form a conjunct operators, whose product have as coefficients the matrix product of the coefficients of the multiplied operators.

Let,

$$A = a^{\epsilon}_{ij} P^{\epsilon}_{ij}$$

$$B = b^{\epsilon'}_{k\ell} P^{\epsilon'}_{k\ell}$$

$$AB = a^{\epsilon}_{ij} b^{\epsilon'}_{k\ell} P^{\epsilon}_{ij} P^{\epsilon'}_{k\ell} = a^{\epsilon}_{ij} b^{\epsilon'}_{k\ell} \delta_{j\ell} \delta^{\epsilon\epsilon'} P^{\epsilon}_{k\ell} = a^{\epsilon}_{ij} b^{\epsilon}_{jk} P^{\epsilon}_{ik}$$

$$a^{\epsilon}_{ij} b^{\epsilon'}_{k\ell} = c^{\epsilon}_{ik}$$

$$AB = c^{\epsilon}_{ik} P^{\epsilon}_{ik}$$

The first term of B.8, can be written:

$$\not{p} p_2 p_2 = -p_2 \not{p} p_2 = -p_2 |p| \hat{\not{p}} p_2 = -|p| p_2 \hat{p} p_2,$$

with $\Lambda^+ - \Lambda^- = \hat{\not{p}}$

$$\begin{aligned} \not{p} p_2 p_2 &= -|p| p_2 \left(\Lambda^+ - \Lambda^-\right) p_2 \\ &= -|p| \left[p_2 \Lambda^+ p_2 - p_2 \Lambda^- p_2\right] \\ &= -|p| \left[P_{22}^+ - P_{22}^-\right]. \end{aligned} \tag{B.15}$$

The second term can be written:

$$|p| p_2 p_1 = |p| p_2 \left[\Lambda^+ + \Lambda^-\right] p_1 = |p| \left[P_{21}^+ + P_{21}^-\right]. \tag{B.16}$$

The third term can be written as:o:

$$|p| p_1 p_2 = |p| p_1 \left[\Lambda^+ + \Lambda^-\right] p_2 = |p| \left[P_{12}^+ + P_{12}^-\right], \tag{B.17}$$

the fourth term can be written as:

$$\not{p} p_1 p_1 = |p| p_1 \left[\Lambda^+ - \Lambda^-\right] p_1 = |p| \left[P_{11}^+ - P_{11}^-\right]. \tag{B.18}$$

collecting all the terms, $\gamma \not{p} \gamma$ can be written as:

$$\gamma \not{p} \gamma = 3|p| \left[P_{22}^+ - P_{22}^-\right] + |p| \left[P_{11}^+ - P_{11}^-\right] + \sqrt{3}|p| \left[P_{21}^+ + p_{21}^- + P_{12}^+ + P_{12}^-\right], \tag{B.19}$$

which in matrix form can be written as:

$$\gamma \not{p} \gamma = \sum_{ij} a_{ij}^{\pm} P_{ij}^{\epsilon}, \tag{B.20}$$

$$a_{ij}^{\pm} = |p| \begin{bmatrix} \pm 1 & \sqrt{3} \\ \sqrt{3} & \pm 3 \end{bmatrix}. \tag{B.21}$$

The term $p\gamma+\gamma p$ in B.7 can be written as:

$$\begin{aligned} p\gamma+\gamma p &= p\left(\sqrt{3}p_2+\hat{\not{p}}p_1\right)+\left(\sqrt{3}p_2+\hat{\not{p}}p_1\right)p \\ &= |p|p_1\left(\sqrt{3}p_2+\hat{\not{p}}p_1\right)+\left(\sqrt{3}p_2+\hat{\not{p}}p_1\right)|p|p_1 \\ &= |p|\left(\sqrt{3}p_1p_2+p_1\hat{\not{p}}p_1+\sqrt{3}p_2p_1+\hat{\not{p}}p_1p_1\right) \\ &= |p|\left(\sqrt{3}p_1p_2+p_1\hat{\not{p}}p_1+\sqrt{3}p_2p_1+p_1\hat{\not{p}}p_1\right) \\ &= |p|\left(\sqrt{3}P_{12}+\left(P_{11}^{+}-P_{11}^{-}\right)+\sqrt{3}P_{21}+\left(P_{11}^{+}-P_{11}^{-}\right)\right), \end{aligned} \tag{B.22}$$

which in matrix form can be written as:

$$b_{ij}^{\pm}=-|p|\begin{bmatrix}\mp 2 & -\sqrt{3}\\ -\sqrt{3} & 0\end{bmatrix}. \tag{B.23}$$

For the last term $m\gamma\gamma$ we have

$$\begin{aligned} m\gamma\gamma &= m\left(\sqrt{3}p_2+\hat{\not{p}}p_1\right)\left(\sqrt{3}p_2+\hat{\not{p}}p_1\right) \\ &= m\left(3p_2p_2+\sqrt{3}p_2\hat{\not{p}}p_1+\sqrt{3}\hat{\not{p}}p_1p_2+\hat{\not{p}}p_1\hat{\not{p}}p_1\right) \\ &= m\left(3p_2p_2+\sqrt{3}p_2\hat{\not{p}}p_1+p_1\hat{\not{p}}p_2+p_1\hat{\not{p}}\hat{\not{p}}p_1\right) \\ &= m\left(3P_{22}+\sqrt{3}\left(P_{21}^{+}-P_{21}^{-}\right)+\sqrt{3}\left(P_{12}^{+}-P_{12}^{-}\right)+P_{11}\right), \end{aligned} \tag{B.24}$$

which in matrix form can be written as:

$$c_{ij}^{\pm}=m\begin{bmatrix}1 & \pm\sqrt{3}\\ \pm\sqrt{3} & 3\end{bmatrix}. \tag{B.25}$$

For the term $\left(\not{p}-m\right)\left(g^{\mu\nu}+P_{11}+P_{22}\right)$, we have

$$\left(\not{p}-m\right)\left(g^{\mu\nu}+P_{11}+P_{22}\right) = \left(\not{p}-m\right)g^{\mu\nu}+\left(\not{p}-m\right)\left(P_{11}+P_{22}\right), \tag{B.26}$$

where,

$$\begin{aligned}\left(\not{p}-m\right)\left(P_{11}+P_{22}\right) &= \not{p}P_{11}+\not{p}P_{22}-mp_{11}-mP_{22}\\ &= |p|\hat{\not{p}}p_1p_1+|p|\hat{\not{p}}p_2p_2-mP_{11}-mP_{22}\\ &= |p|p_1\hat{\not{p}}p_1-|p|p_2\hat{\not{p}}p_2-mP_{11}-mP_{22}\\ &= |p|\left(P_{11}^{+}-P_{11}^{-}\right)-|p|\left(P_{22}^{+}-P_{22}^{-}\right)-mP_{11}-mP_{22}. \end{aligned} \tag{B.27}$$

which in matrix form can be written as:

$$d_{ij}^{\pm}=|p|\begin{bmatrix}\pm1 & 0\\ 0 & \mp1\end{bmatrix}+m\begin{bmatrix}-1 & 0\\ 0 & -1\end{bmatrix}, \tag{B.28}$$

adding the four matrices $a_{ij}^{\pm}+b_{ij}^{\pm}+c_{ij}^{\pm}+d_{ij}^{\pm}$ we have

$$|p|\begin{bmatrix}\pm1 & \sqrt{3}\\ \sqrt{3} & \pm3\end{bmatrix}+|p|\begin{bmatrix}\mp2 & -\sqrt{3}\\ -\sqrt{3} & 0\end{bmatrix}+m\begin{bmatrix}1 & \pm\sqrt{3}\\ \pm\sqrt{3} & 3\end{bmatrix}+|p|\begin{bmatrix}\pm1 & 0\\ 0 & \mp1\end{bmatrix}+m\begin{bmatrix}-1 & 0\\ 0 & -1\end{bmatrix}, \tag{B.29}$$

$$|p|\begin{bmatrix}\pm1\mp\pm1 & \sqrt{3}-\sqrt{3}\\ \sqrt{3}-\sqrt{3} & \pm3\mp1\end{bmatrix}+m\begin{bmatrix}1-1 & \pm\sqrt{3}\\ \pm\sqrt{3} & 3-1\end{bmatrix}=|p|\begin{bmatrix}0 & 0\\ 0 & \pm2\end{bmatrix}+m\begin{bmatrix}0 & \pm\sqrt{3}\\ \pm\sqrt{3} & 2\end{bmatrix} \tag{B.30}$$

$$=\begin{bmatrix}0 & \pm\sqrt{3}m\\ \pm\sqrt{3}m & \pm2|p|+2m\end{bmatrix}, \tag{B.31}$$

what can be written as:

$$\begin{aligned}\pm\sqrt{3}\pm\sqrt{3}m\pm2|p|+2m &= \pm\sqrt{3}m\left(P_{12}^{+}-P_{12}^{-}\right)\pm\sqrt{3}m\left(P_{21}^{+}-P_{21}^{-}\right)\pm2|p|\left(P_{22}^{+}-P_{22}^{-}\right)+2mP_{22}\\ &= \pm\sqrt{3}m\left(P_{12}^{*}+P_{21}^{*}\right)\pm2|p|P_{22}^{*}+2mP_{22}, \end{aligned} \tag{B.32}$$

where $P_{12}^{*} = P_{12}^{+} - P_{12}^{-}$. So finally we can write $\Lambda$ as

$$\begin{aligned}
\Lambda &= \left(\not{p} - m\right) + \gamma \not{p} \gamma - (p\gamma - \gamma p) + m\gamma\gamma \\
&= \sqrt{3} m \hat{\not{p}} \left(P_{12} + P_{21}\right) + 2\hat{\not{p}}|p| P_{22} + 2m P_{22} + \left(\not{p} - m\right) P_{3/2} \\
&= 2\left(\not{p} + m\right) P_{22} + \sqrt{3} m \hat{\not{p}} \left(P_{12} + P_{21}\right) + \left(\not{p} - m\right) P_{3/2}. \qquad \text{(B.33)}
\end{aligned}$$

The propagator is the Green function, G$= \Lambda^{-1}$, $\Lambda$ transform as $\Lambda(a) = R(a)\Lambda R(a)$, then $\Lambda(a)^{-1} = R(a)^{-1}\Lambda^{-1}R(a)^{-1}$ so,

$$\begin{aligned}
\Lambda &= \Lambda_{3/2} + \Lambda_{1/2} \\
&= \left(\not{p} - m\right) P_{3/2} + 2\left(-\not{p} - m\right) P_{22} + \sqrt{3} m \hat{\not{p}} \left(P_{12} - P_{21}\right), \qquad \text{(B.34)} \\
& \qquad \text{(B.35)}
\end{aligned}$$

and then the propagator can be written as:

$$\Lambda^{-1} = \frac{1}{\not{p} - m} P_{3/2} + \begin{bmatrix} 0 & \pm\sqrt{3}m \\ \pm\sqrt{3}m & 2|p| + 2m \end{bmatrix}^{-1}, \qquad \text{(B.36)}$$

where we must find the inverse of the matrix in B.36. Taking into account the inverse of a matrix that can be found as $\begin{bmatrix} a & -b \\ -c & d \end{bmatrix}^{-1} = \frac{\begin{bmatrix} d & b \\ c & a \end{bmatrix}}{(ad - bc)}$, then,

$$\begin{bmatrix} 0 & \pm\sqrt{3}m \\ \pm\sqrt{3}m & \pm 2|p| + 2m \end{bmatrix}^{-1} = \frac{\begin{bmatrix} \pm 2|p| + 2m & \mp\sqrt{3}m \\ \mp\sqrt{3}m & 0 \end{bmatrix}}{3m^2} \qquad \text{(B.37)}$$

$$\Lambda^{-1} = \frac{1}{\not{p} - m} P_{3/2} + \frac{\left(2\not{p} + 2m\right) P_{11} - \sqrt{3}\left(P_{12}^{*} + P_{21}^{*}\right)}{3m^2}. \qquad \text{(B.38)}$$

And as can be seen this is the expression for the propagator in Eq. 3.2

# Appendix C

# ISOSPIN COEFFICIENTS

In this Appendix we calculate the isospin elements $\mathcal{T}$ for the equation 4.17 in three channel of pion−production

$$\nu_{\mu^-} p \to \mu^- p\pi^+ \tag{C.1}$$

$$\nu_{\mu^-} n \to \mu^- n\pi^+ \tag{C.2}$$

$$\nu_{\mu^-} n \to \mu^- p\pi^0 \tag{C.3}$$

$$\mathbf{W}^{\pm} = \mp\frac{1}{\sqrt{2}} \begin{pmatrix} 1 \\ \pm i \\ 0 \end{pmatrix} \tag{C.4}$$

$$\boldsymbol{\tau}_1 = \begin{pmatrix} 0 & 1 \\ 1 & 0 \end{pmatrix}, \quad \boldsymbol{\tau}_2 = \begin{pmatrix} 0 & -i \\ i & 0 \end{pmatrix}, \quad \boldsymbol{\tau}_3 = \begin{pmatrix} 1 & 0 \\ 0 & -1 \end{pmatrix} \tag{C.5}$$

**Process** $\nu_{\mu^-} p \to \mu^- p\pi^+$

$$\mathcal{T}_1(m,m') = \chi^{\dagger}(m')(\boldsymbol{\tau}\cdot\mathbf{W}^*)(\boldsymbol{\tau}\cdot\boldsymbol{\phi}_{\pi}^*)\chi(m)$$

$$(\boldsymbol{\tau}\cdot\mathbf{W}^*)(\boldsymbol{\tau}\cdot\boldsymbol{\phi}_{\pi}^*) = -2 \begin{pmatrix} 1 & 0 \\ 0 & 0 \end{pmatrix} \tag{C.6}$$

$$\mathcal{T}_1(1/2,1/2) = -2\begin{pmatrix} 1 & 0 \end{pmatrix}\begin{pmatrix} 1 & 0 \\ 0 & 0 \end{pmatrix}\begin{pmatrix} 1 \\ 0 \end{pmatrix} = -2 \tag{C.7}$$

**Process** $\nu_{\mu^-} n \to \mu^- n\pi^+$

$$\mathcal{T}_1(m,m') = \chi^\dagger(m')(\boldsymbol{\tau}\cdot\mathbf{W}^*)(\boldsymbol{\tau}\cdot\boldsymbol{\phi}_\pi^*)\chi(m)$$

$$(\boldsymbol{\tau}\cdot\mathbf{W}^*)(\boldsymbol{\tau}\cdot\boldsymbol{\phi}_\pi^*) = -2\begin{pmatrix} 1 & 0 \\ 0 & 0 \end{pmatrix} \tag{C.8}$$

$$\mathcal{T}_1(-1/2,-1/2) = -2\begin{pmatrix} 0 & 1 \end{pmatrix}\begin{pmatrix} 1 & 0 \\ 0 & 0 \end{pmatrix}\begin{pmatrix} 0 \\ 1 \end{pmatrix} = 0 \tag{C.9}$$

**Process** $\nu_{\mu^-} n \to \mu^- p\pi^0$

$$\mathcal{T}_1(m,m') = \chi^\dagger(m')(\boldsymbol{\tau}\cdot\mathbf{W}^*)(\boldsymbol{\tau}\cdot\boldsymbol{\phi}_\pi^*)\chi(m)$$

$$(\boldsymbol{\tau}\cdot\mathbf{W}^*)(\boldsymbol{\tau}\cdot\boldsymbol{\phi}_\pi^*) = -\frac{2}{\sqrt{2}}\begin{pmatrix} 0 & -1 \\ 0 & 0 \end{pmatrix} \tag{C.10}$$

$$\mathcal{T}_1(-1/2,1/2) = -\frac{2}{\sqrt{2}}\begin{pmatrix} 1 & 0 \end{pmatrix}\begin{pmatrix} 0 & -1 \\ 0 & 0 \end{pmatrix}\begin{pmatrix} 0 \\ 1 \end{pmatrix} = \sqrt{2} \tag{C.11}$$

**Process** $\nu_{\mu^-} n \to \mu^- n\pi^+$

$$\mathcal{T}_2(m,m') = \chi^\dagger(m')(\boldsymbol{\tau}\cdot\boldsymbol{\phi}_\pi^*)(\boldsymbol{\tau}\cdot\mathbf{W}^*)\chi(m)$$

$$(\boldsymbol{\tau}\cdot\boldsymbol{\phi}_\pi^*)(\boldsymbol{\tau}\cdot\mathbf{W}^*) = -2\begin{pmatrix} 0 & 0 \\ 0 & 1 \end{pmatrix} \tag{C.12}$$

$$\mathcal{T}_1(1/2,1/2) = -2\begin{pmatrix} 1 & 0 \end{pmatrix}\begin{pmatrix} 0 & 0 \\ 0 & 1 \end{pmatrix}\begin{pmatrix} 1 \\ 0 \end{pmatrix} = 0 \tag{C.13}$$

**Process** $\nu_{\mu^-} n \to \mu^- n\pi^+$

$$\mathcal{T}_2(m,m') = \chi^\dagger(m')(\boldsymbol{\tau}\cdot\boldsymbol{\phi}_\pi^*)(\boldsymbol{\tau}\cdot\mathbf{W}^*)\chi(m)$$

$$(\boldsymbol{\tau}\cdot\boldsymbol{\phi}_\pi^*)(\boldsymbol{\tau}\cdot\mathbf{W}^*) = -2\begin{pmatrix} 0 & 0 \\ 0 & 1 \end{pmatrix} \tag{C.14}$$

$$\mathcal{T}_2(-1/2,-1/2) = -2\begin{pmatrix} 0 & 1 \end{pmatrix}\begin{pmatrix} 0 & 0 \\ 0 & 1 \end{pmatrix}\begin{pmatrix} 0 \\ 1 \end{pmatrix} = -2 \tag{C.15}$$

**Process** $\nu_{\mu^-} n \to \mu^- p\pi^0$

$$\mathcal{T}_2(m,m') = \chi^\dagger(m')(\boldsymbol{\tau}\cdot\boldsymbol{\phi}_\pi^*)(\boldsymbol{\tau}\cdot\mathbf{W}^*)\chi(m)$$

$$(\boldsymbol{\tau}\cdot\boldsymbol{\phi}_\pi^*)(\boldsymbol{\tau}\cdot\mathbf{W}^*) = \frac{2}{\sqrt{2}}\begin{pmatrix} 0 & 1 \\ 0 & 0 \end{pmatrix} \tag{C.16}$$

$$\mathcal{T}_2(-1/2,1/2) = \frac{2}{\sqrt{2}}\begin{pmatrix} 1 & 0 \end{pmatrix}\begin{pmatrix} 0 & 1 \\ 0 & 0 \end{pmatrix}\begin{pmatrix} 0 \\ 1 \end{pmatrix} = \sqrt{2} \tag{C.17}$$

**Process** $\nu_{\mu^-} p \to \mu^- p \pi^+$

$$\mathcal{T}_3(m,m') = -i\chi^\dagger(m')[(\boldsymbol{\Phi}^*_\pi \times \boldsymbol{\Phi}_{\pi'}) \cdot W^*](\boldsymbol{\tau} \cdot \boldsymbol{\Phi}^*_{\pi'})\chi(m)$$

$$(\boldsymbol{\Phi}^*_\pi \times \boldsymbol{\Phi}_{\pi'}) \cdot W^* = -\frac{1}{2}\begin{vmatrix} 1 & 0 & 1 \\ -i & 0 & i \\ 0 & 1 & 0 \end{vmatrix} = i \tag{C.18}$$

$$(\boldsymbol{\tau} \cdot \boldsymbol{\Phi}^*_{\pi'}) = \begin{pmatrix} 1 & 0 \\ 0 & -1 \end{pmatrix} \tag{C.19}$$

$$[(\boldsymbol{\Phi}^*_\pi \times \boldsymbol{\Phi}_{\pi'}) \cdot W^*](\boldsymbol{\tau} \cdot \boldsymbol{\Phi}^*_{\pi'}) = i\begin{pmatrix} 1 & 0 \\ 0 & -1 \end{pmatrix} \tag{C.20}$$

$$\mathcal{T}_3(1/2,1/2) = \begin{pmatrix} 1 & 0 \end{pmatrix}\begin{pmatrix} 1 & 0 \\ 0 & -1 \end{pmatrix}\begin{pmatrix} 1 \\ 0 \end{pmatrix} = 1 \tag{C.21}$$

**Process** $\nu_{\mu^-} n \to \mu^- n \pi^+$

$$\mathcal{T}_3(m,m') = -i\chi^\dagger(m')[(\boldsymbol{\Phi}^*_\pi \times \boldsymbol{\Phi}_{\pi'}) \cdot \mathbf{W}^*](\boldsymbol{\tau} \cdot \boldsymbol{\Phi}^*_{\pi'})\chi(m)$$

$$[(\boldsymbol{\Phi}^*_\pi \times \boldsymbol{\Phi}_{\pi'}) \cdot \mathbf{W}^*](\boldsymbol{\tau} \cdot \boldsymbol{\Phi}^*_{\pi'}) = i\begin{pmatrix} 1 & 0 \\ 0 & -1 \end{pmatrix} \tag{C.22}$$

$$\mathcal{T}_3(-1/2,-1/2) = \begin{pmatrix} 0 & 1 \end{pmatrix}\begin{pmatrix} 1 & 0 \\ 0 & -1 \end{pmatrix}\begin{pmatrix} 0 \\ 1 \end{pmatrix} = -1 \tag{C.23}$$

**Process** $\nu_{\mu^-} n \to \mu^- p\pi^0$

$$\mathcal{T}_3(m,m') = -i\chi^\dagger(m')[(\boldsymbol{\phi}^*_\pi \times \boldsymbol{\phi}_{\pi'}) \cdot \mathbf{W}^*](\boldsymbol{\tau} \cdot \boldsymbol{\phi}^*_{\pi'})\chi(m)$$

$$[(\boldsymbol{\phi}^*_\pi \times \boldsymbol{\phi}_{\pi'}) \cdot W^*](\boldsymbol{\tau} \cdot \boldsymbol{\phi}^*_{\pi'}) = \frac{2i}{\sqrt{2}} \begin{pmatrix} 0 & 1 \\ 0 & 0 \end{pmatrix} \tag{C.24}$$

$$\mathcal{T}_3(-1/2,1/2) = -i \begin{pmatrix} 1 & 0 \end{pmatrix} \frac{2i}{\sqrt{2}} \begin{pmatrix} 0 & 1 \\ 0 & 0 \end{pmatrix} \begin{pmatrix} 0 \\ 1 \end{pmatrix} = \sqrt{2} \tag{C.25}$$

**Process** $\nu_{\mu^-} p \to \mu^- p\pi^+$

$$\mathcal{T}_4(m,m') = i\chi^\dagger(m')[(\boldsymbol{\phi}^*_\pi \times \boldsymbol{\tau}) \cdot \mathbf{W}^*]\chi(m)$$

$$[(\boldsymbol{\phi}^*_\pi \times \boldsymbol{\tau}) \cdot \mathbf{W}^*] = -\frac{1}{2} \begin{vmatrix} 1 & \boldsymbol{\tau}_1 & 1 \\ -i & \boldsymbol{\tau}_2 & i \\ 0 & \boldsymbol{\tau}_3 & 0 \end{vmatrix} = i\boldsymbol{\tau}_3 \tag{C.26}$$

$$\mathcal{T}_4(1/2,1/2) = i \begin{pmatrix} 1 & 0 \end{pmatrix} i \begin{pmatrix} 1 & 0 \\ 0 & -1 \end{pmatrix} \begin{pmatrix} 1 \\ 0 \end{pmatrix} = -1 \tag{C.27}$$

**Process** $\nu_{\mu^-} n \to \mu^- n\pi^+$

$$\mathcal{T}_4(m,m') = i\chi^\dagger(m')[(\boldsymbol{\phi}^*_\pi \times \boldsymbol{\tau}) \cdot \mathbf{W}^*]\chi(m)$$

$$[(\boldsymbol{\phi}_\pi^* \times \boldsymbol{\tau}) \cdot \mathbf{W}^*] = -\frac{1}{2} \begin{vmatrix} 1 & \boldsymbol{\tau}_1 & 1 \\ -i & \boldsymbol{\tau}_2 & i \\ 0 & \boldsymbol{\tau}_3 & 0 \end{vmatrix} = i\boldsymbol{\tau}_3 \tag{C.28}$$

$$\mathcal{T}_4(-1/2,-1/2) = i \begin{pmatrix} 0 & 1 \end{pmatrix} i \begin{pmatrix} 1 & 0 \\ 0 & -1 \end{pmatrix} \begin{pmatrix} 0 \\ 1 \end{pmatrix} = 1 \tag{C.29}$$

**Process** $\nu_{\mu^-} n \to \mu^- p\pi^0$

$$\mathcal{T}_4(m,m') = i\chi^\dagger(m')[(\boldsymbol{\phi}_\pi^* \times \boldsymbol{\tau}) \cdot \mathbf{W}^*]\chi(m)$$

$$[(\boldsymbol{\phi}_\pi^* \times \boldsymbol{\tau}) \cdot \mathbf{W}^*] = \frac{1}{2} \begin{vmatrix} 0 & \boldsymbol{\tau}_1 & 1 \\ 0 & \boldsymbol{\tau}_2 & i \\ 1 & \boldsymbol{\tau}_3 & 0 \end{vmatrix} = \frac{2i}{\sqrt{2}} \begin{pmatrix} 0 & 1 \\ 0 & 0 \end{pmatrix} \tag{C.30}$$

$$\mathcal{T}_4(-1/2,1/2) = i \begin{pmatrix} 1 & 0 \end{pmatrix} \frac{2i}{\sqrt{2}} \begin{pmatrix} 0 & 1 \\ 0 & 0 \end{pmatrix} \begin{pmatrix} 0 \\ 1 \end{pmatrix} = -\sqrt{2} \tag{C.31}$$

**Process** $\nu_{\mu^-} p \to \mu^- p\pi^+$

$$\mathcal{T}_5(m,m') = \chi^\dagger(m')(\boldsymbol{\phi}_\pi^* \cdot \mathbf{W}^*)\chi(m)$$

$$\boldsymbol{\phi}_\pi^* \cdot \mathbf{W}^* = \frac{1}{\sqrt{2}} \begin{pmatrix} -1 & i & 0 \end{pmatrix} \frac{1}{\sqrt{2}} \begin{pmatrix} 1 \\ i \\ 0 \end{pmatrix} = -1 \tag{C.32}$$

$$\mathcal{T}_5(1/2,1/2) = \begin{pmatrix} 1 & 0 \end{pmatrix}(-1)\begin{pmatrix} 1 \\ 0 \end{pmatrix} = -1 \tag{C.33}$$

**Process** $\nu_{\mu^-} n \to \mu^- n\pi^+$

$$\mathcal{T}_5(-1/2,-1/2) = \begin{pmatrix} 1 & 0 \end{pmatrix}(-1)\begin{pmatrix} 0 \\ 1 \end{pmatrix} = -1 \tag{C.34}$$

**Process** $\nu_{\mu^-} n \to \mu^- p\pi^0$

$$\boldsymbol{\phi}^*_\pi \cdot \mathbf{W}^* = \begin{pmatrix} 0 & 0 & 1 \end{pmatrix}\frac{1}{\sqrt{2}}\begin{pmatrix} 1 \\ i \\ 0 \end{pmatrix} = 0 \tag{C.35}$$

$$\mathcal{T}_5(-1/2,1/2) = 0 \tag{C.36}$$

$$\mathcal{T}_6 = -\mathcal{T}_3 \tag{C.37}$$

To calculate isospin coefficients $\mathcal{T}_7$ and $\mathcal{T}_8$, we use the transition matrix $\mathbf{T}$, that can be construct using the Clebsch-Gordan coefficient. The matrix are given by

$$T_1 = \begin{pmatrix} -\frac{1}{\sqrt{2}} & 0 & \frac{1}{\sqrt{6}} & 0 \\ 0 & -\frac{1}{\sqrt{6}} & 0 & \frac{1}{\sqrt{2}} \end{pmatrix}, \quad T_2 = -i\begin{pmatrix} \frac{1}{\sqrt{2}} & 0 & \frac{1}{\sqrt{6}} & 0 \\ 0 & \frac{1}{\sqrt{6}} & 0 & \frac{1}{\sqrt{2}} \end{pmatrix}, \quad T_3 = \begin{pmatrix} 0 & \sqrt{\frac{2}{3}} & 0 & 0 \\ 0 & 0 & \sqrt{\frac{2}{3}} & 0 \end{pmatrix} \tag{C.38}$$

**Process** $\nu_{\mu^-} p \to \mu^- p\pi^+$

$$\mathcal{T}_7(m,m') = \chi^\dagger(m_{t'})(\mathbf{T}\cdot\mathbf{W}^*)(\mathbf{T}^\dagger\boldsymbol{\phi}^*_\pi)\chi(m_t)$$

$$(\mathbf{T}\cdot\mathbf{W}^*)(\mathbf{T}^\dagger\boldsymbol{\phi}_\pi^*) = -\begin{pmatrix} 0 & 0 & \frac{1}{\sqrt{3}} & 0 \\ 0 & -\frac{1}{\sqrt{6}} & 0 & 1 \end{pmatrix}\begin{pmatrix} 0 & 0 \\ 0 & 0 \\ \frac{1}{\sqrt{3}} & 0 \\ 0 & 1 \end{pmatrix} = \begin{pmatrix} \frac{1}{3} & 0 \\ 0 & 1 \end{pmatrix} \tag{C.39}$$

$$\mathcal{T}_7(1/2,1/2) = -\begin{pmatrix} 1 & 0 \end{pmatrix}\begin{pmatrix} \frac{1}{3} & 0 \\ 0 & 1 \end{pmatrix}\begin{pmatrix} 1 \\ 0 \end{pmatrix} \tag{C.40}$$

$$\mathcal{T}_7(1/2,1/2) = -\frac{1}{3} \tag{C.41}$$

**Process** $\nu_{\mu^-} n \to \mu^- n\pi^+$

$$\mathcal{T}_7(-1/2,-1/2) = -\begin{pmatrix} 0 & 1 \end{pmatrix}\begin{pmatrix} \frac{1}{3} & 0 \\ 0 & 1 \end{pmatrix}\begin{pmatrix} 0 \\ 1 \end{pmatrix} \tag{C.42}$$

$$\mathcal{T}_7(-1/2,-1/2) = -1 \tag{C.43}$$

**Process** $\nu_{\mu^-} n \to \mu^- p\pi^0$

$$(\mathbf{T}\cdot\mathbf{W}^*)(\mathbf{T}^\dagger\boldsymbol{\phi}_\pi^*) = -\begin{pmatrix} 0 & 0 & \frac{1}{\sqrt{3}} & 0 \\ 0 & 0 & 0 & 1 \end{pmatrix}\begin{pmatrix} 0 & 0 \\ \sqrt{\frac{2}{3}} & 0 \\ 0 & \sqrt{\frac{2}{3}} \\ 0 & 0 \end{pmatrix} = \begin{pmatrix} 0 & \frac{\sqrt{2}}{3} \\ 0 & 0 \end{pmatrix} \tag{C.44}$$

$$\mathcal{T}_7(-1/2,1/2) = -\begin{pmatrix} 1 & 0 \end{pmatrix}\begin{pmatrix} 0 & \frac{\sqrt{2}}{3} \\ 0 & 0 \end{pmatrix}\begin{pmatrix} 0 \\ 1 \end{pmatrix} \tag{C.45}$$

$$\mathcal{T}_7(-1/2,1/2) = \frac{\sqrt{2}}{3} \tag{C.46}$$

**Process** $\nu_{\mu^-} p \to \mu^- p\pi^+$

$$\mathcal{T}_8(m_t,m_{t'}) = \chi^\dagger(m_{t'})(\mathbf{T}\cdot\boldsymbol{\phi}_\pi^*)(\mathbf{T}^\dagger\cdot\mathbf{W}^*)\chi(m_t) \tag{C.47}$$

$$(\mathbf{T}\cdot\boldsymbol{\phi}^*_\pi)(\mathbf{T}^\dagger\cdot\mathbf{W}^*) = -\begin{pmatrix} 1 & 0 & 0 & 0 \\ 0 & \frac{1}{\sqrt{3}} & 0 & 0 \end{pmatrix}\begin{pmatrix} 1 & 0 \\ 0 & \frac{1}{\sqrt{3}} \\ 0 & 0 \\ 0 & 0 \end{pmatrix} = \begin{pmatrix} 1 & 0 \\ 0 & \frac{1}{3} \end{pmatrix} \tag{C.48}$$

$$\mathcal{T}_8(1/2,1/2) = -\begin{pmatrix} 1 & 0 \end{pmatrix}\begin{pmatrix} 1 & 0 \\ 0 & \frac{1}{3} \end{pmatrix}\begin{pmatrix} 1 \\ 0 \end{pmatrix} \tag{C.49}$$

$$\mathcal{T}_8(1/2,1/2) = -1 \tag{C.50}$$

**Process** $\nu_{\mu^-} n \to \mu^- n\pi^+$

$$\mathcal{T}_8(-1/2,-1/2) = -\begin{pmatrix} 0 & 1 \end{pmatrix}\begin{pmatrix} 1 & 0 \\ 0 & \frac{1}{3} \end{pmatrix}\begin{pmatrix} 0 \\ 1 \end{pmatrix} \tag{C.51}$$

$$\mathcal{T}_8(-1/2,-1/2) = -\frac{1}{3} \tag{C.52}$$

**Process** $\nu_{\mu^-} n \to \mu^- p\pi^0$

$$(\mathbf{T}\cdot\boldsymbol{\phi}^*_\pi)(\mathbf{T}^\dagger\cdot\mathbf{W}^*) = -\begin{pmatrix} 0 & \sqrt{\frac{2}{3}} & 0 & 0 \\ 0 & 0 & \sqrt{\frac{2}{3}} & 0 \end{pmatrix}\begin{pmatrix} 1 & 0 \\ 0 & \frac{1}{\sqrt{3}} \\ 0 & 0 \\ 0 & 0 \end{pmatrix} = \begin{pmatrix} 0 & \frac{\sqrt{2}}{3} \\ 0 & 0 \end{pmatrix} \tag{C.53}$$

$$\mathcal{T}_8(-1/2,1/2) = -\begin{pmatrix} 1 & 0 \end{pmatrix}\begin{pmatrix} 0 & \frac{\sqrt{2}}{3} \\ 0 & 0 \end{pmatrix}\begin{pmatrix} 0 \\ 1 \end{pmatrix} \tag{C.54}$$

$$\mathcal{T}_8(-1/2,1/2) = -\frac{\sqrt{2}}{3} \tag{C.55}$$

# Appendix D

# PROPAGATORS AND LAGRANGIANS FOR BACKGROUND AND NON-RESONANT AMPLITUDES

The propagators and interaction Lagrangians used to built amplitudes $O_{BN}$will be resumed here. First the propagators, which come from the inversion of the kinetic operators present in the free Lagrangians are

$$S(p) = \frac{\not{p}+m_N}{p^2-m^2}, \text{ nucleon} \tag{D.1}$$

$$\Delta(p) = \frac{1}{p^2-m_\pi^2}, \text{ pion} \tag{D.2}$$

$$D_{\mu\nu}(p) = \frac{-g_{\mu\nu}+\frac{p_\mu p_\nu}{m_V^2}}{p^2-m_V^2}, \text{ vector-meson,} \tag{D.3}$$

while the effective strong interacting Lagrangians are

$$\mathscr{L}_{\pi NN}(x) = -\frac{g_{\pi NN}}{2m_N}\bar{\psi}(x)\gamma_5\gamma_\mu\boldsymbol{\tau}\cdot(\partial^\mu\boldsymbol{\phi}(x))\psi(x), \tag{D.4}$$

$$\mathscr{L}_{VNN}(x) = -\frac{g_V}{2}\bar{\psi}(x)\left[\gamma_\mu\left\{\begin{array}{c}\boldsymbol{\rho}^\mu(x)\cdot\boldsymbol{\tau}\\ \omega^\mu(x)\end{array}\right\}-\frac{\kappa_V}{2m_N}\sigma_{\mu\nu}\left(\partial^\nu\left\{\begin{array}{c}\boldsymbol{\rho}^\mu(x)\cdot\boldsymbol{\tau}\\ \omega^\mu(x)\end{array}\right\}\right)\right]\psi(x), \tag{D.5}$$

With $V=\omega,\rho$. Now, we define the effective hadron weak Lagrangians

$$\mathscr{L}_{WNN}(x) = -\frac{g}{2\sqrt{2}}\overline{\psi}(x)\left[\gamma_\mu F_1^V(Q^2) - \frac{F_2^V(Q^2)}{2m_N}\sigma_{\mu\nu}\partial^\nu - F^A(Q^2)\gamma_\mu\gamma_5\right]\sqrt{2}\boldsymbol{W}^\mu(x)\cdot\frac{\boldsymbol{\tau}}{2}\psi(x) + hc. \quad \text{(D.6)}$$

$$\mathscr{L}_{W\pi\pi}(x) = -\frac{g}{2\sqrt{2}}F_1^V(Q^2)\sqrt{2}\left[\boldsymbol{\phi}(x)\times\partial_\mu\boldsymbol{\phi}(x)\right]\cdot\boldsymbol{W}^\mu(x), \quad \text{(D.7)}$$

$$\mathscr{L}_{W\pi NN}(x) = -\frac{g}{2\sqrt{2}}\frac{f_{\pi NN}}{m_\pi}F_1^V(Q^2)\bar{\psi}(x)\gamma_5\gamma_\mu\sqrt{2}(\boldsymbol{\tau}\times\boldsymbol{\phi}(x))\cdot\boldsymbol{W}^\mu\psi(x), \quad \text{(D.8)}$$

$$\mathscr{L}_{W\pi\rho}(x) = \frac{g}{2\sqrt{2}}f_{\rho\pi A}F^A(Q^2)\sqrt{2}\left(\boldsymbol{\phi}(x)\times\boldsymbol{\rho}_\mu(x)\right)\cdot\boldsymbol{W}(x)^\mu \quad \text{(D.9)}$$

$$\mathscr{L}_{W\pi\omega}(x) = -\frac{g}{2\sqrt{2}}\frac{g_{\omega\pi V}}{m_\omega}F_1^V(Q^2)\epsilon_{\mu\alpha\lambda\nu}\left(\partial^\lambda\boldsymbol{\phi}(x)\right)\cdot\left(\partial^\mu\boldsymbol{W}^\alpha(x)\right)\omega^\nu(x). \quad \text{(D.10)}$$